



AKADEMIA GÓRNICZO-HUTNICZA IM. STANISŁAWA STASZICA W KRAKOWIE

DZIEDZINA NAUKI INŻYNIERYJNO-TECHNICZNE

DYSCYPLINA AUTOMATYKA, ELEKTRONIKA, ELEKTROTECHNIKA
I TECHNOLOGIE KOSMICZNE

ROZPRAWA DOKTORSKA

Detekcja pracy wyspowej rozproszonych źródeł energii z
wykorzystaniem metod estymacji fazorów i sieci
neuronowych

Autor: Mohammad Abu Sarhan

Promotor rozprawy: Dr hab. inż. Andrzej Bień, prof. uczelni
Promotor pomocniczy: Dr inż. Szymon Barczentewicz

Praca wykonana: Akademia Górniczo-Hutnicza
im. Stanisława Staszica w Krakowie

Kraków, 2024



FIELD OF SCIENCE ENGINEERING AND TECHNOLOGY

SCIENTIFIC DISCIPLINE AUTOMATION, ELECTRONICS, ELECTRICAL
ENGINEERING AND SPACE TECHNOLOGIES

DOCTORAL THESIS

The Identification of Islanding Incidents in Grid-
Connected Distributed Systems Using Phasor
Measurement Estimation and Artificial Neural Network
Approach

Author: Mohammad Abu Sarhan

First supervisor: Prof. dr hab. inż. Andrzej Bień
Assisting supervisor: Dr. inż Szymon Barczentewicz

Completed in: AGH University of Krakow

Krakow, 2024

The Identification of Islanding Incidents in Grid-Connected Distributed Systems Using Phasor Measurement Estimation and Artificial Neural Network Approach

Mohammad Abu Sarhan

Abstract

The protection techniques in conventional power systems are created under the presumption that, in the event of any abnormal or undesirable circumstances, the parts affected by this abnormal condition will be isolated from the whole power grid. As an alternative, the integrated DG power system when a problem occurs, the microgrid system's loads continue to be powered by the system's current local DG. The microgrid is referred to as being islanded in this situation, which is also referred to as an islanding scenario. Islanding detection is a crucial process that must be carried out in order to ensure the reliability and security of energy distribution networks.

This study presents a new approach to identify islanding incidents by integrating phasor measuring units (PMU) with artificial neural network (ANN). The approach utilizes PMU measurements to derive characteristics such as phasor voltage, voltage frequency, and voltage rate of change of frequency (ROCOF), which are subsequently inputted into an ANN classifier. By utilizing a vast dataset consisting of over one hundred thousand observations of both islanding and non-islanding scenarios, the tests are conducted on several types of inverters in accordance with the requirements outlined in the PN-EN 62116 protocol. The experiments were conducted in three distinct experimental laboratories, where the data and outcomes were analyzed using MATLAB and LabVIEW. The findings exhibit a remarkable level of accuracy when compared to previous methods, with a testing accuracy of 99%, a training accuracy of 99.3%, and a rapid detection time response which was calculated as an average time equals 0.18 seconds. This study presents a pragmatic resolution for issues arising from the islanding phenomena in power networks, therefore improving the reliability and security of the system.

Detekcja pracy wyspowej rozproszonych źródeł energii z wykorzystaniem metod estymacji fazorów i sieci neuronowych

Mohammad Abu Sarhan

Streszczenie

Techniki zabezpieczeń w klasycznych systemach elektroenergetycznych tworzone są przy założeniu, że w przypadku wystąpienia jakichkolwiek nietypowych lub niepożądanych okoliczności, części dotknięte tym anormalnym stanem zostaną odizolowane od całej sieci elektroenergetycznej. Alternatywą są systemy rozproszone w których jedno ze źródeł w mikrosieci pozwala na pracę wyspową układu. Wykrywanie pracy wyspowej jest kluczowym procesem, który należy przeprowadzić, aby zapewnić niezawodność i bezpieczeństwo sieci dystrybucyjnych w kontekście integracji źródeł rozproszonych.

W badaniu przedstawiono nowe podejście do detekcji pracy wyspowej poprzez integrację danych synchrofazorowych z siecią neuronową (SSN). Podejście to wykorzystuje dane pozyskiwane z PMU, tj. napięcie, częstotliwość napięcia i szybkość zmiany częstotliwości napięcia (ROCOF), które są następnie wprowadzane do klasyfikatora SSN. Wykorzystując obszerny zbiór danych składający się z ponad stu tysięcy obserwacji zarówno w scenariuszu wyspowym, jak i scenariuszu pracy synchronicznej przeprowadzono badania na kilku typach falowników, zgodnie z wymaganiami określonymi w normie PN-EN 62116. Eksperymenty przeprowadzono w trzech różnych laboratoriach doświadczalnych, gdzie dane i wyniki analizowano przy użyciu MATLAB-a i LabVIEW. Wyniki wykazują niezwykle skuteczną detekcję na poziomie 99% dokładność uczenia na poziomie 99,3% i krótki czas reakcji na wykrywanie na poziomie 0.18 s. W opracowaniu przedstawiono pragmatyczne rozwiązanie problemów wynikających z pracy wyspowej w sieciach elektroenergetycznych, poprawiając tym samym niezawodność i bezpieczeństwo systemu.

Declaration

I, Mr. Mohammad Abu Sarhan do hereby declare that the dissertation entitled “The Identification of Islanding Incidents in Grid-Connected Distributed Systems Using Phasor Measurement Estimation and Artificial Neural Network Approach” being submitted to **AGH University of Krakow** for the fulfilment of the requirement of obtaining the degree of **Doctor of Philosophy in Electrical Engineering** is original work which has been carried out by myself under the supervision of my supervisors. I also do hereby declare that this original work has not been previously submitted to any other university or institute for the award of any degree or diploma.

Acknowledgements

I would like to use this opportunity to convey my gratitude to my supervisor, Professor Andrzej Bień, for providing me with significant supervision, support, and direction during the entirety of my research journey. Additionally, I would like to express my gratitude to Dr. Szymon Barcentewicz, my co-supervisor, for his additional supervision, technical support, and assistance. In conclusion, I would want to express my gratitude to my parents, my wife, other members of my family, and my friends for never-ending moral support and encouragement during the entirety of my research journey.

Table of Content

1.	Introduction.....	1
1.1	Microgrids.....	3
1.1.1	Benefits and Characteristic of Microgrid.....	4
1.1.2	Obstacles Encountered in the Growth of Microgrids.....	4
1.1.3	Basic Microgrids Components.....	5
1.2	Control of Microgrid.....	7
1.2.1	Control Issues with Microgrids.....	7
1.3	Microgrid Protection.....	9
1.3.1	Challenges in Microgrid Protection.....	10
1.3.2	Aspect Related to the Microgrid Protection.....	12
1.4	Research Problem Formulation.....	18
1.5	Objective of Research Work.....	23
1.6	Thesis Layout.....	24
2.	Literature Review.....	25
2.1	Background.....	25
2.2	Schemes of Islanding Detection.....	27
2.2.1	Passive Methods.....	27
2.2.1.1	Over under Voltage/Frequency Scheme (O/UV, F).....	28
2.2.1.2	Scheme of Frequency Rate of Change (ROCOF).....	29
2.2.1.3	Active and Reactive Power Rate of Change Scheme (ROCOP).....	29
2.2.1.4	Unbalance Voltage Scheme (VU).....	30
2.2.1.5	Scheme of Phase Jump Detection (PJD).....	30
2.2.1.6	Scheme of Total Harmonic Distortion (THD).....	30
2.2.1.7	Frequency over Power Rate of Change Scheme (ROCOFOP).....	31
2.2.2	Active Schemes.....	31
2.2.2.1	Scheme of Active Frequency Drift (AFD).....	32
2.2.2.2	Scheme of Sandia Frequency Shift (SFS).....	32
2.2.2.3	Scheme of Sandia Voltage Shift (SVS).....	33
2.2.2.4	Scheme of Impedance Measurement (IM).....	33
2.2.2.5	Scheme of Slip Mode Frequency Shift (SMFS).....	33
2.2.2.6	Scheme of Active and Reactive Power Variation (ARPV).....	34
2.2.2.7	Scheme of Negative Sequence of Injected Current (NSC).....	35
2.2.2.8	Scheme of Frequency Jump (FJ).....	35
2.2.2.9	Scheme of Perturbation of Phase-Locked Loop (PLL).....	35
2.2.2.10	Scheme of Virtual Capacitor or Inductor (VC).....	36
2.2.3	Hybrid Methods.....	36
2.2.3.1	Scheme of Unbalanced Voltage and Frequency Set-Point.....	37
2.2.3.2	Scheme of Shifted Voltage and Real Power.....	37
2.2.3.3	Scheme of Injected Voltage Fluctuation.....	37
2.2.3.4	Scheme of Hybrid Sandia Frequency Shift and Q-F.....	37
2.2.4	Remote Schemes.....	38
2.2.4.1	Scheme of Power Line Carrier Communication (PLCC).....	38
2.2.4.2	Scheme of Signal Produced by Disconnect (SPD).....	39
2.2.4.3	Scheme of Supervisory Control and Data Acquisition (SCADA).....	39

2.2.4.4	Transfer Trip Scheme.....	39
2.2.4.5	Impedance Insertion Method.....	39
2.2.4.6	Scheme of Phasor Measurement Unit.....	40
2.2.5	Scheme of Signal Processing.....	40
2.2.5.1	Scheme of Fourier Transformer.....	41
2.2.5.2	Scheme of Wavelet Transformer.....	41
2.2.5.3	Scheme of S- Transformer.....	41
2.2.5.4	Time-Time Transformer Method.....	41
2.2.5.5	Miscellaneous Signal Processing Based Methods.....	42
2.2.6	Scheme of Computational Intelligence.....	42
2.2.6.1	Scheme of Artificial Neural Network (ANN).....	43
2.2.6.2	Scheme of Probabilistic Neural Network (PNN).....	43
2.2.6.3	Scheme of Decision Tree (DT).....	43
2.2.6.4	Scheme of Fuzzy Logic (FL).....	43
2.2.6.5	Scheme of Adaptive Neuro-Fuzzy Inference System (ANFIS).....	43
2.2.6.6	Scheme of Support Vector Machine (SVM).....	44
2.2.6.7	Scheme of Naive Bayesian Classifier (NB).....	44
2.2.6.8	Scheme of Deep Learning (DL).....	44
2.3	Difficulties in Choosing Islanding Detection Techniques.....	45
2.4	Evaluation of Islanding Detection Techniques' Performance.....	45
2.4.1	Assessing the Appropriateness According to DGs Category.....	46
2.4.2	Applicability of Multi-DGs Networks.....	46
2.4.3	Non-Detected Zone.....	47
2.4.4	Quality Factor.....	47
2.4.5	Response Time.....	47
2.4.6	Execution Expense.....	48
2.4.7	Power Quality Degradation.....	48
2.4.8	Load Type.....	48
2.4.9	Reliability.....	48
2.4.10	Compatibility with Multiple IDMs.....	49
2.4.11	Vulnerability to Cyber-Attacks.....	49
2.5	Standards of Islanding Detection.....	49
2.6	Comparison of IDMs.....	50
2.7	Conclusions.....	54
3.	Multiple-Criteria Decision Assessment.....	55
3.1	Background.....	55
3.2	Approach to Solving an MCDA Problem in General.....	57
3.3	Categories for Multiple-Criteria Decision Making (MCDM).....	59
3.4	Literature Review on Analytic Hierarchy Process (AHP).....	61
3.5	Background of Analytic Hierarchy Process (AHP).....	62
3.6	Theory of Analytic Hierarchy Process (AHP).....	63
3.7	Prioritization of Analytic Hierarchy Process (AHP).....	64
3.8	Consistency of Analytic Hierarchy Process (AHP).....	64
3.9	The Pairwise Scale of Analytic Hierarchy Process (AHP).....	65
3.10	Summary of Analytic Hierarchy Process (AHP).....	66
3.11	Analysis of Multiple-criteria Decision Analysis (MCDA).....	66

3.12	Analysis using Expert Choice Software.....	73
3.13	Conclusion.....	76
4.	Phasor Measurement Estimation.....	77
4.1	Background.....	77
4.2	Wide Area Measurement System.....	78
4.2.1	Phasor Measurement Unit.....	79
4.2.2	Phasor Measurement Technique.....	82
4.2.3	Discrete Fourier Transform.....	82
4.2.4	Estimation of Frequency Amplitude and Frequency Rate of Change.....	83
4.3	Phasor Measurement Unit Techniques for Islanding Detection.....	84
4.4	Phasor Measurement Unit Technique for Feature Extraction.....	86
4.5	Conclusion.....	93
5.	Islanding Detection Classification.....	94
5.1	An overview of Theory of Artificial Neural Network.....	94
5.2	Artificial Neural Network Model.....	95
5.3	Artificial Neural Network Architecture.....	96
5.3.1	Single Layered Feed Forward ANN.....	97
5.3.2	Multilayered Feed Forward Network (MFFN).....	97
5.3.3	Back Propagation (BP) Algorithm.....	98
5.4	Proposed Islanding Detection Method.....	100
5.5	Microgrid Systems under Test.....	102
5.6	Conclusion.....	107
6.	Results and Discussion.....	109
6.1	Islanding Detection Scenarios.....	109
6.2	ANN Classifier Model Parameters and Training.....	113
6.3	ANN Model Parameters Evaluation.....	114
6.4	Comparisons.....	118
6.5	Detection Time.....	120
6.6	Conclusion.....	121
7.	Conclusion and Future Scope.....	123
7.1	Conclusion.....	123
7.2	Major Contribution.....	123
7.3	Future Scope.....	125

List of Tables

Table 2.1.	Criteria of islanding identification.....	50
Table 2.2.	Analysis of islanding identification schemes determined by their positive aspects and drawbacks.....	51
Table 2.3.	Analysis of islanding identification determined by numerous factors.....	52
Table 2.4.	Analysis of islanding identification schemes determined by the time required to respond.....	52
Table 3.1.	MCDA matrix.....	58
Table 3.2.	Scale of AHP pair-wise scale.....	65
Table 3.3.	A concise contrast between islanding identification schemes determined by execution expense.....	67
Table 3.4.	A concise contrast between islanding identification schemes determined by undetectable area.....	67
Table 3.5.	A concise contrast between islanding identification schemes determined by power quality.....	68
Table 3.6.	A concise contrast between islanding identification schemes determined by response time.....	68
Table 3.7.	Matrix of pair-wise assessment.....	71
Table 3.8.	Matrix of inputs.....	71
Table 3.9.	Normalized matrix.....	72
Table 3.10.	Alternative ranking.....	73
Table 4.1.	A comparison between PMU and SCADA data.....	77
Table 4.2.	Techniques for detecting islanding using PMU parameters.....	85
Table 4.3.	Features extracted from PMU.....	87
Table 4.4.	Scenarios of Islanding for grid-linked PV Inverter.....	87
Table 4.5.	Phasors readings.....	88
Table 4.6.	Frequency readings.....	89
Table 4.7.	ROCOF readings.....	89
Table 4.8.	Scenarios of Islanding for grid linked synchronous generator system.....	89
Table 4.9.	Phasors readings.....	90
Table 4.10.	Frequency readings.....	91
Table 4.11.	ROCOF readings.....	91
Table 4.12.	Scenarios of islanding for grid linked PV system and synchronous generator.....	91
Table 4.13.	Phasors readings.....	92
Table 4.14.	Frequency readings.....	93
Table 4.15.	Results for ROCOF.....	93
Table 5.1.	Power assumption for inverters and loads.....	105
Table 5.2.	Power assumption for inverters and loads.....	107
Table 6.1.	Some samples of the data set used for training the classifier.....	113
Table 6.2.	ANN parameters specification.....	114

Table 6.3.	ANN contingency table.....	115
Table 6.4.	Constraint values of the ANN model.....	116
Table 6.5.	ANN model results.....	118
Table 6.6.	Naïve Bayes contingency table.....	118
Table 6.7.	Constraint values of the ANN model.....	119
Table 6.8.	GLM Logistic Regression contingency table.....	119
Table 6.9.	Constraint values of the GLM Logistic Regression model.....	119
Table 6.10.	Linear Discriminant contingency table.....	120
Table 6.11.	Constraint values of the GLM Logistic Regression model.....	120
Table 6.12.	Comparison of response time between the proposed model and tested inverters.....	121

List of Figures

Fig. 1.1.	Microgrid structure	3
Fig. 1.2.	Islanding phenomena concept.....	13
Fig. 1.3.	Islanding detection methods.....	13
Fig. 1.4.	Principle operation of passive schemes.....	14
Fig. 1.5.	Principle operation of active scheme.....	15
Fig. 1.6.	Principle operation of hybrid scheme.....	16
Fig. 1.7.	Principle operation of signal processing scheme.....	16
Fig. 1.8.	Principle operation of computational Intelligent schemes.....	17
Fig. 1.9.	Test system for the investigation of islanding formulation.....	18
Fig. 1.10.	Test system following islanding occurrence.....	19
Fig. 2.1.	Types of islanding condition.....	26
Fig. 2.2.	Passive methods.....	28
Fig. 2.3.	Active methods.....	31
Fig. 2.4.	Hybrid methods.....	36
Fig. 2.5.	Remote methods.....	38
Fig. 2.6.	Signal processing-based methods.....	40
Fig. 2.7.	Schemes of computational intelligence.....	42
Fig. 2.8.	Islanding detection criteria.....	46
Fig. 2.9.	Non-detected zone.....	47
Fig. 3.1.	MCDA steps.....	59
Fig. 3.2.	Various MCDM classifications.....	61
Fig. 3.3.	Proposed hierarchy structure.....	71
Fig. 3.4.	The framework of proposed hierarchy model.....	74
Fig. 3.5.	Pair-wise assessment in relation to (1) execution expense, (2) undetectable area, (3) quality of power, and (4) time to respond.....	74
Fig. 3.6.	The determination of priorities pair-wise assessment for (1) execution expense, (2) undetectable area, (3) quality of power, and (4) time to respond.....	75
Fig. 3.7.	Optimizing global priorities using the optimum mode.....	75
Fig. 3.8.	Functioning sensitivity.....	76
Fig. 4.1.	WAM structure.....	79
Fig. 4.2.	The PMU's functional block diagram.....	79
Fig. 4.3.	A sinusoidal signal's phasor representation.....	82
Fig. 4.4.	Measurement platform.....	87
Fig. 4.5.	Voltage and current for first, second , and third scenarios.....	88
Fig. 4.6.	Amplitude of voltage phasor, frequency and ROCOF for scenarios 1, 2, and 3.....	88
Fig. 4.7.	Voltage and current for scenarios 4, 5, and 6.....	90
Fig. 4.8.	Amplitude of voltage phasor, frequency and ROCOF for scenarios 4, 5, and 6.....	90
Fig. 4.9.	Voltage and current for scenarios 8, 9, and 10.....	92

Fig. 4.10.	Amplitude of voltage phasor, frequency and ROCOF for scenarios 8, 9, and 10.....	92
Fig. 5.1	ANN model.....	96
Fig. 5.2	ANN architecture classification.....	96
Fig. 5.3	FNN-single layer.....	97
Fig. 5.4	Multilayered FNN.....	98
Fig. 5.5	ANN structure with backpropagation algorithm.....	99
Fig. 5.6	Proposed islanding identification scheme.....	101
Fig. 5.7	Flowchart of the proposed scheme.....	101
Fig. 5.8	Schematic diagram of reflex laboratory.....	102
Fig. 5.9	Reflex laboratory system.....	103
Fig. 5.10	Schematic diagram of energy center laboratory.....	104
Fig. 5.11	Test bench for inverters.....	104
Fig. 5.12	Schematic diagram of dynamic power system laboratory.....	106
Fig. 5.13	Dynamic power systems laboratory setup.....	106
Fig. 6.1	Inverter voltage during unintentional islanding for scenario 1.....	110
Fig. 6.2	Inverter voltage during unintentional islanding for scenario 2.....	110
Fig. 6.3	Inverter voltage during unintentional islanding for scenario 3.....	111
Fig. 6.4	Inverter voltage during unintentional islanding for scenario 4.....	111
Fig. 6.5	Inverter phasor voltage, frequency, and ROCOF during unintentional islanding for (a) scenario 1, (b) scenario 2, (c) scenario 3, and (d) scenario 4...	112
Fig. 6.6	Confusion matrix for training.....	115
Fig. 6.7	Confusion matrix for training (a) voltage vs frequency (b) voltage vs ROCOF	118
Fig. 6.8	Comparison of accuracies between the proposed model and other methods....	120

List of Publications

Published Journal Papers

1. Use of analytical hierarchy process for selecting and prioritizing islanding detection methods in power grids / Mohammad Abu SARHAN, Andrzej BIEŃ, Szymon BARCZENTEWICZ // International Journal of Electrical and Computer Engineering. — 2024 — vol. 14 no. 3, s. 2422–2435. **(Q2, 70 Points)**
2. An extensive review and analysis of islanding detection techniques in DG systems connected to power grids / Mohammad ABU SARHAN // Energies. — 2023 — vol. 16 iss. 9 art. no. 3678, s. 1–22. **(Q1, 140 Points)**
3. A review of electricity and renewable energy sectors status and prospect in Jordan / Mohammad ABU SARHAN, Andrzej BIEŃ, Szymon BARCZENTEWICZ, Rana HASSAN // Przegląd Elektrotechniczny. — 2021 — R. 97 nr 9, s. 123–129. **(Q4, 70 Points)**
4. Energy sector of Pakistan – a review / Rana Muneeb HASSAN, Andrzej BIEŃ, Szymon BARCZENTEWICZ, Mohammad ABU SARHAN // Przegląd Elektrotechniczny. — 2021 — R. 97 nr 10, s. 33-37. **(Q4, 70 Points)**

Published Conference Papers

1. Dynamic voltages and currents in the microgrids while unintentional islanding / Mohammad ABU SARHAN, Szymon BARCZENTEWICZ, Andrzej BIEŃ // W: KNER: I Konferencja Naukowa Energetyki Rozproszonej KNER'2023 : Kraków, 26 września 2023 : streszczenia. — [Kraków : AGH], [2023].
2. Experimental study of power definitions in non-sinusoidal condition / Mohammad ABU SARHAN, Andrzej BIEŃ, Szymon BARCZENTEWICZ // W: EEET 2022 : 5th international conference on Electronics and Electrical Engineering Technology (EEET) : 2-4 December 2022, Beijing, China : proceedings. — Piscataway : The Institute of Electrical and Electronics Engineers, Inc., cop. 2022 — S. 126-131. **(20 Points)**
3. Global maximum power point tracking (GMPPT) control method of solar photovoltaic system under partially shaded conditions / Mohammad ABU SARHAN, Andrzej BIEŃ, Szymon BARCZENTEWICZ, Rana HASSAN // W: ICARA 2022 [Dokument elektroniczny] : 8th International Conference on Automation, Robotics and Applications : 18–20 February 2022 : virtual conference. — Piscataway : IEEE, cop. 2022. — S. 209–216. **(20 Points)**

Submitted Journal Papers (Accepted)

1. Hybrid Islanding Detection Method Using PMU-ANN Approach for Inverter-based Distributed Generation Systems. / Mohammad ABU SARHAN, Szymon BARCZENTEWICZ, Tomasz Lerch // IET Renewable Power Generation. **(Q2, 100 Points)**

1. Introduction

The term "Power Grid" has historically represented the electric network, that carries out the four fundamental operational functions of generation, transmission, distribution, and control. The high-capacity conventional generators that were situated far from the end consumers were controlled centrally by the conventional power system. Because centralized generating is more common, the distribution system's power flow is only ever going in one direction. As a result, the conventional electric system's straightforward infrastructure made it simple to adjust to changing demand. The electrical networks today, however, are faced with several stressors that the engineers of the past century could never have foreseen [1]. The grids are undergoing significant transformation because of numerous difficult criteria. The following are some of the main trends that pose a threat to the operation of conventional grids:

- Energy conversion and observance of the environment.
- The implementation of renewable energy resources.
- Intermittent power generation and control methods of renewable energy resources.
- An increase in energy-consuming machinery.
- Better defense mechanisms and the accompanying technologies.
- Demand for better customer service and operational effectiveness.
- A greater need for grid dependability due to the aging of the current infrastructure and rising energy consumption.

In order to enhance the integration of the new applications that recently become popular such distributed generator, plug-in electric means, storage systems, and demand response strategy, the renovation and revolution of traditional grids become crucial. Electric distribution grid must quickly make the transition from only one-way, blind physical operations through electromechanical mechanisms to the "Smart Grid" to meet the difficulties and changes in utilities and electric system operators [2].

Future grids and intelligent grids are other names for smart grids. A smart grid is described as "an electric network that possesses the characteristic of economically integrating various operational behavior and action-based generators, consumers, and those that perform both, to achieve an

efficient and sustainable power network with enhanced power quality, security, and safety along with the reduced system loss" [3]. Electricity is implemented in a smart grid in both directions. As a smart network, it communicates and develops a sophisticated automated power distribution system using cyber-secure digital communication technology. The future-grid is highly functional and has novel features including smart controlling and monitoring, self-recover, energy management, and instantaneous pricing [4]. The following objectives and requirements are achieved using smart grids:

- An improvement in the effectiveness and capacity of the current power services.
- Facilitating the use of electric vehicles, storage systems, and renewable energy sources.
- Adapting to and accommodating a variety of distributed power generation sources.
- Utilization of resources and system performance optimization.
- Power quality and system dependability improvements.
- Automation in the management of the operation's self-healing and maintenance.
- Enhancement of the system's disruption tolerance limit.
- support for the economic decarbonization process.
- Extremely resilient to cyberattacks.
- Increasing consumer choice by allowing for new markets, products, and services.
- The end-users are informed of all information and given choices for effectively utilizing their supply.
- Control over the entire electric power system, including integrated control over generation, transmission, distribution, substations, and end users.

The question is whether the smart grid will have an impact on or conflict with the existing distribution system's architecture to achieve the enhanced function mentioned above. If so, how should the utility system modify and implement the modifications now to convert the current conventional distribution network into a sophisticated and intelligent grid for the future? It would take decades to transform the current system into a "Smart Grid." Additionally, efforts to redesign the current grids are unable to keep up with several factors, including aging infrastructure, an increase in the frequency and intensity of weather occurrences, and a rising danger of physical and cyberattacks [5]. Consequently, many societies, businesses, and institutions are establishing "Microgrids" to push up and improve their electrical systems' resistance to the flaws in the

conventional "Macro-Grids." However, for the electricity system to operate a microgrid, more attention must be paid to the related problems and difficulties.

1.1 Microgrids

Microgrids, which primarily operate at the distribution system level, could be regarded as a clearly identifiable component of the smart grid. It incorporates power production and storage sources that are close to the loads and gives the customer's community complete control over each component, allowing the micro-system to supply 80% to 100% of the power needs. In other words, the microgrid is defined as "A cluster of distributed energy resources and end-users interconnected within the specific electric borders and functions like a sole controllable system relating to the utility grid" by the United States Department of Energy Microgrid Exchange Group. The plug-and-play electrical network is a notable characteristic of the microgrid as it has the ability to function alone or in collaboration with the power networks. The user's text is "[6]." Figure 1.1 illustrates the arrangement and connections of the microgrid's structure. These small-scale grids provide electricity with enhanced reliability, safety, and robustness by allowing users to select the amount and type of renewable energy sources that can be integrated into the network. The capacity of microgrids to efficiently include a wide range of different distributed power generating sources, especially those that are renewable, can be affirmed [7].

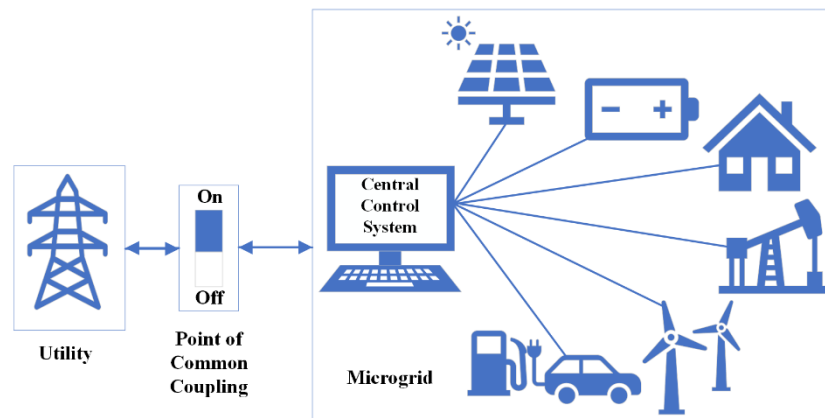


Fig. 1.1. Microgrid structure

1.1.1 Benefits and characteristics of microgrid

The remote centralized power system is significantly shifted toward a decentralized distributed power system thanks to the microgrid. Microgrids are designed to function with great operational resilience while being able to isolate themselves from larger grids [8]. Both the islanded/standalone mode (also known as grid-forming mode) and the grid-connected mode (also known as grid-following mode) are feasible options for their operation. Islanded mode refers to the state in which a microgrid autonomously manages and provides the system load demand, runs, and controls power generation, and maintains system stability without relying on any higher-level control [9].

The utilization of microgrids in the system offers several primary advantages or benefits:

- The system has the capability to operate in both Grid-connected and Standalone modes, providing flexibility.
- Offers excellent efficiency at a lower cost.
- Offers an energy resource an extremely dynamic response.
- Aids in balancing climatic changes.
- Assists with the integration of a range of power sources.
- Supports local employment creation and economic prosperity.
- reduces the system's transmission losses.
- enhances the dependability of the power supply.
- Provides the opportunity to decrease electricity bills.
- lessens grid congestion and effectively manages peak loads.
- Installation takes less time than with a conventional power plant.
- Provides improved cyber security.
- The risk is spread out, which is generally preferable to highly focused exposure to potential risks.

1.1.2 Obstacles encountered in the growth of microgrids

Despite the numerous potential benefits the microgrid may have, they face the following difficulties and drawbacks.

- DGs have a high installation cost.

- inability to operate various plug-and-play power sources due to lack of technical knowledge.
- Standards still need to be examined and reorganized for microgrids to operate well in active distribution systems.
- legal and administrative obstacles.
- a suitable market infrastructure to restrain a microgrid's monopoly.

1.1.3 Basic microgrid components

A. Distributed power generation sources

The consumers of microgrids receive power, heating, and cooling from the sources of power generation. They can be divided into two categories, thermal power sources (such as natural gas, biogas, and co-generation plants) and renewable power sources (such as solar, wind, and micro hydroelectric facilities). In some instances, the sources are categorized according to how they operate as synchronous generator-based power sources and inverter-based power sources, respectively.

It is crucial that the distributed generators (DGs) produce enough power to sustain all the important and uninterruptible demands of a microgrid that runs independently. Most often, when microgrids are formed, renewable energy sources like solar, wind, micro-hydro, etc. are incorporated [10]. However, the intermittent and fluctuating nature of the generation from various sources could lead to system instability. If the microgrids run concurrently with the main grid, the disturbances are managed by the main grid; otherwise, the internal microgrid component (i.e., storage devices) makes up for the instabilities. Hence, the system integrates several forms of generation, such as natural gas, biogas, diesel back-up generation, and batteries, to provide support to the renewable power sources in a self-sufficient microgrid [11]. Consequently, the power sources in the microgrid must consist of a blend of controllable resources and the primary source of electricity for the minimum level of demand.

- Distributed generator advantages
 - Reliable supply of electricity.
 - Cut down the losses of power transmission.
 - Alleviates the tension resulting from limited feeding capacity.
 - Promotes the utilization of sustainable energy sources.

- Challenges in incorporating distributed generators into power systems
 - Difficulties related to the quality of power.
 - Variation in the voltage levels which the network operates.
 - Alterations in the network's fault levels.
 - Redesigning network components is necessary.
 - System inertia variation (system with minimal inertia).

B. Decentralized storage systems

The microgrid tends to integrate many distributed generators (DGs), whereas the active and reactive power requirements of clients inside the microgrid are known to fluctuate [12]. This poses a threat to the microgrid's stability, which can be managed by incorporating decentralized power storage technologies. The storage technologies within a microgrid fulfill multiple functions. Some of the functions include ensuring system power quality, regulating system voltage and frequency, serving as a backup power supply, assisting in the black-start process, maintaining reserves, and performing demand-response management. The technologies used to create several sorts of storage devices, including thermal, mechanical, chemical, electrical, electromagnetic, and fossil fuel storage [13]. The charging and discharging of each device in a microgrid made up of many storage mechanisms with various capabilities and operational sorts must be effectively coordinated. The idea could be expressed simply as follows: storage devices with lesser capacities shouldn't discharge or fully charge more quickly than those with greater capacities [14]. These storage devices can be divided depending on their working efficacy, which is determined by their particular energy and specific power. Batteries and compressed air storage devices are examples of high specific energy storage devices, whereas flywheels, supercapacitors, and super-magnetic storage devices are examples of high specific power storage devices.

C. Consumers or End-Users

The classification of consumers in the microgrid can be mainly divided into different kinds of loads such as constant power load, constant current load, and constant impedance load. On the other hand, the loads can be classified as critical, non-critical, and vital loads. The loads which have higher priority and considered very important for the emergency system are defined as critical

loads. The critical loads have to be delivered by a constant power supply have control and command capabilities [12]. Lighting and heating are considered as vital loads. While loads include high voltage AC loads found in minor office buildings, motels, workshops, and similar establishments are an example of non-critical loads. Nevertheless, the application of load management schemes to control these loads is needed to ensure the system stability according to the power generation [15].

1.2 Control of Microgrid

An interface scheme based on computers is called the central control system of microgrid (MCCS). Almost every aspect of how the microgrid operates is under the control of the software. The system data are examined and controlled using supervisory control, and data acquisition (SCADA) system. Also, power demand, the power production, and market pricing are regulated and monitored using some forecasting schemes.

To achieve an ideal power supply at the lowest possible cost, an economic dispatch and unit commitment are applied [16]. MCCS manages information that is both centralized and decentralized. The MCCS manages all microgrid's data while handling the centralized processing. In contrast, just a small portion of the data acquired by the real-time process is handled by the MCCS during the decentralized processing [17].

To ensure a safe, dependable, and cost-effective operation, the central controller collaborates with every component that is part of the microgrid system. Regardless of the principal operation method of the microgrid, MCCS plays a very important function to control and integrate the distributed generators optimally (particularly renewable resources). The control approach is designed in a such way that can display the microgrid from the perspective of the grid as a self-governed unit as the control of the microgrid becomes a significant component.

1.2.1 Control issues with microgrids

Microgrid is a modified and improved operating system that has been mounted and incorporated into the low-voltage distribution system (LV). Because of this, the operating features of the traditional (i.e., current) distribution system change. With an increase in microgrids, the variances or differences in the features dramatically rise. This makes it difficult to develop a workable controller that accounts for variations in the LV system [18]. The microgrid's operational control also strives to boost efficiency by optimizing energy output and consumption. Microgrids also

carry over some traits like managing extreme imbalance and varied distributed power sources. Another difficult job is dealing with missing input parameters when managing the microgrid in centralized or decentralized mode [19].

Additionally, microgrid controllers support two operating modes: grid-connected (also known as grid-following) and autonomous (also known as island or grid-forming) modes. A changeover between the two modes is necessary for microgrid operations. Additionally, the change between modes results in a significant mismatch between generation and load [20]. As a result, the system voltage and frequency levels experience significant changes, and the control system becomes more complex. Furthermore, if there are many scattered micro sources connected to the microgrid, the plug-and-play functionality of the microgrid poses a significant problem [21].

The control and protective aspects of the microgrid are highly impacted by the transient faults, which are pointedly impacted by the electronic control unit presence in the microgrid. To achieve effective control and security in the microgrid, it is essential to first determine the operation mode. The operation modes of microgrids are monitored by local, central, or supervisory controllers.

The modes in which the microgrids operate are presented as:

A. Grid-connected operating mode

The microgrid's local power sources and loads in this mode function in accordance with utility-side parameter measurements. The system utility is mostly used to govern how the entire microgrid runs. To manage the microgrid's internal operations, the supervisory control of the microgrid gathers signals and data from the main grid. When operating in current control mode, the microgrid controllers regulate the injected active and reactive power of every power source. The other name of this mode is grid-following mode.

B. Islanded operating mode

In this operating mode, the microgrid's supervisory control unit and local controllers are exclusively accountable for the efficient running of the system. The microgrid controllers' function in voltage control mode, maintaining the operating limits for the voltage and frequency of the microgrid. This method of operation is as well defined as the grid-forming mode. Both centralized and decentralized control schemes of microgrid are options for the controller's control technique.

C. Mesogrid operating mode

The style of this operating mode involves a group of microgrids operating in parallel with the utility grid in a predetermined coordinated manner, each having its own local and supervisory controllers. The mesogrid, which is made up of all the microgrids, functions as a fictitious power plant that runs on orders sent to the local controllers via their supervisory control. Information is sent to each microgrid supervisory control from the mesogrid supervisory control. Additionally, the utility grid provides information to the supervisory controller of the mesogrid. Each power source operating in a microgrid has special control over and obligations toward its PCC during this control process.

1.3 Microgrid Protection

The typical distribution system has a single direction of current flow, and protective devices like relays, fuses, and circuit breakers are consistently installed across the network to identify and isolate failures. However, the complexity of the network is getting more when the distribution generator is included and integrated into a radial distribution system because the amount and direction of current flow change dramatically [22]. Additionally, as they can function both in an autonomous and grid-connected mode, DG units in microgrids need protection. Because the fault current shifts by the move to the operating mode, the protection issue grows. In a traditional distributed system, the protection strategy is built around the detection of short-circuit current and is configured to work for fault currents of large amplitudes in a radial network topology. Nonetheless, the high magnitude fault currents are absent while the microgrids are in their islanded operating mode. Additionally, the microgrid's integrated distributed sources are primarily converter interfaced, which limits its ability to feed fault current [23]. Because the overcurrent limitations in microgrids may be so low, traditional protection techniques and protective equipment may not be able to identify, operate, and isolate failures.

Furthermore, power flows in both directions, from the main grid to the load side and back again from the power source of microgrid to the utility. Therefore, the flow of power is determined by either a big power production or a significant power demand) [24]. Simply it could be stated that the strength and direction of the fault current can be altered due to the addition of micro-sources, which could cause the conventional protection technique to fail.

The production capacity, design, and placement of DG units have a significant impact on the fault current in the microgrid system. This causes a breakdown in communication between the protective devices, which in turn causes false tripping, unintended islanding, malfunctioning auto-reclosers, and a failure to identify faults [25]. As a result, creating a protection strategy is necessary for the integration of microgrids into the LV system. To develop a protection plan for the microgrid that is effectually coordinated and operated, the current protection system needs data collecting and information sharing. The following are particular of the variables to be considered when constructing the microgrid protection strategy [26]:

- Microgrid design.
- Configuration topology of a microgrid.
- A type of DG.
- The DG's location.
- The DG's power-generating capability.
- Type of communication.
- Communication links' delay time.
- Technique for data analysis and fault finding.
- Relay type.
- Fault category.
- Grounding procedure.
- The microgrid's use of smart transformers.

1.3.1 Challenges in microgrid protection

The design of its protective system is a significant technical problem that comes when the microgrids are deployed in the LV distribution system. The main issues that make microgrid protection so difficult can be summed up as follows:

A. Short-circuit level variation

Based on the operating modes of microgrid either grid-connected or islanded mode, the size of fault currents greatly varies.

B. Discrimination by device

Since the generating sources are located at the network's end in typical power systems, the fault currents get less the farther away you are from them. Discrimination is based on this variance in fault current magnitude. An island-based microgrid system with converter-interfaced power sources cannot use this tactic, though. The fault current magnitude stays constant because the inverter-based DG's fault current is further constrained by distance [27]. As a result, the zone of protection shrinks, and the standard relays are unable to safeguard the feeder lines' ends.

C. Reversed flow of power

Since the location of power sources can be on both sides of the load, the power flow in microgrids is bidirectional in each of its feeders. Additionally, the power flow reverses direction if the microgrid's local generation is greater than the regional demand. The power quality of the system tends to be compromised by the reverse power flow, which causes voltage volatility [28].

D. False tripping

When relays are activated for faults outside the protective zone, a false trip is caused. The current produced by the DG in a microgrid during any fault condition adds to the fault in a nearby feeder. As a result, the healthy feeder's protection equipment may function to cut itself off from the circuit. The term "un-necessary feeder outage" or "sympathetic tripping" can also be used to describe relay fault and tripping behaviors [29].

E. Unsynchronized reclosing

In the smart power systems, reclosers are essential to link the powered power systems together. Though, a significant protection concern occurs if the energized distributed generator is connected with the utility side without taking the synchronism between both reclosers into account. As a result, the delicate devices and DGs integrated into the power system may sustain significant damage [30].

F. Single phase connection

The microgrid contains some DGs that inject single-phase power, which throws off the three-phase current's delicate balance. As a result, stray current flows to earth because of the imbalance current passing through the neutral conductor. This needs to be under control or overloading scenarios could result [31].

G. Islanding

The fault currents are supplied by the utility and grid-connected microgrid if any abnormal condition occurs. In this case, the reclosers of utility side work to isolate the effected components and resolve transient condition. However, the fault current is kept to be delivered by the DGs in the microgrid system, damaging the system's hardware in the process. If this protective component is ignored, the fault occurrence could develop into a systemic permanent fault [32].

It should be emphasized that neither of the aforementioned problems may be investigated in the "single wire earth return" power system. This kind of power system is typically used to provide distant loads at a reasonable price using a one conductor and an earth return line [33].

1.3.2 Aspect related to the microgrid protection

Numerous solutions related to this issue have been discussed in the literature to overcome the aforementioned problems. However, the detection of an islanding occurrence is the most difficult problem with microgrid safety.

- Islanding phenomena detection

The protectional techniques in conventional power systems are created under the presumption that, in the event of any abnormal or undesirable circumstances, the parts affected by this abnormal condition will be isolated from the whole power grid. As an alternative, the integrated DG power system when a problem occurs as shown in Figure 1.2, the microgrid system's loads continue to be powered by the system's current local DG. The microgrid is referred to as being islanded in this situation, which is also referred to as an islanding scenario [34, 35]. The two sorts of islanding scenarios are intentional and unintentional islanding events. With the objective of preventing cascaded breakdowns or organizing power management, intentional islanding is planned and carried out. The control and protection of the microgrid are carefully considered when creating these scenarios. Intentional islanding enhances the system's power quality because it is a methodical process [36]. Unintentional islanding, on the other hand, is a surprising event. If its existence is not promptly discovered, it could result in system failure, present safety risks to line workers, harm end users' equipment, upset voltage and frequency stability, and complicate attempts to reopen the microgrid to the utility [37].

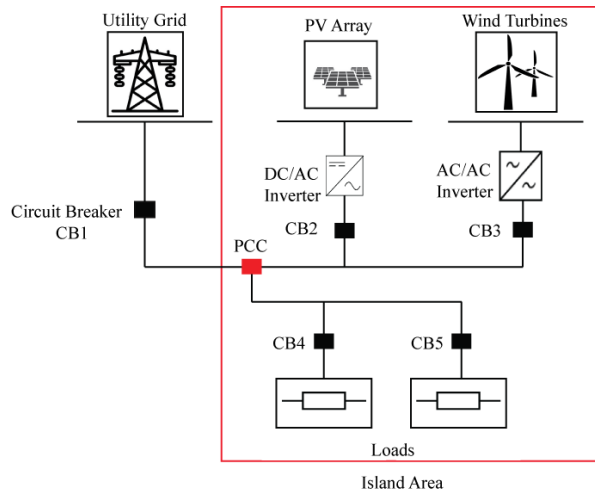


Fig. 1.2. Islanding phenomena concept

As a result, there is a clear conflict between numerous standards, including IEC 62116, IEEE 929-2002, IEEE 1547, etc., about the functioning of DG in an islanded operating mode [35],[38],[39]. However, the requirements prevent the power sources from being fully utilized in accordance with the demand of local power, which may not be financially feasible. Thus, ongoing initiatives have been yielded by the scholars to develop effective detection algorithms through paying attention to a number of technological elements which can ease microgrid operational security.

The difficulty of detecting an islanding incident is heightened by the short window of opportunity for discovery. Faster detection aids in the microgrid system's rapid stabilization. Therefore, islanding scenarios must be identified within 2 seconds, according to IEEE 1547 standards [35],[40].

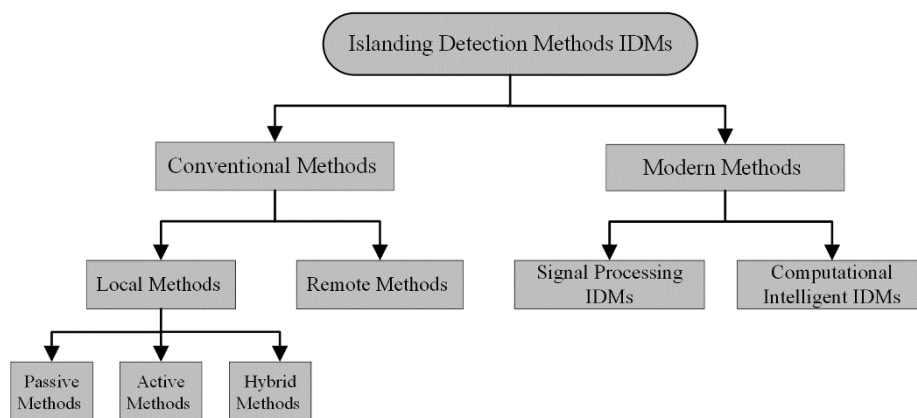


Fig. 1.3. Islanding detection methods

Numerous methodologies that depend on electrical parameters like voltage, impedance frequency, and power are presented in the literature survey on islanding detection. The four main categories into which islanding detection techniques fall are conventional and modern schemes as shown in Figure 1.3. Passive techniques work by monitoring changes and variations in the grid properties at coupling point (PCC). Different network injections are changed through active procedures, and the impact of the changes on the system parameters is then investigated. In hybrid methods, active and passive strategies are employed. The collection and sharing of data between main source and DG side forms the basis of remote approaches. The extraction of system features is the cornerstone of how signal processing-based approaches operate. Computational intelligence-based techniques operate by training the data and recognizing the pattern. Here is a basic explanation of how islanding detection techniques work.

- Passive Methods

When using passive schemes, system quantities like voltage, impedance, current, frequency, or power are monitored at coupling point. When the system operates in a normal condition, these quantities will be within acceptable ranges. However, when islanding happens, these quantities will change and rise over the permitted boundary limits. Examining and identifying these oscillations takes place using the relays utilized in the system protection to off the major circuit breakers to stop the islanding process. The procedure for passive islanding detection is given in Figure 1.4. Passive schemes include various techniques over/under frequency or voltage (O/UF, V), change rate of frequency, reactive power, active power (ROCOF, ROCOP), and etc. [41]–[43].

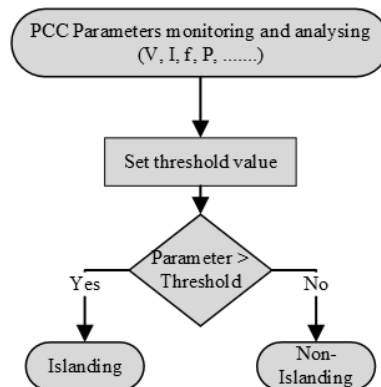


Fig. 1.4. Principle operation of passive schemes

- Active Methods

When active methods are applied, a little external disturbance signal is introduced into the DG output. The system quantities will swing and exceed the tolerable ranges because of this injection while the grid is in an islanding situation. The procedures needed for active schemes are given in Figure 1.5. Various techniques come under the umbrella of active methods such as Sandia frequency, voltage shift schemes (SFS, SVS), schemes of measuring the impedance (IM), and etc. [44]– [47].

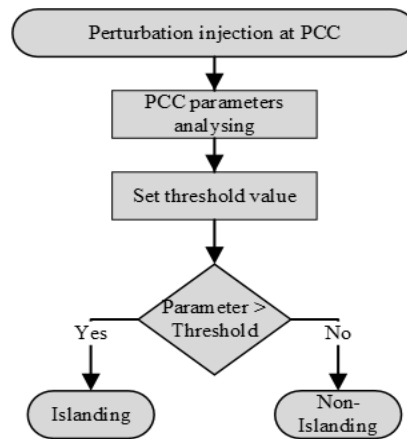


Fig. 1.5. Principle operation of active scheme

- Hybrid Methods

In order to build hybrid techniques, passive and active schemes are combined. Implementing a hybrid technique involves two steps. In the first step, the islanding is predominantly identified using a passive scheme. If the islanding is still there after the first step has been applied, an active scheme is utilized to precisely identify it. The procedures needed for hybrid islanding detection are shown in Figure 1.6. Hybrid approaches include a variety of ways, such as the imbalance of voltage level scheme, scheme of injecting voltage fluctuation, and etc. [48]-[50].

- Remote Schemes

Communication between the main source and the DG side is the main factor that remote schemes depend on. According to the assessment of the utility to the condition of circuit breakers, an islanding incident is located. The necessary tripping signal is subsequently sent, which triggers the

DG unit. Various schemes come under the umbrella of remote schemes such as scheme of inserting impedance, SCADA scheme, PLCC scheme, and etc. [51], [52].

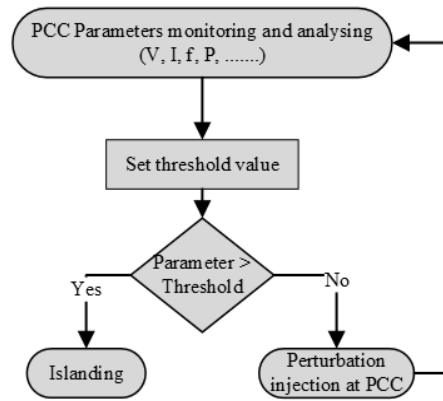


Fig. 1.6. Principle operation of hybrid scheme

- Signal Processing-based Methods

In order to reduce the NDZ of passive methods in islanding detection, signal processing techniques are used. When compared to passive methods, the merit of these schemes is the capability of extracting some important unique features from the measured waveform at the coupling point. To determine whether the system works in an islanding situation, the obtained features might be used in the second stage by an artificial intelligence classifier. The procedures required for signal processing-based islanding detection scheme are given in Figure 1.7. Many techniques come under the umbrella of this scheme such as Wavelet, Fourier transformers, etc. [53]-[54].

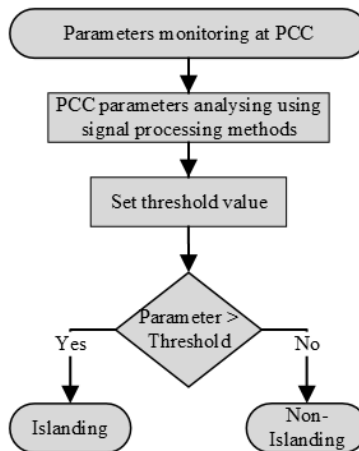


Fig. 1.7. Principle operation of signal processing scheme

- Computational Intelligent Schemes

The accuracy of the system can be enhanced by signal processing schemes especially when the DG system is more complicated. But when it comes to NDZ, signal processing schemes fail to completely eliminate the NDZ. In this case, providing more intelligence to the islanding detecting relay boosts the system performance. Multiple factors can be handled simultaneously using islanding detection techniques that use computational intelligence. With such methods, selecting threshold values is not necessary, but there has been a significant processing burden. The procedure for computationally intelligent islanding detection is shown in Figure 1.8. Artificial neural networks, fuzzy logic, decision trees, support vector machines, and other computational intelligence-based approaches are just a few examples [55]– [57].

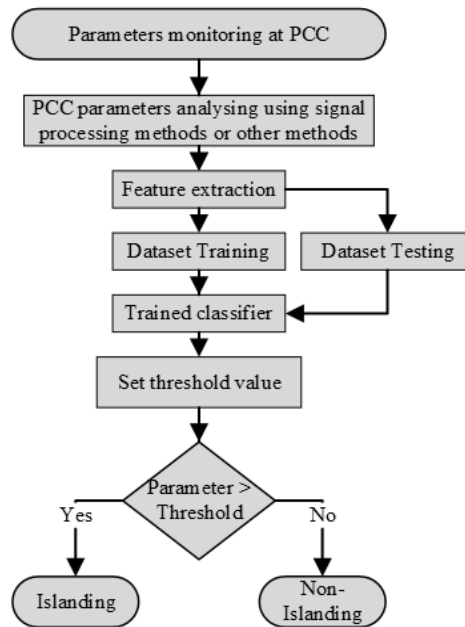


Fig. 1.8. Principle operation of computational Intelligent schemes

1.4 Research Problem Formulation

The test system taken into consideration for islanding scenario formation is presented in Figure.1.9. The system is typical to the test system for IEEE 1547's DG related standards. The following are some of the conditions for the RLC load.

- The frequencies of grid and resonant load are similar.
- The value of Q_f (load's quality factor) is equal to 2.5.

- The power produced by DG and the power absorbed by load are equal, less, or greater.

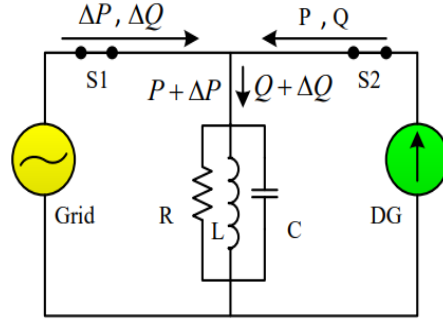


Fig. 1.9. Test system for the investigation of islanding formulation

The islanding forms when switch S1 is released, and the DG keeps supplying the power to the RLC load. During the absence of a mechanism to cause a deviation, the frequency and voltage were running at their nominal rates. The RLC load is characterized by the following.

$$R = \frac{V^2}{P} \quad (1.1)$$

$$L = \frac{V^2}{(2\pi \times f \times Q_f \times P)} \quad (1.2)$$

$$C = \frac{Q_f \times P}{(2\pi \times f \times V^2)} \quad (1.3)$$

$$f = \frac{1}{2\pi\sqrt{LC}} \quad (1.4)$$

Where R is the load resistance, C is the load capacitance, L is the load inductance, P is the active power, f is the frequency, and Q_f is the quality factor. The most horrible scenario of islanding is the scenario in which the network is operated at Unity Power Factor (UPF) and has the equal DG and RLC load power capacity as described in equations (1.1) through (1.4). The reference reactive power Q amount is determined to zero to run the circuit at UPF. The system will now operate at UPF, and the matched active power will be 100%. There is typically an imbalance between load

and generation in actual scenarios, which the grid makes up for. The grid supplies the mismatched load in a grid-connected operation. The passive parameters, such as frequency and voltage are driven to new amounts as an islanding event appears. When an islanding occurs, as seen in Figure.1.10, the new resonant frequency is given by.

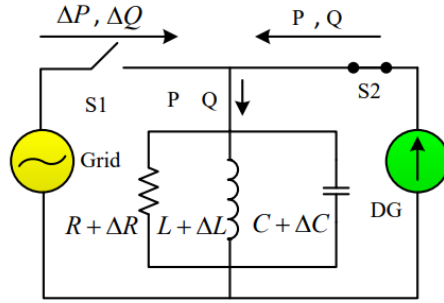


Fig. 1.10. Test system following islanding occurrence.

$$f' = \frac{1}{2\pi\sqrt{(L + \Delta L)(C + \Delta C)}} \quad (1.5)$$

Thus, the frequency change is calculated as:

$$\frac{f' - f}{f} = \frac{\frac{1}{2\pi\sqrt{(L + \Delta L)(C + \Delta C)}} - \frac{1}{2\pi\sqrt{LC}}}{\frac{1}{2\pi\sqrt{LC}}} \quad (1.6)$$

$$\frac{f' - f}{f} = \frac{\sqrt{LC}}{\sqrt{(L + \Delta L)(C + \Delta C)}} - 1 \quad (1.7)$$

For permissible lower and upper threshold values of frequency, the following requirement should be upheld:

$$\frac{f_{min} - f}{f} \leq \frac{\sqrt{LC}}{\sqrt{(L + \Delta L)(C + \Delta C)}} - 1 \leq \frac{f_{max} - f}{f} \quad (1.8)$$

Eq. (1.8) can be changed to (1.9) in the worst case of islanding $\Delta L \times \Delta C = 0$.

$$\left(\frac{f}{f_{max}}\right)^2 - 1 \leq \frac{\Delta L}{L} + \frac{\Delta C}{C} \leq \left(\frac{f}{f_{min}}\right)^2 - 1 \quad (1.9)$$

The relationship between the ΔL , ΔC and can be calculated as:

$$\Delta Q = V^2 \left(\frac{1}{2\pi f(L + \Delta L)} - 2\pi f(C + \Delta C) \right) \quad (1.10)$$

$$\Delta Q = V^2 \left(\frac{1}{2\pi fL\left(\frac{1 + \Delta L}{L}\right)} - 2\pi fC\left(\frac{1 + \Delta C}{C}\right) \right) \quad (1.11)$$

$$\Delta Q = \frac{Q_L}{\frac{1 + \Delta L}{L}} - Q_C \left(\frac{1 + \Delta C}{C} \right)$$

$$Q_L = Q_C = Q_f \times P$$

Thus, ΔQ is normalized as following:

$$\frac{\Delta Q}{P} = \frac{Q_f}{\left(\frac{1 + \Delta L}{L}\right)} - Q_C \left(\frac{1 + \Delta C}{C} \right)$$

$$\frac{\Delta Q}{P} = Q_f \times \frac{1 - \left(\frac{1 + \Delta L}{L}\right)\left(\frac{1 + \Delta C}{C}\right)}{\left(\frac{1 + \Delta L}{L}\right)}$$

$$\frac{\Delta Q}{P} = Q_f \times \frac{1 - \left(\frac{1 + \Delta L}{L}\right)\left(\frac{1 + \Delta C}{C}\right)}{\left(\frac{1 + \Delta L}{L}\right)}$$

$$\frac{\Delta Q}{P} \approx Q_f \times \frac{\frac{-\Delta L}{L} - \frac{\Delta C}{C}}{\left(\frac{1 + \Delta L}{L}\right)} \approx -Q_f \left(\frac{\Delta L}{L} + \frac{\Delta C}{C}\right) \quad (1.12)$$

Consider the following two approximations:

$$\Delta L \times \Delta C = 0$$

$$\frac{1 + \Delta L}{L} = 1$$

Using (1.9) and (1.12),

$$Q_f \left(1 - \left(\frac{f}{f_{min}}\right)^2\right) \leq \frac{\Delta Q}{P} \leq Q_f \left(1 - \left(\frac{f}{f_{max}}\right)^2\right) \quad (1.13)$$

The link between voltage and active power can be obtained in exactly the same way demonstrated below.

Prior to islanding, the value of active power is provided by $P = \frac{V^2}{R}$

Upon islanding, it is provided by $P = \frac{V^2}{(R + \Delta R)}$

Since the system is functioning under current control mode, the active power balancing is:

$$\frac{V^2}{(R + \Delta R)} = \frac{(V + \Delta V)^2}{R + \Delta R} = \frac{V^2}{R}$$

$$\frac{\Delta R}{R} = 2 \frac{\Delta V}{V} + \left(\frac{\Delta V}{V}\right)^2 \quad (1.14)$$

The RLC load consumed ΔP which is delivered by the network before islanding is:

$$\Delta P = \frac{V^2}{R + \Delta R} - \frac{V^2}{R}$$

Given thru the normalization of ΔP is:

$$\frac{\Delta P}{P} = \frac{\frac{V^2}{R + \Delta R} - \frac{V^2}{R}}{\frac{V^2}{R}} = \frac{-\Delta R}{R + \Delta R} = -\frac{\frac{\Delta R}{R}}{\frac{\Delta R}{R} + 1} \quad (1.15)$$

Equation (1.14) being substituted for (1.15):

$$\frac{\Delta P}{P} = \frac{2 \frac{\Delta V}{V} + \left(\frac{\Delta V}{V}\right)^2}{2 \frac{\Delta V}{V} + \left(\frac{\Delta V}{V}\right)^2 + 1} = \frac{1}{\left(\frac{\Delta V}{V} + 1\right)^2} - 1 \quad (1.16)$$

The highest and lowest rates of voltages are provided in compliance with IEEE guidelines. The formula (1.16) can be changed to:

$$\left(\frac{V}{V_{max}}\right)^2 - 1 \leq \frac{\Delta P}{P} \leq \left(\frac{V}{V_{min}}\right)^2 - 1 \quad (1.17)$$

when the rates of maximal and minimal voltage, maximal and minimal frequency, and quality factor are provided as 110%, 88%, 51 Hz, 49 Hz, and 2.5 from equations (1.13) and (1.17), they are adjusted as follows:

$$-17.36\% \leq \frac{\Delta P}{P} \leq 29.13\%$$

$$-10.3\% \leq \frac{\Delta Q}{P} \leq 9.71\%$$

According to mathematical modeling, there are no variances in the measured parameters during grid-connected operation. Many parameters are changed to new levels after islanding. These variations allow the islanding to be verified.

1.5 Objective of Research Work

- The primary goal of the research is to develop an effective islanding detection technique that offers quick and accurate results.
- Aims to give an in-depth overview of the majority of islanding detection techniques currently in use in literature, conventional and modern techniques.
- To provide a comprehensive analysis of islanding detection problem by studying the islanding phenomenon classification and detection to propose a better approach that is compared with the existing islanding detection techniques.
- To provide a fault analysis of microgrid integrated with DGs by examining three different real-time microgrid systems consisting of different types of DGs such as PV system, wind turbine, and synchronous generator according to IEEE standards.
- To use a decision-making approach namely the analytical hierarchy process (AHP) to assess and analyze islanding detection techniques based on various criteria such as the response time, and non-detected zone to compare between those methods based on the selected criterion.
- To design an advanced signal processing approach based on phasor measurement estimation to be used for the features extraction of the faulty voltage signal specifically the voltage amplitude, the frequency, and the rate change of frequency. Also, to design an artificial intelligence detector (artificial neural network) combined with the PMU approach to classify the islanding incidents according to the obtained features of the faulty voltage signal with more accuracy and less detection time.
- To provide an evaluation of the proposed method's performance with other artificial intelligence techniques such as Naïve bayes, GLM logistic regression, and LD in order to assess each method's validity.

1.6 Thesis Layout

- Chapter 2 presents the review of the literature based on my own research.
- Chapter 3 presents a decision-making-based assessment of islanding detection techniques.
- Chapter 4 presents feature selection and extraction in detail for multiple DG system islanding detection.

- Chapter 5 presents an overview of various classifiers that may be used to quickly and precisely detect islanding based on the type of inverters allied to the system and features extracted.
- Chapter 6 provides all of the work's results and discussions.
- Chapter 7 presents the conclusion and future scope of the work.

2. Literature Review

2.1 Background

For electrical power systems to operate normally, there must be no interruptions or distortions in the power supply to the end consumers. However, this normal operation is challenging to achieve due to several issues, including malfunctions and switching events in a useful power setup. Such unusual circumstances and occurrences must be acknowledged and categorized for different objectives, like prevention, maintaining, and assessment objectives.

Due to several economic and environmental concerns, more renewable energy resources are increasingly incorporated in recent power systems. A power electronic interference is used to link the distribution generators such as PV inverters, synchronous generators, and wind turbines with the main utility side to establish a smart distribution network in which the power is not flowing unidirectionally because the power is produced and fed back to the grid. Integration of DG into the primary grid has numerous advantages, including expanded network throughput, reduced power losses, higher power quality, and reduced gas emissions. Conversely, this merging may result in different concerns related to system operation that affect the stability and dependability of the system, such as problems with reverse power flow and islanding.

To expand the capability to supply less expensive, environmentally friendly, and reliable power supplies, the electrical power system must be upgraded by utilizing various solutions that facilitate the integration of distributed generation (DG) with the actions of end users.

The islanding phenomena occurs after the main grid is severed from the DG, but the end users keep receiving power. In this instance, the phenomena must be detected while utility-controlled generation is not present to stop supplying power to the system. Alternatively, if the generation in the islanding zone is effective at frequency and voltage rates above the normal, the apparatus may be dented, and employees who mistakenly believe the wires are not powered may experience a shock hazard from the energized lines.

Islanding can happen either intentionally or unintentionally as presented in Figure 2.1. When intentional islanding occurs, the variation of network parameters will be handled, and the fluctuation of frequency and voltage is monitored by the control scheme of the distribution

generator. Conversely, when unintentional islanding occurs, the variation of parameters will not be easily handled and monitored which causes increasing the parameters rating above the boundary limits, therefore a switching scheme is required to detect this abnormal condition and shut down the whole system accordingly. The following are the main reasons why the electricity system can become islanded.

- A grid failure that causes the CB to open and that the protection devices and inverter are unable to detect.
- Unexpected CB opening brought on by short circuit issues and system failure.
- Unexpected changes to the load switching and network switching.
- Intentional CB opening for grid-side or distribution-level maintenance.
- Human mistakes and environmental acts.

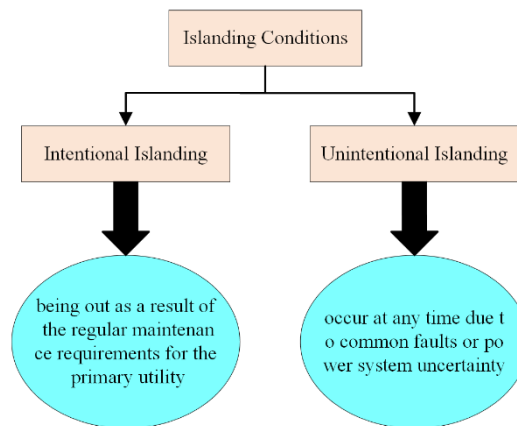


Fig. 2.1. Types of islanding condition

The creation of islands in the power system has a few causes. Safety and providing consumers with high-quality power are two key variables. Customers trust the quality of power, yet they must install an anti-islanding mechanism inside their DG inverters because of the reasons mentioned below.

- The load cannot keep up with the increased voltage that the client equipment receives when the DG system is islanding.
- The customer's equipment and occasionally DG are damaged by the voltage and frequency being outside of standards.

- Since grid customers and field employees are unaware that DG supplies power to the islanding area, they are in danger.
- Because the grid synchronization parameters are not synchronized, automatic recoupling the DG with the main grid could cause harm to the DG and loads.

Many islanding detection methods have been developed and implemented proposed. The approaches proposed to identify islanding remain have numerous drawbacks and limitations, including the inability to identify islanding especially once a non-detected zone (NDZ) is existing, issues pertaining to the reliability of the network and the quality of power, incorrect operation as there is numerous DG, the need to install extra hardware or circuits, and high implementation costs. Further investigation and improvement of strategies for detecting islanding is required to overcome such limitations and drawbacks [58].

The main objective of this chapter is to review the extensive use of the schemes used to identify the islanding incident in DG grid-connected networks. The fundamentals of every islanding approach will be discussed. Additionally, a comparison of the benefits and drawbacks of each strategy is made. A conclusion is offered later. This chapter highlights and discusses the schemes of islanding detection that were not extensively covered in detail by prior studies, giving researchers and experts who want to learn the most recent information about islanding detection methods a more solid background than other recent reviews do. Additionally, additional factors that have not been covered in other publications but that influence the selection of is-landing detection methods include dependability and sensitivity to cyber-attacks.

2.2 Schemes of Islanding Detection

Numerous classifications for islanding detection approaches, including both conventional and modern strategies are described below. Following is a description of each method:

2.2.1 Passive Methods

Measurements of system quantities such as frequency, voltage, or impedance at the coupling point (PCC) are essential to the fundamental function of passive methods. Significant fluctuations of such parameters that surpass the permitted threshold values are seen when islanding occurs. Protective relays keep an eye on the variations and, if necessary, the major circuit breaker is turned

on. A variety of schemes come under the umbrella of passive scheme as presented in Figure 2.2. The following provides in-depth explanations of passive strategies:

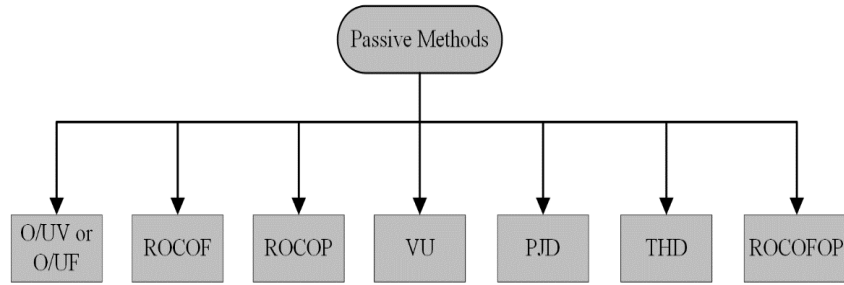


Fig. 2.2. Passive methods

2.2.1.1 Over under Voltage/Frequency Scheme (O/UV, F)

Using this scheme, the conventional protective relays which are linked to the power system operate to find out any abnormal situations that may appear during the operation of the primary utility network. The DG side inverters are prevented from delivering any power to the connected load via the triggering of the protective relays which sense any variations of the network parameters amplitudes. The disparity of active and reactive power between the DG inverter and load can greatly affect the response of the utility network during the disconnection and before the switch opens to establish the islanded part. To prevent islanding, a voltage amount shift will be observed and identified if there is a positive differential in active power (ΔP) between the DG inverter and load. If there is a non-zero difference in reactive power (ΔQ), the inverter will be turned off. This is because it would cause a load voltage phase shift and a divergence from the frequency of the inverter current [59].

$$\Delta P = P_{Load} - P_{DG} \quad (2.1)$$

$$\Delta Q = Q_{Load} - Q_{DG} \quad (2.2)$$

Because both voltage and frequency are considered, such techniques are straightforward and economical. If there is a distinct power imbalance, this scheme can be applicable. Therefore, the surpass of system parameters will cause the network to function as an islanding mode within a time range of 4 ms to 2s [60,61].

2.2.1.2 Scheme of Frequency Rate of Change (ROCOF)

Using this scheme, the frequency rate of change (df/dt) is monitored and compared with the allowed boundary limits during the abnormal condition using a phase-locked loop (PLL) for a certain period of time to ensure that the frequency relays do not take too long to trip [62,63]. The frequency rate of change can be calculated using the following formula:

$$\frac{df}{dt}(k) = \frac{f(t_k) - f(t_k - \Delta t)}{\Delta t} \quad (2.3)$$

The frequency is $f(t_k)$ at the k^{th} time sample and the measured value of frequency Δt prior to the k^{th} segment time is called $f(t_k - \Delta t)$ i.e. $t_k - \Delta t$. Particularly Whenever there's a significant disparity in power across the load and DG sides, this approach is very trustworthy and efficient. This method, however, fails to distinguish between frequency changes brought on by islanding and load variations since it is very vulnerable to load variations. As a result, it may be a suitable approach for loads with little fluctuations [63].

2.2.1.3 Active and Reactive Power Rate of Change Scheme (ROCOP)

Using this scheme, the power rate of change (dP/dt) is monitored and measured over a defined time interval, as load fluctuations are likely to happen during grid disturbances. This change (dP/dt) during the abnormal situations is significantly greater than its measurement prior to islanding. Therefore, during the deactivation of the main grid it is measured for some sample cycles to be compared with the boundary limit, and if it is greater than the permitted limits, a decision is made to cease supplying power to the consumers [64].

The speed of this scheme to recognize the problem is not impacted by the disparity of power between the DG and load sides. Likewise, it is possible that the unsynchronized reconnection of the power supply to the distribution generator is promptly detected in order to guarantee the solidity of the power network's functioning. The technique still exhibits non-detected zone (NDZ), even if there is not any power disparity between the inverter and the load. Nevertheless, while the power disparity intensifies, this scheme will excel in identifying the islanding circumstances.

2.2.1.4 Unbalanced Voltage Scheme (VU)

In this scheme, the voltage of each phase at the coupling point is utilized to accurately identify the occurrence of islanding. The loss of the major utility source will lead to a voltage imbalance of the DG output. When the voltage disparity is greater than the preassemble boundary limits, the islanding process will be chosen. The voltage imbalance (V_{ut}) is determined as the discrepancy among the voltages of the negative and positive sequences, as shown below [65].

$$V_{ut} = \frac{N_{st}}{P_{st}} \quad (2.4)$$

This approach does not depend on system fluctuations and has a minimal detection error. The NDZ, however, is rather large [66].

2.2.1.5 Scheme of Phase Jump Detection (PJD)

In order to use this technique, you must monitor the phase shift among the current and voltage coming from the DG inverter through a sudden phase jump. Under islanding conditions, due to the phase shift the current of the inverter remains constant, while the voltage will vary in direction which is identified using an adjusted PLL. Hence, the voltage path alternation will raise the phase discrepancy leading to the disconnection of the inverter if the voltage surges over the allowable threshold [67].

Using this approach, the power quality is not impacted negatively, also this scheme is simple to use and has quick detection time. The detection window is between 10 and 20 ms [68]. However, the load switching in this method makes it difficult to determine the threshold, which could lead to certain inaccuracies in the islanding distinguishing.

2.2.1.6 Scheme of Total Harmonic Distortion (THD)

The assessment of total harmonic distortion at the coupling point is the main factor that this scheme depends on. During the normal condition, the impedance of the network will be low, therefore the produced inverter harmonics will be small with no big effect or distortion on the coupling point. But, during the abnormal condition this produced harmonics may be big and may lead to have a significant harmonics distortion at the coupling point. The surpass of this harmonic distortion is

compared with the specific threshold value to determine if the system is under islanding or not [69].

The simplicity of implementing and functioning this scheme even when there are multiple DGs connected to the network is a plus. Establishing the limit values, though, poses a challenge due to the potential for error detection caused by any disruption in the grid.

2.2.1.7 Frequency over Power Rate of Change Scheme (ROCOFOP)

Using this scheme, the islanding is identified by computing the derivative of the frequency with respect to the load power (df/dp). The (df/dp) is more responsive than (df/dt) if there is only a slight power disparity among the load and the inverter. This scheme is effective when there is a minimal power disparity between the load and the inverter [70].

2.2.2 Active Schemes

Modifying the DG inverter output by introducing an external small disturbance waveform is the primary objective of active schemes. During the abnormal condition, the system parameters will be modified by this injection. When the power difference between the DG inverter and load is zero, these schemes identify the islanding incidents effectively compared to passive schemes which are not capable of performing the detection in such cases. Nevertheless, the network may experience issues related to harmonic distortion and power quality when employing these solutions. The phrase "active methods" encompasses a range of strategies, as seen in Figure 2.3. Here is a concise explanation of active approaches.

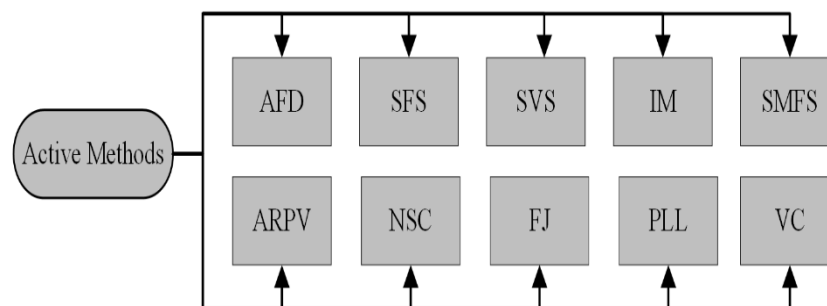


Fig. 2.3. Active methods

2.2.2.1 Scheme of Active Frequency Drift (AFD)

In this scheme, by the use of the DG inverter a slightly altered electric current signal is injected at the coupling point. During the normal condition, the network is stable due to the inverter output voltage and current stay fixed. However, during the abnormal condition the voltage amplitude passes through zero because of the signal injection carried out which led to boost the phase error among the DG current and output voltage. The boosted phase error is then reduced by measuring the inverter frequency drift. The islanding state is identified once the frequency reaches the threshold rate and then deviates again [71].

The following equation defines the inverter altered current signal as the chopping fraction:

$$CF = \frac{2t_z}{T_{vutil}} \quad (2.5)$$

Where the variable t_z represents the dead time, while T_{vutil} represents the voltage across the period.

The main benefits of this approach are its ease of usage and low NDZ. When there are numerous inverters present, this method might not be competent to distinguish islanding due to variations in frequency bias, different inverters exhibit unique characteristics. This kind of load has a big impact on how effective this method is as well. The duration of detection and NDZ will experience an increase especially when the connected loads are not purely resistive. Therefore, in systems connected to only one inverter and resistive loads, this method performs well for islanding detection.

2.2.2.2 Scheme of Sandia Frequency Shift (SFS)

Using this scheme the frequency of voltage inverter is modulated using positive feed-back that's why it is thought as an expansion of the AFD scheme [72]. The DG phase angle error is introduced when islanding occurs, and this error remains until it surpasses the cutoff point. In this method, the choice of parameters, such as the accelerating gain (k) and the chopping frequency (Cf_o), determines how effective the islanding detection is. The SFS parameters are as follows:

$$\theta_{inv} = \pi(Cf_o + k(f - f_n)) \quad (2.6)$$

where Cf_o and k are the SFS parameters, f is the islanding frequency, f_n is the nominal frequency, and ϕ_{inv} is the inverter phase angle.

This technique can identify islanding in less than six cycles [73]. In contrast to alternative active strategies, this one has the most minimal NDZ. Additionally, this scheme effectively lessens the influence of sudden reactions in the system while detecting power quality and efficiency.

2.2.2.3 Scheme of Sandia Voltage Shift (SVS)

The core principle of this strategy is akin to that of the previous scheme, which hinges on amplifying the constructive response to the voltage at the coupling point. During the normal condition, no visible alterations occur. However, during the abnormal condition, a voltage change occurs. This shift is then detected and amplified by the positive feedback mechanism, outside the limit rate. As a result, the O/UV relay is activated, causing the system to shut down [74].

With this simple method, the NDZ is little. But the quality of the power could be compromised by this technology.

2.2.2.4 Scheme of Impedance Measurement (IM)

Using this scheme, the abnormal condition can be identified by the voltage shift those results from current perturbation and the impedance alteration of the DG output induced by the failure of the main power supply. To track this shift and identify islanding, the inverter's measured impedance is calculated as dv/di . When detecting a single DG source, this method's NDZ is minimal; however, when detecting several inverters, its efficacy may decrease. Furthermore, because it is essential to determine the exact amplitude of system impedance, it is difficult to set the impedance threshold value [75].

2.2.2.5 Scheme of Slip Mode Frequency Shift (SMFS)

Using this scheme, affirmative feedback is delivered to disrupt the voltage phase of the DG inverter, and thereafter the deviation of frequency is measured to distinguish the islanding incident [76]. The following formula presents the phase angle of the inverter current and voltage which changes in a sinusoidal manner with frequency.

$$\theta_{SMFS} = \theta_m \sin \left[\left(\frac{\pi}{2} \right) \left(\frac{f^{k-1} - f_n}{f_m - f_n} \right) \right] \quad (2.7)$$

θ_m represents the highest phase angle at the frequency f_m , f_n denotes the nominal frequency, and f^{k-1} refers to the frequency of the previous cycle.

During the normal condition, the inverter of the distribution generation side operates at zero phase angle frequency. Conversely, during the absence of the utility grid the phase angle error will increase due to the fluctuation of both inverter frequency and voltage. As a result, the inverter will encounter challenges in operation at its nominal frequency, and the uncertainty that causes the system to function either above or below the frequency range will intensify the frequency disturbance.

When compared to other active approaches, the SMFS has a lower NDZ and is easier to apply. Moreover, this method's effectiveness is excellent when dealing with several inverter systems. Conversely, the application of SMFS may result in a reduction in the power quality of the network and may affect the transient network reliability.

2.2.2.6 Scheme of Active and Reactive Power Variation (ARPV)

This approach detects islanding by monitoring variations in voltage amplitude and frequency while adjusting the injected inverter power. During the absence of the utility source, the load absorbs the active power produced by the inverter. In order to reach a full active power equilibrium among the inverter and load the voltage alteration must satisfy the subsequent equation:

$$P_{DG} = P_{Load} = \frac{V^2}{R} \quad (2.8)$$

Therefore, if the voltage change is greater than the threshold value, islanding will be detected. Once the frequency is beyond the limits the islanding incident is present because the disruption in reactive power affects the change in frequency [77].

The NDZ remains small, and this method's implementation is straightforward. Nevertheless, the power quality and transient stability of the system may be impacted by using this strategy.

Furthermore, this strategy becomes less successful in systems with various parallel connected inverters.

2.2.2.7 Scheme of Negative Sequence of Injected Current (NSC)

To monitor the negative sequence voltage at the coupling point and identify the abnormal incident, this method entails introducing a negative sequence current into the system. During the normal condition, the offered impedance by the injected sequence current is small, that's why the voltage at coupling point will not alter. Conversely, during the abnormal condition, the negative current that is injected will head towards the load, causing an imbalanced voltage at the coupling point. The defined criteria will be followed in order to detect islanding if this voltage surpasses the threshold [78]. This approach is not used to display NDZ, and the load change has no effect on the effectiveness of NSC.

2.2.2.8 Scheme of Frequency Jump (FJ)

The possession of specific dead zones within the disrupting current signal is the common thing between this scheme and AFD. These dead zones are inserted into the system for each of the three cycles of the inverter output current signal. Under normal circumstances, the voltage frequency remains constant; nevertheless, it will change during the abnormal condition. This method is thought to be an enhanced variant of the scheme of active frequency drift. FJ may fail to recognize the islanding incident, though, if there are many inverters equipped with the system [79].

2.2.2.9 Scheme of Perturbation of Phase-Locked Loop (PLL)

This method depends on creating a changed current reference angle by adding the second harmonic components to the reference current of the DG inverter. During the normal condition, the voltage is stabilized by the main network, preventing any appreciable variations in the generated current. However, a dispute in the voltage at the coupling point is identified, then consequently, the islanding incident can be adequately diagnosed, during the loss of the main grid as the result of the inclusion of second harmonic elements [80].

PLLs of several kinds are applied to be utilized for the identification of islanding incidents. Certain approaches entail adjusting the PLL in order to continuously change the stable equilibrium point, while extra techniques require altering the PLL small-signal's properties in order to achieve a monotonic instability performance under islanding conditions. Because the stiff grid may isolate

the feed-forward loop's influence and ensure the PLL's stability in grid-tied situations, The PLL, which has been updated to include a small-signal feedforward loop, is showing promising results [81].

This method's modest NDZ and low detection error rate allow it to be used in systems with multiple parallel-connected inverters. During normal conditions, this scheme might, nevertheless, produce a minor disturbance in comparison to other active ways.

2.2.2.10 Scheme of Virtual Capacitor or Inductor (VC)

The DG inverter functions as a virtual inductor or capacitor in this way by employing frequency amplitudes that are lower or higher than the rated frequency. Hence, once the main grid is unplugged, the frequency and voltage of load will vary due to this virtualization even while generation and consumption are balanced. Although this approach can quickly identify islanding, the quality of the electricity may be compromised [82, 83].

2.2.3 Hybrid Methods

Active procedures aim to minimize the potential negative detection zone (NDZ) that may occur when using passive methods. This, in turn, increases the accuracy of islanding detections. On the other hand, active techniques will cause problems with system power quality since disturbance signals would gradually enter the system. To address these problems, hybrid systems are developed by amalgamating the benefits of both active and passive schemes. Various techniques come under the umbrella of hybrid methods as presented in Figure 2.4. A description of hybrid islanding strategies follows.

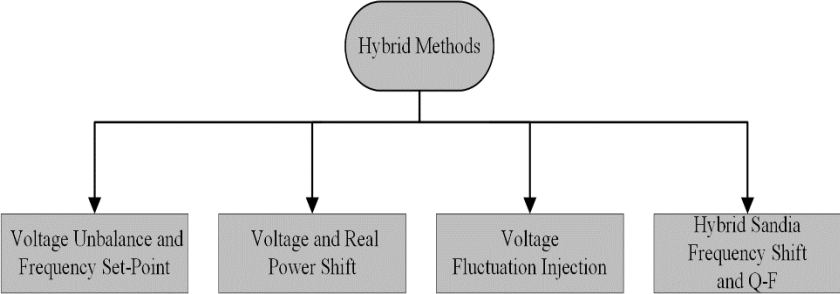


Fig. 2.4. Hybrid methods

2.2.3.1 Scheme of Unbalanced Voltage and Frequency Set-Point

Positive feedback is employed as an active strategy, while voltage imbalance is utilized as a passive approach in the design of this scheme. Monitoring the output voltages of the inverter is a standard procedure for determining voltage imbalance. DGs experience disruptions and an increase in voltage imbalance with each event. If the jump is higher than the predetermined thresholds, islanding will be called. This method can be used to differentiate between conditions that result in islanding and load-switching [84].

2.2.3.2 Scheme of Shifted Voltage and Real Power

Using this scheme, the passive element is represented by the average rate of voltage change, whereas the active element is represented by the shifted real power. Islanding is detected at the side of the distributed generators (DGs) where the voltage signal is continuously monitored, when the average rate of voltage change is consistently positive for more than five cycles. However, it is unable to detect islanding if the disruption lasts for less than five cycles. The true power transfer method can be quite effective [85].

2.2.3.3 Scheme of Injected Voltage Fluctuation

Using this scheme, the rates of voltage and frequency change are combined to identify islanding incidents. Initially, the detection of islanding is achieved by monitoring the frequency and voltage change rate of the PCC. If one of the DGs surpasses the threshold value, the others will trip. In the second step of verification, a high-impedance load that switches on and off repeatedly is employed to create a voltage perturbation. The utility side mitigates the coupling point voltage disturbance occurred due to the switching of high-impedance load when they are attached. On the other hand, islanding is detected by tracking the effect of the periodic perturbation at the PCC voltage when the primary grid connection is severed. The detection time of this scheme is not influenced by the quality factor which is less than 0.216 s. However, in large DG units, its effectiveness is reduced [75].

2.2.3.4 Scheme of Hybrid Sandia Frequency Shift and Q-F

To reduce NDZ, a Q-f droop curve is added to the Sandia Frequency technique, as the ideal gain, k_f , depends on the load quality factor. Whenever the value of quality factor exceeds five, this gain value could be excessive, which could result in inaccurate detection and unstable systems. Once connected, reactive electricity is controlled by the main grid. During abnormal conditions, the

inverter runs at unity power factor and does not create any reactive power, therefore a frequency disruption arises between the actual and nominal network frequencies. This technique monitors the variation in frequency to sense islanding, using a detection interval of 1.4 seconds [86].

2.2.4 Remote Schemes

Using this scheme, the inverter and main power supply are communicated with each other to identify any abnormal conditions. The main advantage of implementing this scheme is that the power quality is maintained plus there is no NDZ. But still, this approach is regarded as a relatively costly and sophisticated one. Various approaches come under the umbrella of this scheme as presented in Figure 2.5. The techniques for detecting islanding are listed below.

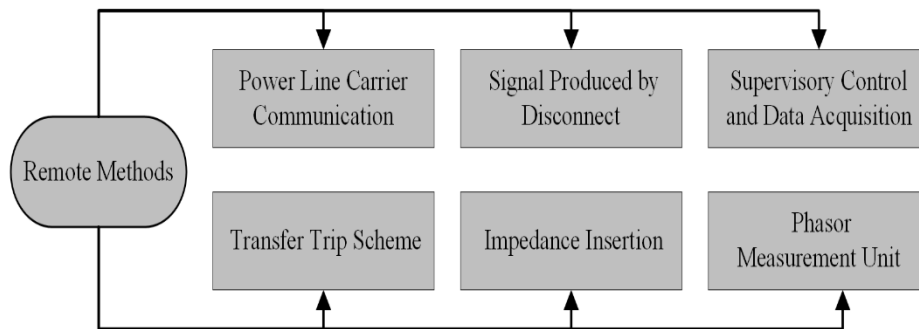


Fig. 2.5. Remote methods

2.2.4.1 Scheme of Power Line Carrier Communication (PLCC)

Using this scheme, a power line and transmission signal are both emitted by a transmitter situated on the grid side. The receiver is additionally configured on the DG side. Once the main grid is connected, the receiver receives a low-energy signal. When the microgrid is in the islanding state, the PLCC signal will be interrupted, directing that the system faces abnormal condition [78].

Applying this scheme is devoid of any adverse consequences on the grid transient response, no NDZ, and no degradation of power quality. Furthermore, this strategy works quite well when applied to several inverter systems. However, this approach is costly commercially, particularly for low-power ratings DG systems. As a result, can be employed with high-power ratings DG systems in microgrids.

2.2.4.2 Scheme of Signal Produced by Disconnect (SPD)

Using this scheme, the abnormal condition is recognized by analyzing the transmission signal among the main supply and the inverters. Although this scheme is similar to PLCC scheme but here the transmission signal utilizes alternative forms such phone lines or microwave. Such an approach fully controls the DG as well as the main grid, and it lacks an NDZ. Nevertheless, the cost is high, and the design is intricate [87].

2.2.4.3 Scheme of Supervisory Control and Data Acquisition (SCADA)

Using this scheme, the auxiliary contacts of main relays are monitored to identify any abnormal condition in the network. The SCADA system will send tripping signals to the associated circuit breakers to be unplugged in the event of islanding [88]. Although this technology is quite good in detecting islanding, it is not thought to be appropriate for small-scale systems due to its high cost and requirement for several instruments, tools, mechanisms, and communication channels in multiple inverter grids. Furthermore, this method's detection speed may be poor in the event of system disturbances.

2.2.4.4 Transfer Trip Scheme

With the use of this scheme, a central control unit oversees and links all relays in the isolated area to distributed generator side. The transfer trip mechanisms identify the islanded components when the main grid is disconnected and thereafter transmit the required signal to trip the circuit breaker of the distributed generator [89]. Full communication support is necessary for this technology, and common media utilized include radio, leased telephone lines, and contemporary forms of communication like satellite, wireless networking, and Ethernet optical fiber. For this reason, the primary drawback of this approach is the complexity of the design. Nonetheless, this approach has a very high efficacy with a small NDZ and quick islanding identification.

2.2.4.5 Impedance Insertion Method

This technique entails adding a low-value impedance or capacitor bank to the utility grid [67]. The unbalanced reactive power deviates from the equilibrium between generation and consumption. Both voltage and frequency can be changed at the coupling point, then frequency relays are used on the side of main supply to measure changes in frequency. This method is effective and has a

quick reaction time to detect islanding. Despite being expensive, this solution does not meet some standards since installing the capacitor bank after severing the connection of main grid takes too long. Nonetheless, this approach has a very high efficacy with a small NDZ and quick islanding identification.

2.2.4.6 Scheme of Phasor Measurement Unit

Using this scheme, a time broadcast or conventional coding like GPS is used by a local clock to obtain a time synchronization source. This method is employed to control the amplitude and phase angle of voltage or current phasor. Two units are utilized, with one positioned adjacent to the main supply and the other located alongside the DGs. Additionally, it is time-stamped before being sent to the recipient. In this manner, DG synchronization with the grid can be easily ascertained [90, 91].

2.2.5 Scheme of Signal Processing

The implementation of this scheme is to minimize the non-detected zones that passive schemes fail to identify during the islanding incident. These techniques are thought to have an additional advantage by obtaining some unique feature of the assessed signals at the coupling point (frequency, voltage, and current). in contrast to passive techniques. The final traits can then be used as an input for a method of classification using machine learning, artificial intelligence, or any other methods to determine whether the system is under abnormal condition or not [92]. Various approaches come under the umbrella of this scheme as presented in Figure 2.6. Below is a discussion and presentation of signal processing techniques.

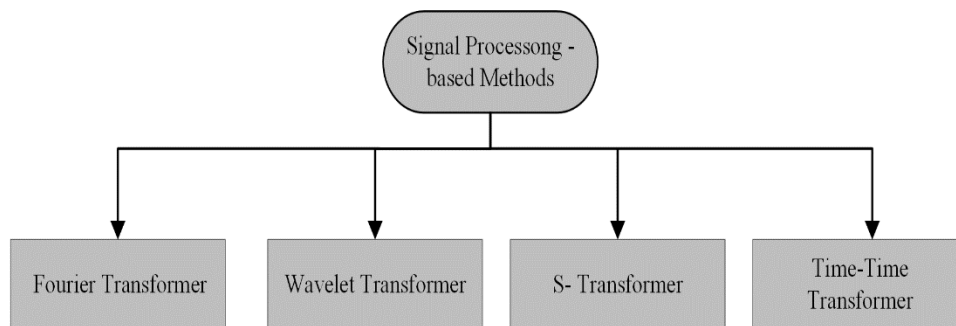


Fig. 2.6. Signal processing-based methods

2.2.5.1 Scheme of Fourier Transformer

Using this scheme, utilizing the frequency domain some required features of certain levels of the frequency signal are extracted. Short-time Fourier transform, and discrete Fourier transform are examples of this scheme which are employed to provide efficient and fast islanding detection strategies. However, sparse spectrum estimation and low-frequency resolution are this method's main shortcomings [93].

2.2.5.2 Scheme of Wavelet Transformer

Such method extracts the properties of distorted voltage, frequency, or current using a wavelet transformer. The abnormal condition is observed once the wavelet coefficient of the recorded signal exceeds the specified value. The low-frequency band restriction, the challenging limit rate choice, Various sampling frequencies impact, and the mother wavelet choice on the transformer are some of disadvantages of this approach. The d-q axis of three-phase complex power is utilized to evaluate high-frequency elements using wavelet packet transformer [94, 95]. There are two types of wavelet transformers in the wavelet transformer method: discrete and continuous.

2.2.5.3 Scheme of S- Transformer

Using this scheme, the time-domain function is transformed to a 2D frequency-domain function. The obtained voltage or current data at the coupling point is utilized to construct the S-matrix and associated time-frequency contours. The spectral energy content of time-frequency contours, which account for both magnitude and frequency irregularities, is computed to observe the abnormal incident [96]. This method's primary disadvantage is that it requires more computer resources and takes longer to process than other approaches.

2.2.5.4 Time-Time Transformer Method

Using this scheme, a time-time distribution inside a specific frame is provided to convert 1D time-domain signal to a 2D time-domain signal. Thus, the distribution of low-high frequency elements is uneven. Such a scheme is effective even when dealing with signals that contain noise because it provides a perspective of the signal that is specific to a certain time period, achieved through the use of a scaled window [93].

2.2.5.5 Miscellaneous Signal Processing Based Methods

The autocorrelation function method uses constrained summation restrictions to retrieve information from the power or energy signals. Using The Kalman filter approach, harmonic characteristics of the recorded current or voltage are obtained by employing a time-frequency domain approach. The Hilbert-Huang transformer is a distinctive signal processing method that integrates the empirical mode decomposition and Hilbert transformer for analyzing non-linear and non-stationary signals. The income signal is divided into several modes with inherent characteristics that have restricted bandwidth using the variational mode decomposition approach. The morphological filters use nonlinear signal processing techniques. Mathematical morphology is a scheme of evaluating data in the time domain that involves the study of the concept of sets, integrated geometry, and the shape of signals. The transient monitoring function approach calculates the discrepancy between the initial signal and the predicted or regenerated signal, using the precision of the signal approximation.

2.2.6 Scheme of Computational Intelligence

Using signal processing schemes, the accuracy of islanding detection can be enhanced. However, signal processing techniques are unable to totally reduce the NDZ in more sophisticated DG systems. In these situations, enhancing the islanding detecting relay's intelligence can improve performance. The detection of islanding can be accomplished by the simultaneous processing of various factors by computationally sophisticated approaches. With those methods, choosing threshold values is not necessary, but there is a significant processing cost. The term "computational intelligent-based methods" refers to a variety of techniques as presented in Figure 2.7. The schemes of computational intelligence are explained below.

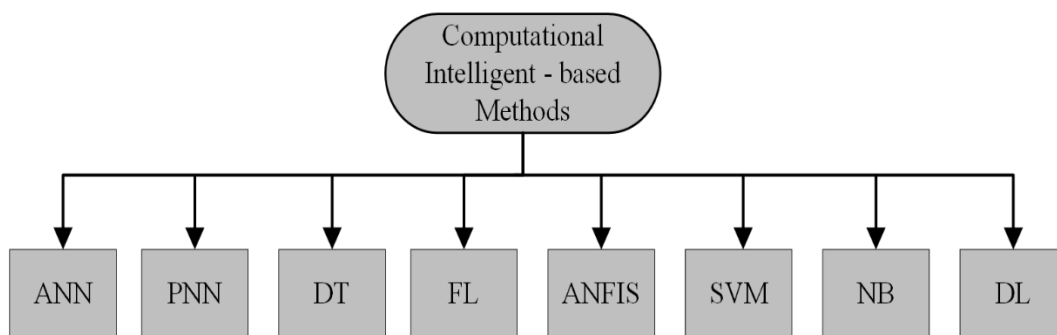


Fig. 2.7. Schemes of computational intelligence

2.2.6.1 Scheme of Artificial Neural Network (ANN)

Using this scheme, the important characteristics of the recorded data are gained to be used to pinpoint changes in the parameters of the network. For multiple DGs, such a method works precisely and efficiently. But the greatest flaw in this strategy is the protracted duration of data processing [97].

2.2.6.2 Scheme of Probabilistic Neural Network (PNN)

Due to ANN's limited computation time, this scheme is proposed to boost the performance of ANN. Four layers are used by the scheme of Bayesian classifier: output layer with feed-forward mechanism, input layer, pattern layer, and summation layer [98]. Learning is not required to use those levels and carry out their responsibilities. You can rely on this method for locating islanding.

2.2.6.3 Scheme of Decision Tree (DT)

Using this scheme, which is considered one of the hierarchical approaches, complex decision-making challenges are divided into manageable possibilities. The extracted necessary characteristics of voltage or current signal for abnormal condition identification are obtained using discrete wavelet transformer or wavelet packet transformer. After being extracted, this scheme examines the given feature data set to identify occurrences of islanding incident [99]. This technique optimizes the limit setting of relays to achieve the smallest possible detection area during abnormal conditions, regardless of the specific conditions and configurations.

2.2.6.4 Scheme of Fuzzy Logic (FL)

Fuzzy logic is employed to solve the problem computationally by utilizing a rule foundation. The model built using the rule bases is called a fuzzy inference system. Decision tree transformation, which integrates fuzzy membership functions and rule foundation to improve the fuzzy system, has been proposed by FL for islanding detection [100]. Therefore, this approach yields positive and effective outcomes in terms of islanding detection. However, noisy input has a significant impact on fuzzy classifiers because of the highest and lowest possible combinations.

2.2.6.5 Scheme of Adaptive Neuro-Fuzzy Inference System (ANFIS)

Using this scheme, the versatility of fuzzy logic and efficacy of artificial neural network are combined together. An active approach is developed for islanding incident identification, which

the ANFIS scheme is used to replace the traditional proportional-integral (PI) controller-based d-axis injection in the system [101]. The fundamental advantage of the ANFIS technique is that it lowers the not-detected zones whilst still maintaining power quality standards.

2.2.6.6 Scheme of Support Vector Machine (SVM)

This method evaluates the signal and structure by defining a decision boundary to split the required training data. SVM and auto-aggressive processing are used to determine the typical operations usual functions of coupling point acquired voltage and current data. This scheme is accurate and has a fast detection rate. However, it is quite difficult for practical implementation due to the approach and data training [102, 103].

2.2.6.7 Scheme of Naive Bayesian Classifier (NB)

This scheme is recognized as a classifier based on probabilities that are based on the Bayes theorem. A particular dataset feature must be individual of each alternative dataset parameter for such a classifier to work. When dealing with big input vectors, this approach performs better than certain other classifiers. This approach was developed for islanding detection to categorize the islanding incidents; the implementation was assessed using SVM scheme and confirmed by fourfold crossing-validation [104]. To choose the most outstanding characteristic retrieved at the coupling point, several schemes, involving ANN, random forest, SVM, DT, and NB, are employed to distinguish the islanding incident based on consecutive feature approaches. When compared to other classifiers, the NB classifier's outputs are very accurate [105].

2.2.6.8 Scheme of Deep Learning (DL)

Using this scheme, the need for an individual characteristic's extraction approach is eliminated by automatically learning the most outstanding characteristics obtained from the initial input datasets. As a result, the time of calculation which is required during the characteristic extraction is reduced. An image dataset is fed into a convolution neural network (CNN) as part of a deep learning technique for islanding identification. A continuous wavelet transform is used to convert the time series into scaled picture data [106]. Deep neural network (DNN) and stacked auto-encoder were proposed as methods for islanding detection. Wavelet multi-resolution spectral analysis was then used to recover the characteristics, which were then fed into the DNN [107].

2.3 Difficulties in Choosing Islanding Detection Techniques

There are numerous difficulties when integrating DGs with utility grid networks, particularly when it comes to islanding techniques. The choice of schemes used for islanding identification is heavily impacted by a few variables, involving the DG units' categories, configurations of DG connection, DG lifespan, scalability in the years ahead, and DG locations.

Although numerous methods have been put out to identify islanding, none of them are flawless. As a result, choosing the best technique to identify islanding and evaluate its applicability in grid-connected distributed generation systems is challenging. It is not possible to utilize the islanding detection selection criteria with deterministic values due to their uncertainty. Consequently, addressing all the factors that influence the choice of islanding detection method requires a high level of knowledge.

Furthermore, as smart grids replace conventional electrical networks, several difficulties could arise. An obstacle in smart grids is the presence of many electrical power pathways, which can lead to numerous flaws in the islanding identification mechanism. Intelligent meters may successfully decrease the expenses of intricacies associated with the identification of islanding in smart power networks.

2.4 Evaluation of Islanding Detection Techniques' Performance

The primary variables that determine how well IDM performs are its operational precision and time response. As shown in Figure 2.8, there are numerous factors that may be applied to assess the applicability and efficacy of islanding detection techniques. Taking into consideration specific criteria, the most suitable approach can function well in each situation. These requirements are covered in detail below.

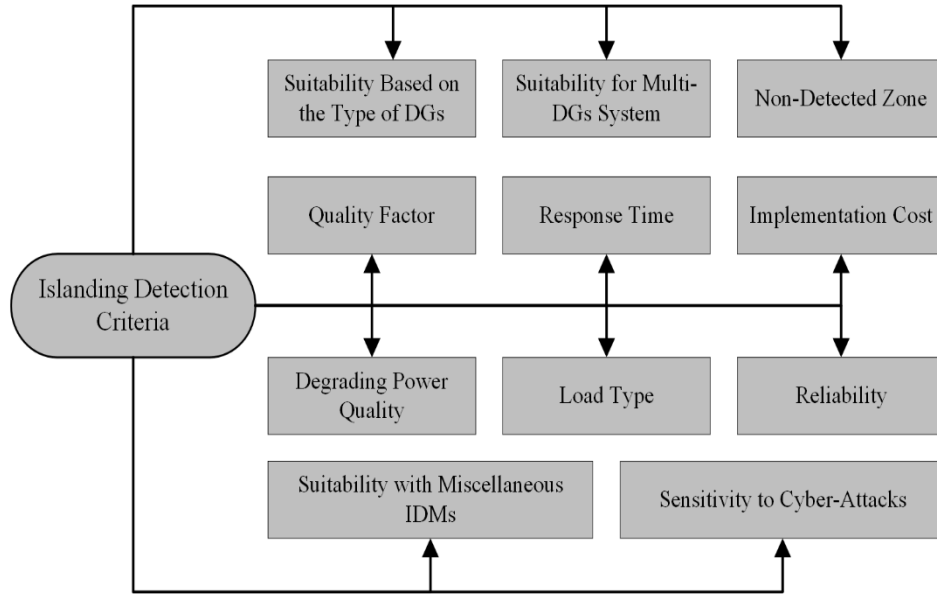


Fig. 2.8. Islanding detection criteria

2.4.1 Assessing the Appropriateness According to DGs Category

The category of DGs is either inverters based which employed in photovoltaic systems or rotational based which are employed in wind turbine systems. Certain techniques used to identify the islanding incident work well with PV systems but not with wind turbine networks. For instance, the techniques of shifted frequency work well with PV systems but not in systems based on rotation. Techniques based on changes in terminal voltage are appropriate for systems that rotate, but they are not suitable for systems that use inverters.

2.4.2 Applicability of Multi-DGs Networks

Once there are multiple DGs in the system, their functioning may be impacted by the relationship among various DG types. Considering such, the sensitivity of Effective evaluation of the detection method is required. Various parameters, including the generating type, can influence the multi-DGs system's choice of islanding detection, the capacity generator ratio, and the existence of reverse power flow. If a pair inverter coupled to the same coupling point but have unequal rating, for example, the higher rating inverter may exhibit dominant actions during the abnormal condition. Furthermore, unintentional tripping may happen because of disturbance injections if the network connected to various inverters which used the same scheme of islanding recognition technique. To prevent such situations, disturbances must be timed to coincide.

2.4.3 Non-Detected Zone

As shown in Figure 2.9, this zone refers to the region where there is a zero discrepancy in power and the scheme of islanding observing may fail to do the work correctly. As a result, voltage and frequency variation can be very minimal when the power of inverter and load are alike, which has a significant impact on the detection effectiveness. When comparing the NDZ of passive and active approaches, the former has a larger NDZ and is therefore less effective.

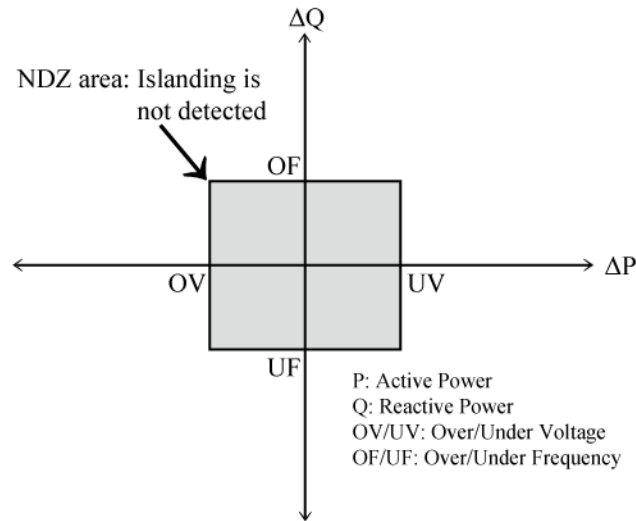


Fig. 2.9. Non-detected zone

2.4.4 Quality Factor

One crucial component in evaluating the efficacy and performance of IDMs is the quality factor. The definition of this factor is the product of the maximal retained energy and the reciprocal dissipated energy during a period of time for a specific frequency. Non-detected zone and the quality factor have a proportionate relationship, and when standards are established, it is imperative to maintain this relationship within the permitted ranges.

2.4.5 Response Time

The time that the scheme of islanding identification taken to respond is crucial and must be minimized as much as possible because of the detrimental effects of islanding on utility staff and network components. Most islanding detection techniques have response times that are in the half-second to two-second range, which is somewhat long, particularly when an island is operating

autonomously and continuously. The time that remote schemes are taken to respond during the abnormal condition is speedier than active schemes which are faster than passive schemes.

2.4.6 Execution Expense

This expense is said to represent a trade-off between system quality and cost. Assessing other approaches, passive schemes are the least expensive. Although the complexity and requirement for additional components make remote techniques the most expensive to implement.

2.4.7 Power Quality Degradation

DGs are required to meet both the generation and power quality standards. Power quality issues include frequency shifts, voltage swings, harmonic deformation, and interference from electromagnetic fields. Degrading the power quality in the system can be greatly impacted by the application of an is-landing detecting mechanism. For example, despite the fact that active schemes modify the power quality by using injected disturbances they rely on, passive approaches do not impair the power quality.

2.4.8 Load Type

The system's operating voltage and the effectiveness of the islanding detection technique are greatly impacted by the design and kind of load. For example, efficient detection of the islanding state will be challenging if the connected load is RLC, particularly if there is power difference between inverter and load is zero. Conversely, non-detected zone would decrease, and the islanding detection method's effectiveness will rise if the grid is coupled to additional non-linear loads [108].

2.4.9 Reliability

To trip the system only when an islanding condition exists and prevent any unintentional trips, the islanding detection mechanism must be accurate and dependable. As a result, techniques for detecting islanding must be able to differentiate between variations in voltage and frequency that result from factors aside from islanding, for example potential underloaded or overloaded circumstances. Nevertheless, the network parameters may go over the permitted limits when certain disruptions occur, including load switching. The rate of detection error (E), which is computed as [109], is the false detection that islanding detection methods may produce in this situation.

$$E = \frac{N_{error}}{N_{error} + N_{correct}} \quad (2.9)$$

where N_{error} and $N_{correct}$ represent, respectively, the error and correct detection times.

2.4.10 Compatibility with Multiple IDMs

An increasing number of inverters are being integrated into the electricity system, which opens up new possibilities for the usage of several IDMs connected to the same or adjacent feeders. As a result, when combining new inverters to a common feeder, integration between the various islanding detection techniques must be considered. Although they have no effect on other methods, passive methods can readily have an impact on further approaches, as active methods.

2.4.11 Vulnerability to Cyber-Attacks

A cyberattack in islanding identification may arise from the introduction of erroneous data into the system. Erroneous data injection modifies the relay's threshold setting to a different value, resulting in erroneous islanding detection and wasteful load shedding and generation rescheduling [110]. As a result, the islanding detection technique needs to be able to deal with online threats.

As was already noted, several factors can be considered while choosing islanding detection techniques. More criteria may be considered, or some criteria may be disregarded, depending on the application type and end-user.

2.5 Standards of Islanding Detection

The criteria for the management, cooperation, and functioning of DGs inverters within the main power grid have been established by several international organizations, including IEEE and IEC. These standards' primary goal is to set forth precise specifications for the integrated power system networks' functionality, security, and safety, as well as for their monitoring and upkeep. When constructing islanding detection methods, specialists can benefit from the complete guidance provided by the standards, which consider many parameters such response time, quality factor of load, operational boundaries for voltage and frequency. Table 2.1 lists the most often used criteria for the identification of islanding incidents that assess the detection mechanism effectiveness. With a few signals processing-based techniques, like the scheme of time-time transformers, which

requires 25 seconds to observe the islanding incident, most of the previously discussed islanding detection methods can meet the prerequisites for IEEE and IEC regulations of observing the islanding incident in a period under 2 seconds. However, many islanding detection techniques such as continuous wavelet transformer, scheme of measured impedance, scheme of active drifted frequency, fail to meet the requirements of other standards, like the Korean standards, which specify that the response time of islanding identification is under 0.5 second.

Table 2.1. Criteria of islanding identification.

Criteria	Frequency Boundaries	Voltage Boundaries	Time of Detection	Quality Factor
IEEE Std. 1547-2003	$59.3 \text{ Hz} \leq f \leq 60.5 \text{ Hz}$	$0.88 \text{ v} \leq V \leq 1.10 \text{ v}$	$t < 2 \text{ s}$	1
IEEE Std. 929-2000	$59.3 \text{ Hz} \leq f \leq 60.5 \text{ Hz}$	$0.88 \text{ v} \leq V \leq 1.10 \text{ v}$	$t < 2 \text{ s}$	2.5
Korean Criteria	$59.3 \text{ Hz} \leq f \leq 60.5 \text{ Hz}$	$0.88 \text{ v} \leq V \leq 1.10 \text{ v}$	$t < 0.5 \text{ s}$	1
French Criteria	$49.5 \text{ Hz} \leq f \leq 50.5 \text{ Hz}$	$0.88 \text{ v} \leq V \leq 1.06 \text{ v}$	instantly	2
IEC 62116	$f_0 - 1.5 \text{ Hz} \leq f \leq f_0 + 1.5 \text{ Hz}$	$0.85 \text{ v} \leq V \leq 1.15 \text{ v}$	$t < 2 \text{ s}$	1
Canadian Criteria	$59.5 \text{ Hz} \leq f \leq 60.5 \text{ Hz}$	$0.88 \text{ v} \leq V \leq 1.10 \text{ v}$	$t < 2 \text{ s}$	2.5
Japanese Criteria	Set value	Set value	Passive: $t < 0.5 \text{ s}$ Active: $0.5 \leq t < 1 \text{ s}$	0(+rotating machinery)
AS4777.3-2005	Set value	Set value	$t < 2 \text{ s}$	1
VDE 0126-1-1	$47.5 \text{ Hz} \leq f \leq 50.2 \text{ Hz}$	$0.80 \text{ v} \leq V \leq 1.15 \text{ v}$	$t < 0.2 \text{ s}$	2
UL 1741	Set value	Set value	$t < 2 \text{ s}$	≤ 1.8

2.6 Comparison of IDMs

Every islanding detection technique has pros and cons that should be considered when selecting the best IDM to utilize in the network, according to the research that was conducted. Table 2.2 provides a summary of the positive aspects and drawbacks of the various schemes of islanding identification. The selection of islanding recognition approaches, as seen in Tables 2.3 and 2.4, relies on an in-depth comparison that considers many criteria to be addressed before execution. These elements include the expense of execution, the non-detected zone, the time taken to respond, and other relevant considerations.

Table 2.2. Analysis of islanding identification schemes determined by their positive aspects and drawbacks.

Schemes		Positive Aspects	Drawbacks
Local Schemes	Passive	Minimalist affordable readily accessible shorter time to respond power quality remains uncompromised	enormous NDZ undependable threshold determining
	Active	rapidity tiny NDZ minimal detection error rate	disruption introduced power quality worsening inadequate time to respond
	Hybrid	optimal effectiveness insignificant NDZ efficient in multi-inverters network	power quality worsening reasons time rises rapidly
Remote Schemes		rapidity utmost dependability minimal detection error efficient in multi-inverters network	delayed response time pricey
Signal Processing Schemes		rapidity eliminate NDZ improved effectiveness higher resolution resilient to noise level window dimensions can vary Processing is framed based	prone to distorted waves sophisticated calculations only low frequency band can be recovered restricted to estimating specific harmonics
Computational Intelligence Schemes		highly precise minimize NDZ threshold adjustment is unnecessary	Substantial training data set required extremely conceptual

Table 2.3. Analysis of islanding identification determined by numerous factors.

Schemes	Pricing	Power Quality	NDZ	Dependability	Computational Load	Multi DGs Application	Vulnerability to Cyber-Attacks
Local Schemes	Passive	least	no consequence	expansive	limited	minimal	can be applied
	Active	least	Marginally deteriorated	compact	reliable	moderate	cannot be applied
	Hybrid	least	Marginally deteriorated	compact	reliable	intensive	can be applied
Remote Schemes	exorbitant	no consequence	very compact	reliable	intensive	can be applied	highly susceptible
Signal Processing Schemes	least	no consequence	very compact	exceptionally reliable	moderate	can be applied	responsive if new data format is instantly modified using the unit of signal processing
Computational Intelligence Schemes	costly	no consequence	very compact	exceptionally reliable	intensive	can be highly applied	responsive if the classifier is trained for bogus data

Table 2.4. Analysis of islanding identification schemes determined by the time required to respond.

Schemes	Time to Respond
Passive Schemes	
Over under Voltage/Frequency	4 ms–2 s
Active and Reactive Power Rate of Change	24–26ms
Frequency Rate of Change	24 ms
Total Harmonic Distortion	45 ms
Phase Jump	10–20ms
Frequency over Power Rate of Change	100 ms
Active Schemes	
Drifted Active Frequency	Within 2 s
Measured Impedance	0.77–0.95 s
Sandia Shifted Frequency	0.5 s
Slip Mode of Shifted Frequency	0.4 s
Sandia Shifted Voltage	0.5 s
Active and Reactive Power Variation	0.3–0.75 s
Negative Sequence of Injected Current	60 ms

Perturbation of Phase-locked loop	120 ms
Virtual Capacitor	20–51 ms
Frequency Jump	75 ms
Virtual Inductor	13–59 ms
Hybrid Schemes	
Unbalanced Voltage & Frequency Set-Point	0.21 s
Injection of Voltage Fluctuation	Within 0.216 s
Remote Schemes	
Power Line Carrier Communication	200 ms
Supervisory Control and Data Acquisition	0.1–0.3 s
Signal Generated by Disconnect	100–300ms
Transfer Trip Scheme	<10 ms
Signal Processing Schemes	
Fourier Transformer	Within 2 cycles
Hilbert Huang Transformer	Less than 2 cycle
Wavelet Transformer	continuous WT (CWT) 0.6 s discrete WT (DWT) 24–26ms
Time-Time Transformer	25 s
S- Transformer	26–28ms
Kalman Filter	50–70ms
Computational Intelligence Schemes	
Decision Tree	0.041 s
Support Vector Machine	0.040 s
Adaptive Neuro-Fuzzy Inference System	0.062 s
Fuzzy Logic	0.070 s
Naive Bayesian classifier	0.12 s

2.7 Conclusions

This chapter presents and thoroughly reviews several islanding detection techniques. There are two types of islanding detection techniques: conventional and modern. Modern approaches involve the utilization of computational intelligence and signal processing schemes, whereas conventional schemes encompass remote and local (passive, active, and hybrid) schemes. The fundamental idea behind passive techniques is observing the fluctuations in grid boundaries, including frequency or voltage shifts at coupling point. Due to their low cost and ease of practical implementation, passive methods are highly preferred for usage in systems. On the other hand, the undetected zone is often extensive when using passive approaches. Active approaches examine the impact of injecting some external disturbances to the network during abnormal conditions. Hybrid schemes are developed by employing both passive and active schemes. Both active and hybrid schemes necessitate additional tools for disruption, potentially increasing installation costs and complexity. The DGs inverters and main power source must communicate to gather data in order to let remote approaches work. Although they are more difficult than local approaches, remote schemes don't contain any undetectable areas. The fundamental basis of signal processing schemes lies in gathering distinctive characteristics. When compared to alternative islanding detection techniques, signal processing schemes are the most preferred when considering expense, dependability, non-detected zone, and precision; as a result, they are often advised for use in industrial applications. Computational intelligence schemes are built upon the basis of identification of patterns and data processing. The undetected area is smaller, and the computational techniques are highly reliable. These techniques, however, are expensive and need a lengthy time for detection. Furthermore, the examined studies have demonstrated that every method has some benefits and drawbacks. The pick of the approach to be applied in the system might be determined by considering a number of factors, including undetected areas, execution expense, quality factor, and so on. As a result, it is challenging to choose the best approach among others to offer a comprehensive answer in every situation. But in the next chapter, a multi-criteria approach is used to weigh the factors, like a group decision-making tool, which can provide a precise assessment to determine the most effective islanding identification scheme by considering the scenarios, applications, or conditions that the network is encountering.

3. Multiple-Criteria Decision Assessment

3.1 Background

The method of decision-making should always be considered when determining any choice. Making decisions is a complex cognitive procedure that involves addressing issues by considering multiple aspects with the goal of achieving an objective conclusion. The procedure is capable of being categorized into two categories: irrational or rational, and it may additionally depend on either implicit or explicit presumptions which are molded by a range of genetic, ethnic, psychological, and interpersonal variables. Each of these features, including competence and risk assessments, may affect the level of intricacy in a process for making decisions. Currently, technological advances in computing are being utilized to automatically calculate and estimate ways to solve issues related to decision-making, using different mathematical concepts, economic concepts, and mathematical formulas, enabling the resolution of complicated decision-making difficulties.

Multiple-Criteria Decision Analysis (MCDA), which has been dubbed a revolution in the area [111,112] is considered to be among the most accurate techniques for making choices. Benjamin Franklin's research on the idea of moral algebra resulted in one of the earliest studies on multiple-criteria choice-making. Throughout the beginning of the twentieth century, numerous experimental and theoretical researchers have been concentrating on MCDA approaches to explore their potential for numerical modeling. The goal is to provide a structure which is useful in structuring decision-making problems and generating judgments among different options.

This approach considers several qualitative and quantitative elements that should be regulated to identify the best possible solution. As an example, Among the least common factors considered in making choices is the expense or pricing and the standard of the operations [113]. Moreover, in such scenarios, panels of experts allocate distinct weights to the criteria, considering the relative significance of every criterion within that particular context.

MCDA is often utilized to address the challenges which occur in individuals' everyday activities. Still, Criteria evaluation becomes of greatest significance while the dispute concerns larger matters, like funding scales. Consequently, under these conditions, the foundation for decision-making must be sound structuring and explicit evaluation of all the criteria using suitable

implements and software package. When it comes to the real-world setting, MCDA is utilized in the development, organization, and decision-making procedures of circumstances in which the field in question possesses a number of criteria that need to be satisfied in order to end up at an ideal outcome which the deciders desire [113].

In the last century, several scientists developed and refined different MCDA approaches. The degree of algorithmic complexity, criteria weighing techniques, preference valuation criteria representation, uncertainty in information and the sort of information collection are the primary distinctions between these approaches [114].

Furthermore, each type of MCDM has unique advantages and disadvantages that should be discussed in detail depending on the approaches. The Analytic Hierarchy Process (AHP), for instance, has problems since criteria and alternatives are interdependent. Nevertheless, it is a user-friendly tool. Conversely, it is possible to use imprecise input in the Theory of Fuzzy Set (FST), albeit developing such technique remains challenging. The benefit shared by all MCDM techniques is that they consider the disproportionate and inconsistent effects of actions. On the downside, due to the inherent characteristics of this issue, the solutions generated by these methodologies need to strike a balance among numerous goals, which prevents the ideal point from being reached [115].

There are several uses for MCDM across a wide range of fields and professions, including engineering and energy sector. Several islanding identification approaches were presented and categorized under four classes as explained in the previous chapter. There are several considerations that need to be made while selecting the best methodology to be implemented in the system, as each approach has pros and cons. As such, it is imperative to devise a streamlined process for ascertaining which islanding detection technique is best suited for system integration. To address this issue, the assessment of multiple-criteria decisions is a beneficial technique.

The utilization of MCDA is carried out while a choice must be made after considering several contradictory and unfavorable assessments. These conflicts will be revealed, and an appropriate plan of action will be created to result in an open process. MCDA has already been used in the power systems review process. The analytical hierarchy process (AHP), evacuation management decision support system (EMDSS), fuzzy sets, elimination and choice expressing reality (ELECTRE), and other MCDA approaches are just a few that can be used to address some of the problems in this field [116].

This chapter contrasts two types of islanding detection methods: traditional methods, which include remote and local approaches, and modern techniques, which include signal processing and computational intelligence-based approaches. The analytical hierarchy method (AHP) is employed for the purpose of examining and ranking each solution according to a variety of criteria, such as reaction times, power quality, non-detected zones, and implementation costs.

3.2 Approach to Solving an MCDA Problem in General

Several components and ideas are included in MCDA, according to the type of choice making issue as presented here:

- "Differing possible courses of action" are called alternatives.
- "A measurable characteristic of an alternative" is the definition of the attribute.
- "Considering the performances of an alternative on the specific criteria for deciding on the alternative" is the definition of aggregation.
- According to definitions, variables are used to represent the options are "components of alternatives' vector."
- "Feasible alternatives" stands the representation of decision space.
- "Elements utilized to quantify an alternative to its attribute by assigning numbers or symbols to the attribute" is the process of defining the measures.
- "Tools for evaluating and comparing alternatives from the standpoint of the consequences of their selection" is the process of defining the criteria.
- "How an alternative fulfills the need of a decision-maker regarding a given attribute" is the definition of a preference.
- According to the issue sort which may consist of ordering, sorting, and choosing issues; different decisions must be made [117,118].

An MCDA problem can be interpreted in a variety of ways. The procedure can be thought of as selecting the most outstanding (most desired) option from the list of available alternatives. Another way to think about it is to classify the options into several preference groups and subsequently pick a limited number among options. Those issues also seek to identify non-dominated or efficient alternatives. This idea aids individuals to pick up some solutions from a group of non-dominated options since it is impossible to transition from one non-dominated solution to another without

sacrificing no less than a single criterion [111]. An MCDA problem is defined mathematically as follows:

$$A = \{A_i \mid i = 1, 2, \dots, m\} \quad (3.1)$$

where m is alternatives number, and A is a distinct, finite set of them.

$$C = \{C_j \mid j = 1, 2, \dots, n\} \quad (3.2)$$

where n is the criteria number and C is a set of particular criteria by which A is evaluated. Although the alternatives are naturally homogeneous, the criteria do not need this point. In other words, criteria can have distinct units with no links between them and can have competing aims (some with minimizing goals and others with maximizing goals).

$$W = \{w_j \mid j = 1, 2, \dots, n\} \quad (3.3)$$

W is a collection of normalized weights which are allocated based on the significance of every criterion. An MCDA problem can be defined simply using the mathematical form of sets that was previously addressed. The information that is gathered is typically arranged in a matrix form, shown in Table 3.1.

Table 3.1. MCDA matrix.

MCDA Matrix	C_1	C_2	...	C_n
A_1	x_{11}	x_{12}	...	x_{1n}
A_2	x_{21}	x_{22}	...	x_{2n}
...	x_{ij}	...
A_m	x_{m1}	x_{m2}	...	x_{mn}

The value of A_i in relation to C_j is represented by x_{ij} in this matrix, and the weights' vector ($W = \{w_1, w_2, \dots, w_n\}$) and the matrix (M) serve as the primary inputs for the MCDA issues. The alternatives are actually scored by MCDA, which then ranks them from best to worst. Figure 3.1 depicts all the MCDA problems' primary steps.

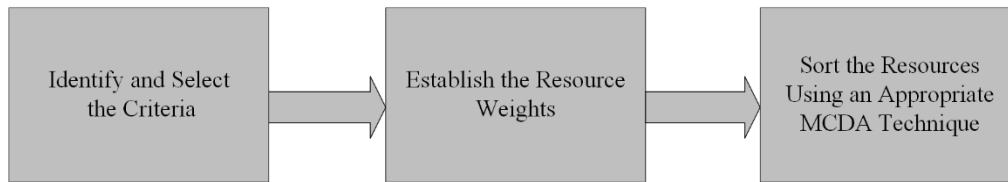


Fig. 3.1. MCDA steps

It should be mentioned that, for greater simplicity, the MCDM approach can be used to modify the rows and columns in the matrix.

3.3 Categories for Multiple-Criteria Decision Making (MCDM)

As previously stated, there are multiple Multi-Criteria Decision Making (MCDM) strategies available, each with distinct characteristics which may be linked to a diverse set of criteria, including the nature of the problems these techniques address and the caliber of the solutions they provide. Hence, it is imperative to ascertain the categorization of issues related to MCDM in order to gain a more comprehensive comprehension about the MCDM methodologies, that facilitates the choice of an appropriate resolution for the challenges at hand. Various typologies and subgroups that consider distinct features of the difficulties are identified in numerous research. After listing several of these main divisions, an in-depth description of the majority of widely used categorization approach is given.

First, a crucial approach considers the kind of aggregation strategy that is employed to assess the criteria which may be used for the sorting of Multiple Criteria Decision Making (MCDM). The aggregation strategies employed in this methodology, as mentioned by Zopounidis and Doumpos [119], are outlined below:

Outranking relation: This approach and associated binary structure enable researchers to examine the options by determining the level of outranking once enough arguments are provided to establish that one option is equivalent to the other.

Utility functions: An alternative's performance after accounting for all relevant criteria is its usefulness. When alternatives are sorted into preset sets, this strategy is utilized as an index to aid in decision-making.

Discriminant function: Such kinds of structures aren't suitable to be implemented as a preferred model, despite their similarities to the utility function. The ordering of preferences across criteria

domains and decision classes is not a basis for these models' operation. Furthermore, the method is linear and employs quantitative criteria, either directly or by assessing qualitative aspects.

Function-free models: Refer to models that possess a figurative structure. A specific decision rule is employed to evaluate the general effectiveness of the options.

Moreover, the research additionally employs the subsequent classifications:

Furthermore, apart from the aforementioned category classification, MCDM may additionally be classified into three additional groups: partial, non-compensatory, and compensatory. This strategy relies on the possibility of the adverse characteristics being balanced out by the beneficial characteristics.

Group or individual decision-making: One easy way to differentiate between MCDM approaches is to look at the number of decision-makers when determining if the decision-making process is individual or group-based [120].

Qualitative, quantitative, or certain/uncertain information: It is possible to classify information in several ways depending on its nature.

Tradeoff and non-tradeoff-involved approaches: there exist two main types of weighting methods for MCDM problems: tradeoff-based and non-tradeoff-based methods. These methods can be used to differentiate between the two types of MCDM problems [118].

MODM or MADM: Two categories of criteria are recognized in one of the most widely applied methods: (1) characteristics and (2) goals. In addition, the model challenges were categorized in two main categories based on the number of choices [121]. As a result, there are two broad subcategories of MCDM problems: multi-attribute decision making (MADM) and multi-objective decision making (MODM). The terms "innumerable" and "numerable" are alternative designations for the sub-groups, with "innumerable" referring to those with an infinite number of permissible responses, and "numerable" referring to those with a finite number of permissible answers. More information on these sub-groups can be found in the paragraphs that follow.

MODM, or continuous problems of choice making, is an approach that specifically deals with decision spaces which have an ongoing variety of possibilities and infinite number of potential results. A viable region, or the place where the alternatives are located, is thought to be the answer to this decision-making conundrum. It is an optimization problem for which there wasn't a clear-cut solution selected. These kinds use implicit attributes and criteria as goals. Here, there is a

significant degree of interaction among decision-makers despite the lack of a clear objective and alternative.

MADM: Discrete problems, usually referred to as explicitly known choice alternatives, are the focus of MADM. These alternatives have a finite number. It's an evaluation problem where the answer is selected from a limited set of alternatives. Goals, attributes (which serve as criteria), and options are evident in these MCDM kinds; but the constraints are not evident, and decision-makers' ability to communicate with one another is constrained.

The various classification techniques covered above are compiled in Figure 3.2

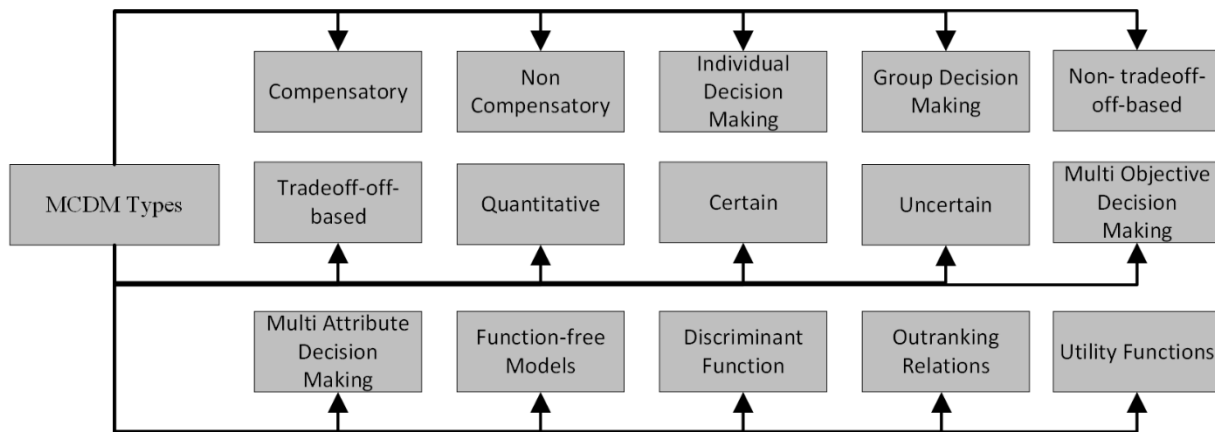


Fig. 3.2. Various MCDM classifications

The primary techniques for making decisions that consider many criteria are known as multicriteria choice modeling (MCDM) approaches. This post aims to provide a comprehensive overview of the fundamental concepts, applications, and diverse forms of MCDM approaches. MCDMs are widely recognized as one of the increasingly prevalent methodologies for decision-making and are utilized in a variety of sectors. MCDM techniques can be categorized based on a variety of factors. Based on the findings of this part, the strategy known as AHP was mentioned more often compared to other selected approaches, and MADM approaches received greater consideration than MODM varieties throughout the investigation.

3.4 Literature Review on Analytic Hierarchy Process (AHP)

The globe is an intricate structure with many interdependent elements from the environment, people, and industry. Systems or interactive environments need decision-making processes that

can make decisions about the system using an analytical and comprehensive approach. AHP is an MCDM technique that is suitable for intricate structures. It allows for the analysis of both qualitative and quantitative aspects of choice-making [122]. AHP may be used to perform evaluations whether the scales are extremely small or extremely huge [123]. For these tiny and big magnitudes, the pairwise comparison procedures employed with AHP are more appropriate compared to a rating system that takes single choice at a certain time period. AHP simplifies a difficult choice or issue into a hierarchy and several pairwise comparisons. AHP is an MCDM approach that permits the application of practice, insight, vision, and quantitative data. Decision-makers who aren't experts can nevertheless join the procedure because AHP is simple to understand. Hence, AHP is a chosen MCDM structure by several experts [124,125]. The AHP's capacity to settle multi-objective decision scenarios is another benefit. Ultimately, AHP not only enables the researcher to handle various data formats but also assesses the consistency of decision makers' inputs [126-128]. The significance of measuring consistency in group decision-making and consensus was emphasized [129,130]. To increase uniformity among SMEs, Stoklasa et al. suggested doing an initial priority ranking prior to conducting a pairwise comparison. After evaluating the AHP, it was determined that it's critical to provide choices to the issue that improve the effectiveness of decision-making [131].

3.5 Background of Analytic Hierarchy Process (AHP)

AHP was established by Thomas L. Saaty that has been demonstrated that it is a successful approach for deciding using multiple criteria. Saaty invented the AHP as a MCDM technique to convert ambiguous subjective estimates to a system of measurable criteria and ratio measures, ultimately resulting in a single measure. The research revealed a wide range of possible uses of AHP in the fields of social science, administration, and technology. AHP is suitable for MCDM, particularly when there are multiple Small and Medium Enterprises (SMEs) engaged in assessing different factors or parameters that impact the ultimate choice [132,133]. The factors involved can be categorized as either quantitative or qualitative, concrete, or immaterial, and subjective or not quantifiable. Saaty endeavored to elucidate the underlying assumptions following initial resistance to the legitimacy of the AHP [134]. Saaty not only focused on enhancing the conceptual basis of the AHP, but also investigated its advantages for group decision-making. He determined that the AHP is a proficient instrument for evaluating qualitative criteria. Saaty summarized the advantages of utilizing AHP as a MCDM structure for collaborative decision-making as presented below:

1. AHP offers a comprehensive approach for resolving problems that are unorganized.
2. It has the ability to identify answers to difficult problems.
3. It can make connections in a complicated mode between interdependent parts.
4. It can deconstruct complicated issues into straightforward components dispersed across different degrees of the hierarchical structure.
5. AHP allows for the juxtaposition of elements at identical degree of hierarchy in order to figure out their priority.
6. AHP transforms subjective evaluations within quantifiable measures.
7. AHP makes it possible to confirm the data's consistency.
8. An overall/decomposed priority of the alternatives with respect to the issue is provided by AHP.
9. AHP draws conclusions from a range of viewpoints.
10. AHP permits modifications and iteration to enhance outcomes.

Due to these benefits, AHP has an extensive variety of applicability by practitioners as well as researchers.

3.6 Theory of Analytic Hierarchy Process (AHP)

AHP is based on several axioms, just like any other theory [135]. The inverse relationship principle, which expresses that if criterion A is four times larger than criterion B, then criterion B is equivalent to a quarter of criterion A. The homogeneity axiom, which is the second axiom, states that to prevent significant judgment errors, the criteria or sub criteria being compared should be fewer than one order apart. The phrase of hierarchical synthesis, which denotes the criteria or sub criteria are independent of the lower-level criteria, is the final axiom. This axiom encourages pairwise comparisons as a bottom-up method of weight determination.

When the individual in charge failed to adhere to both of the overarching criteria of AHP, AHP could provide inaccurate results: two key components of the structure's definition are (a) the hierarchical framework and (b) the priorities. It must be capable of demonstrating how a scientific theory might present the appropriate solutions to a recognized issue in order to support the theory. In order to establish the validity of the AHP, Saaty looked at the compatibility index as a way to gauge how near priority vectors are to one another [134]. However, using MCDM makes it possible to obtain several priority vectors that might be similar. Measurably close to Saaty's

compatibility index S . Participants in the AHP provided varying evaluations, which led to the diverse priority vectors. These discrepancies in assessments can be quantified using a second metric called the consistency index, or CI. The decision-maker must keep an eye on these two indices to make sure the problem has a legitimate solution and to prevent these possible problems.

3.7 Prioritization of Analytic Hierarchy Process (AHP)

The analytical foundation for the AHP is established through the computational framework of coherent matrices and the calculation of weights utilizing the right eigenvector of the matrices.

The priority order is shown by the matrix's eigenvector, or relative weight, and the consistency of decision makers' decisions is indicated by the eigenvalue [136]. Saaty's eigenvector method is compatible with the geometrical mean approach, weighed least-squares (WLS) approach, logistic goal programming approach, and logarithmic approach [137].

Some of the issues with the eigenvector were also addressed in [138], which defined an alternate strategy known as the linear programming approximation. It was demonstrated that the least squares approach can yield an eigenvector solution [139]. To prevent rank reversal, it was suggested using the geometric mean technique in place of the eigenvector [140]. All these variants were employed by researchers in their pursuit of improved optimization. The eigenvalue approach, the modified dominant eigenvalue scheme, direct least squares scheme, and weighted least squares scheme, and logarithmic least squares scheme were among the several prioritization techniques studied in [141], which used real data in their comparisons and discovered strong concordance between various approaches.

3.8 Consistency of Analytic Hierarchy Process (AHP)

AHP is a technique for systematically gathering data from decision-makers. Measurements based on perceptions or exact measurements may be part of the procedure. A consistent judgment matrix is produced by the judgments rendered using a ratio scale. For many criteria used in decision-making, it is impossible to achieve consistency, according to [130]. By using a hierarchy, which enables a two- or three-step assessment procedure, decision makers can reduce these criteria. A cross-weight strategy to prevent inconsistency was used [142]. The consistency of the judgment matrix can also be tested with the AHP. When it comes to consistency, the SMEs' inconsistent responses are quantifiable. The consistency ratio (CR), which can be computed by decision

makers, is the ratio of the random index to the consistency index (CI). According to [134], a ratio of consistency below 0.1 was deemed adequate. The judgment metric needs to be refined by decision makers if the CR is higher than 0.1. The final priorities of the alternative schemes or solutions to the target can only be determined by the CR when the weights of the criteria are aggregated.

3.9 The Pairwise Scale of Analytic Hierarchy Process (AHP)

The three phases of the AHP are synthesis or fusion, preference measurement, and decomposition. It is a type of organized intricacy. Decision-makers must divide the issue into a hierarchical framework with levels of uniform criteria to keep things simple. The objective or the issue is specified at the top of the hierarchy. Every subsequent level presents a definition of a cluster or distinct criterion of the level above. The explicit measurement level, or the characteristics, is the natural lowest level. When ranking the alternative options, the qualities might be the third or fourth level; Saaty recommended using a pairwise comparison scale with a range of 1 to 9. According to the research conducted by psychologist George Miller in the 1950s, Saaty gave the justification for employing a discrete scale ranging from 1 to 9. Miller found that in order to preserve consistency, people could not concurrently discern between an excessive number of alternatives-roughly seven- [134]. The majority of AHP practitioners employ the basic Saaty scale, which has nine extreme levels of importance (1 being equivalent to importance and 9 being extreme) as presented in Table 3.2.

Table 3.2. Scale of AHP pair-wise scale.

Degree of relative significance	Meaning	Explanation
1	Equally significant	The property is equally influenced by two criteria
3	Slightly preferable	One criterion is marginally more favorable than another based on experience and judgment.
5	Highly preferable	One criterion is strongly preferred over another by experience and judgment
7	Very highly preferable	A criterion has a strong preference, and its dominance is shown in actual use.
9	Exceptionally preferable	Highest potential order of affirmation is found in the

		evidence supporting one criterion above another.
2,4,6,8	Intermediary judgment between two consecutive judgments	
Reciprocals	When activity A and activity B are compared, when task A is assigned one of the aforementioned numbers, then activity B will be assigned the reciprocal of that value.	

3.10 Summary of Analytic Hierarchy Process (AHP)

Since Saaty first presented AHP as a decision-making procedure, the approach is becoming more and more well-liked. A study of literature on the AHP application from 2005 to 2009 was conducted in [143]. It conducted a review of over 232 academic journal application articles before incorporating them into their study. The manufacturing sector accounted for most applications, with management of environmental, farming, electricity and energy, transport, construction, and healthcare following closely behind. Given the increasing number of options available, choosing machine tools in the industrial sector can provide difficult decision-making challenges. In summary, the AHP helps define a complicated problem in terms of criteria and sub criteria by utilizing a top-down analysis to generate the relative relevance using a pairwise comparison in a bottom-up manner. It examined a prevalent critique of AHP, which is the potential for inconsistent outcomes [144]. Some have raised problems about the prioritization process and the non-evolutionary computing methodology [141]. But the researchers discovered that by defining an inconsistency index, they could deal with these issues of inconsistency. To verify the accuracy of comparisons, some researchers computed the inconsistency index [126, 134].

Decision-makers can utilize the measuring model produced by the AHP to assess potential alternatives or solutions. Three fundamental functions were identified by [135], in their summary of the AHP: (a) constructing complexity; (b) evaluating on a ratio scale; and (c) combining to enable the recognition of the best solution. It was noted that further work is required to define measurement solidity, with a particular emphasis on ordering and approximating solidity [145].

3.11 Analysis of Multiple-criteria Decision Analysis (MCDA)

Multiple techniques and practices are utilized by MCDA which is a management approach to facilitate choice-making in complicated circumstances where multiple criteria need to be considered. Several MCDA approaches were implemented and examined by different researchers.

Among these approaches, AHP is considered a trustworthy and appropriate approach for resolving islanding identification issues that involve multiple ambiguities and criteria. Using this approach, alternative choices are rated and ranked using numerical rating system by setting subjective criteria for variables that are intangible.

The suitability and effectiveness of islanding identification schemes are assessed by employing various factors. Every situation might be effectively managed by employing the most suitable approach, considering the variables evaluated. The following are the precise details of the prerequisites.

- Execution Expense

The expense for execution is regarded as a trade-off among the expense of the entire system and its level of functionality. The most cost-effective schemes relative to other schemes are passive schemes, while remote schemes are the costliest. A concise contrast between islanding identification schemes determined by their corresponding expenses is provided in Table 3.3.

Table 3.3. A concise contrast between islanding identification schemes determined by execution expense.

Scheme	Execution Expense
Passive Scheme	Affordable
Active Scheme	Affordable
Hybrid Scheme	Affordable
Remote Scheme	Very exorbitant
Signal Processing Scheme	Affordable
Computational Intelligence	Exorbitant

- Undetectable Area

The undetectable area is the region characterized by power balance between the inverter and load in which the islanding incident observing is more complicated due to the deviation of system parameters could be minimized. For instance, the effectiveness of active schemes is higher than passive schemes in terms of undetectable areas. A concise contrast between islanding identification schemes determined by their corresponding undetectable area is provided in Table 3.4.

Table 3.4. A concise contrast between islanding identification schemes determined by undetectable area.

Scheme	Undetectable Area
Passive Scheme	Big
Active Scheme	Tiny
Hybrid Scheme	Tiny

Remote Scheme	Very Tiny
Signal Processing Scheme	Very Tiny
Computational Intelligence	Very Tiny

- The Quality of Power

Aside from the need to generate power, the distributed generators must also adhere to power quality standards. Power quality concerns encompass frequency and voltage variability, deformation of harmonics, and electromagnetic noise. The network capacity to detect islanding, where the DGs operate independently from the main grid, greatly affects power quality. Passive schemes do not harm power quality, while active schemes involving injections and disruptions may have a negative impact. A concise contrast between islanding identification schemes determined by their corresponding power quality is provided in Table 3.5.

Table 3.5. A concise contrast between islanding identification schemes determined by power quality.

Scheme	Power Quality
Passive Scheme	Zero Impact
Active Scheme	Marginally Deteriorated
Hybrid Scheme	Marginally Deteriorated
Remote Scheme	Zero Impact
Signal Processing Scheme	Zero Impact
Computational Intelligence	Zero Impact

- Response Time

As a result of the detrimental effects that islanding can have on grid equipment and technicians, the time which the scheme needs to respond to this abnormal condition is critical and must be maximally rapid. The majority of schemes respond to the islanding incidents in a period ranging from 0.5 to 2 seconds, which is quite lengthy. A concise contrast between islanding identification schemes determined by their corresponding response time is provided in Table 3.6.

Table 3.6. A concise contrast between islanding identification schemes determined by response time.

Scheme	Time To Respond
Passive Scheme	Rapidly Fast
Active Scheme	Slightly Fast
Hybrid Scheme	Slow
Remote Scheme	Slow
Signal Processing Scheme	Rapidly Fast
Computational Intelligence	Fast

The most effective scheme of islanding identification is selected by employing AHP strategy which examines the functional capabilities across numerous situations. The hypothesized hierarchy framework which is used for such assessment is described below.

- The determination of the proper scheme of islanding identification is the primary objective of this task.
- The choice of solution will be based on several criteria, including the execution expense, undetectable area, quality of power, and time to respond.
- The available alternatives for the decision-making process include the four categories of islanding observing scheme were discussed briefly in the previous chapter.

The problem is structured using an inverted tree which consists of different stages. The apex stage refers to the main purpose, the second stage refers to the sub-objectives which add value to the main purpose, the third stage refers to the third-level goals. The specific goals are regarded as criteria in this research. At a lower hierarchical level, the attainment of each aim is achieved by evaluating the possibilities and making pairwise comparisons between them. Table 3.7 presents the conducted comparative analysis at the basic scale ranges.

An $n \times n$ matrix is constructed using the quantity of alternatives, denoted as n . a_{ij} are appended to Matrix A, in which j represents the alternative that juxtaposed with i which denotes the foundational alternate for contrast. The value 5 is assigned to A_{ij} , which may be interpreted as an indication that i is in control of j , provided that i 's contribution to the criterion being evaluated is exceptionally substantial in comparison to j . Understanding the correlation between matrix A, its higher eigenvalue λ , and the associated vector x constitutes the initial stage in deriving the priority vector x , as illustrated subsequently:

$$a_{ji} = 1/a_{ij} \quad (3.4)$$

When assessments are consistent:

$$a_{jk} = a_{ik}/a_{ij} \quad (3.5)$$

In the context of evaluating i , k and j represent two alternatives.

$$A_x = \lambda x \quad (3.6)$$

Comparisons are conducted by constructing matrices using the identical process and scale as demonstrated in Table 5. The criteria priorities are utilized as factors to compute the alternatives priorities inside every criterion, ultimately determining the alternatives priorities in relation to the general goal. Prior to computing the priorities for each matrix with n choices, evaluations are done based on relation 1 and the condition that the diagonal $a_{ij} = 1$.

The subsequent are the sequential procedures for constructing AHP system:

- **Phase 1:** Construct a hierarchy consisting of three different stages. The objective is to reach Stage 1, which serves as the target. Stage 2 represents the standards that need to be met, while Stage 3 consists of different alternatives, as depicted in Figure 3.3.
- **Phase 2:** Build a matrix for performing the pairwise assessment. Table 3.7 demonstrates that Saaty's nine-point range is the basis for the elements of every matrix. The importance assigned to different criteria is evident in the pairwise assessment.
- **Phase 3:** Create the matrix of inputs according to the information provided in Table 3.8. The scale of this matrix is determined according to individual experience.
- **Phase 4:** Build the normalization matrix according to the information provided in Table 3.9. The matrix is normalized by the division of each component into the entire components.
- **Phase 5:** The weight of each criterion is computed as shown in Table 3.9.
- **Phase 6:** The alternatives are ranked as shown in Table 3.10.

Sufficient data is collected, and their consistency is examined in order to determine if the decision made is consistent or not. The consistency ratio (CR) is calculated as the ratio of the consistency index (CI) to the random inconsistency (RI). The CI is determined using the formula $CI = (n_{max} - n) / (n - 1)$, while the RI is calculated using the formula $RI = 1.987(n - 2) / n$. In order for complete inconsistency to be deemed agreeable, the consistency ratio must be equal to or below 10%. If not, the quality of judgment data has to be improved. The study demonstrates a high level of consistency, with a coefficient of 0.04, as indicated in the subsequent section.

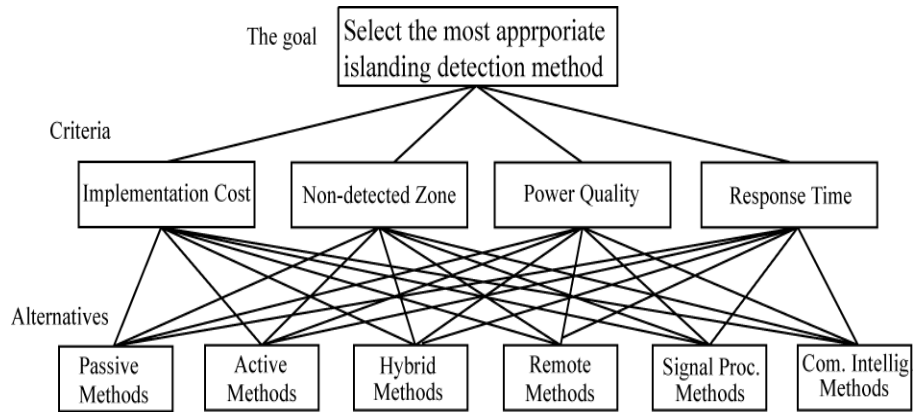


Fig. 3.3. Proposed hierarchy structure

Table 3.7. Matrix of pair-wise assessment.

Degree of relative significance	Meaning
1	Equally significant
3	Slightly preferable
5	Highly preferable
7	Very highly preferable
9	Exceptionally preferable
2,4,6,8	Intermediary judgment between two consecutive judgments

Table 3.8. Matrix of inputs.

	Initial Passive	Active	Hybrid	Remote	Signal Processing	Computational intelligent
Criterion 1	Execution Expense					
Passive	1	3	5	9	5	7
Active	1/3	1	3	5	3	5
Hybrid	1/5	1/3	1	5	1	7
Remote	1/9	1/5	1/5	1	1/7	1/3
Signal Processing	1/5	1/3	1	7	1	7
Computational intelligent	1/7	1/5	1/7	3	1/7	1
Sum	1.987	5.066	10.342	30	10.285	27.333
Criterion 2	Undetectable Area					
Passive	1	1/5	1/5	1/7	1/9	1/9
Active	5	1	1/3	1/9	1/9	1/9
Hybrid	7	3	1	1/9	1/9	1/9
Remote	7	9	9	1	1/3	1/3
Signal Processing	9	9	9	3	1	1
Computational intelligent	9	9	9	3	1	1
Sum	38	31.2	28.53	7.37	2.67	2.67
Criterion 3	Power Quality					

Passive	1	9	7	1	1	1
Active	1/9	1	1/3	1/9	1/9	1/9
Hybrid	1/7	3	1	1/7	1/7	1/7
Remote	1	9	7	1	1	1
Signal	1	9	7	1	1	1
Processing						
Computational	1	9	7	1	1	1
intelligent						
Sum	4.254	40.000	29.333	4.254	4.254	4.254
Criterion 4	Time to Respond					
Passive	1	5	9	7	1	3
Active	1/5	1	5	3	1/5	1/3
Hybrid	1/9	1/5	1	1/3	1/9	1/7
Remote	1/7	1/3	3	1	1/7	1/5
Signal	1	5	9	7	1	3
Processing						
Computational	1/3	3	7	5	1/3	1
intelligent						
Sum	2.787	14.533	34.000	23.333	2.787	7.676

Table 3.9. Normalized matrix.

Normalization								
Criterion 1	Execution Expense						Weight	W%
	Passive	Active	Hybrid	Remote	Signal	Computational		
					Processing	Intelligent		
Passive	0.503	0.592	0.483	0.300	0.486	0.256	0.436667	43.66
Active	0.167	0.197	0.290	0.166	0.291	0.182	0.2155	21.55
Hybrid	0.100	0.065	0.096	0.166	0.097	0.256	0.13	13
Remote	0.055	0.039	0.019	0.033	0.013	0.012	0.0285	2.85
Signal	0.100	0.065	0.096	0.233	0.097	0.256	0.141167	14.11
Processing								
Computational	0.071	0.039	0.013	0.1	0.013	0.036	0.045333	4.53
intelligent								
Criterion 2	Undetectable Area							
Passive	0.026	0.006	0.007	0.019	0.042	0.042	0.024	2.40
Active	0.132	0.032	0.012	0.015	0.042	0.042	0.046	4.60
Hybrid	0.184	0.096	0.035	0.015	0.042	0.042	0.069	6.90
Remote	0.184	0.288	0.315	0.136	0.125	0.125	0.196	19.6
Signal	0.237	0.288	0.315	0.407	0.375	0.375	0.333	33.3
Processing								
Computational	0.237	0.288	0.315	0.407	0.375	0.375	0.333	33.3
intelligent								
Criterion 3	Power Quality							
Passive	0.235	0.225	0.239	0.235	0.235	0.235	0.234	23.4
Active	0.026	0.025	0.011	0.026	0.026	0.026	0.023	2.3
Hybrid	0.034	0.075	0.034	0.034	0.034	0.034	0.041	4.1
Remote	0.235	0.225	0.239	0.235	0.235	0.235	0.234	23.4
Signal	0.235	0.225	0.239	0.235	0.235	0.235	0.234	23.4
Processing								
Computational	0.235	0.225	0.239	0.235	0.235	0.235	0.234	23.4
intelligent								
Criterion 4	Time to Respond							
Passive	0.359	0.344	0.265	0.300	0.359	0.391	0.336	33.6
Active	0.072	0.069	0.147	0.129	0.072	0.043	0.089	8.9

Hybrid	0.040	0.014	0.029	0.014	0.040	0.019	0.026	2.6
Remote	0.051	0.023	0.088	0.043	0.051	0.026	0.047	4.7
Signal Processing	0.359	0.344	0.265	0.300	0.359	0.391	0.336	33.6
Computational intelligent	0.120	0.206	0.206	0.214	0.120	0.130	0.166	16.6

Table 3.10. Alternative ranking.

Criterion 1		Execution Expense	
	Weight (%)		Ranking
Passive	43.66		1st
Active	21.55		2nd
Hybrid	13		4th
Remote	2.85		6th
Signal Processing	14.11		3rd
Computational intelligent	4.53		5th
Criterion 2		Undetectable Area	
Passive	2.40		5th
Active	4.60		4th
Hybrid	6.90		3rd
Remote	19.6		2nd
Signal Processing	33.3		1st
Computational intelligent	33.3		1st
Criterion 3		Power Quality	
Passive	23.4		1st
Active	2.3		3rd
Hybrid	4.1		2nd
Remote	23.4		1st
Signal Processing	23.4		1st
Computational intelligent	23.4		1st
Criterion 4		Time to Respond	
Passive	33.6		1st
Active	8.9		3rd
Hybrid	2.6		5th
Remote	4.7		4th
Signal Processing	33.6		1st

3.12 Analysis using Expert Choice Software

There are three significant elements of the proposed hierarchy model as illustrated in Figure 3.4 namely the main purpose, which is choosing the scheme of islanding identification, the criteria which are the execution expense, the undetectable area, quality of power, and time to respond, and the alternative which refers to the four categories of islanding identification scheme as discussed previously. The pair-wise assessment is carried out to evaluate the components once the model is prepared. This assessment is performed by evaluating the alternatives based on the criteria

mentioned in Figure 3.5. According to Saaty's 1–9 scale, the judgments are decided and if any alternative is assessed by itself, it will assign a value of "1" which will be presented along the main diagonal of the matrix.

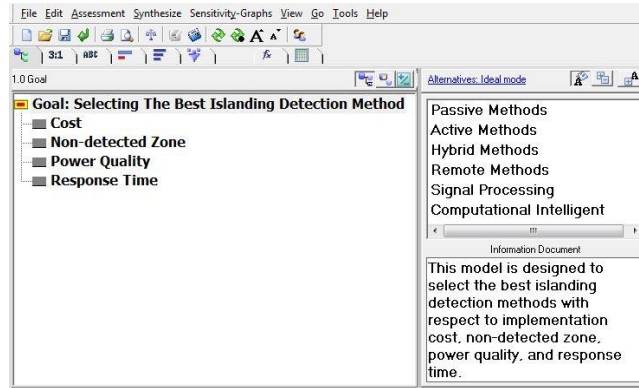


Fig. 3.4. The framework of proposed hierarchy model

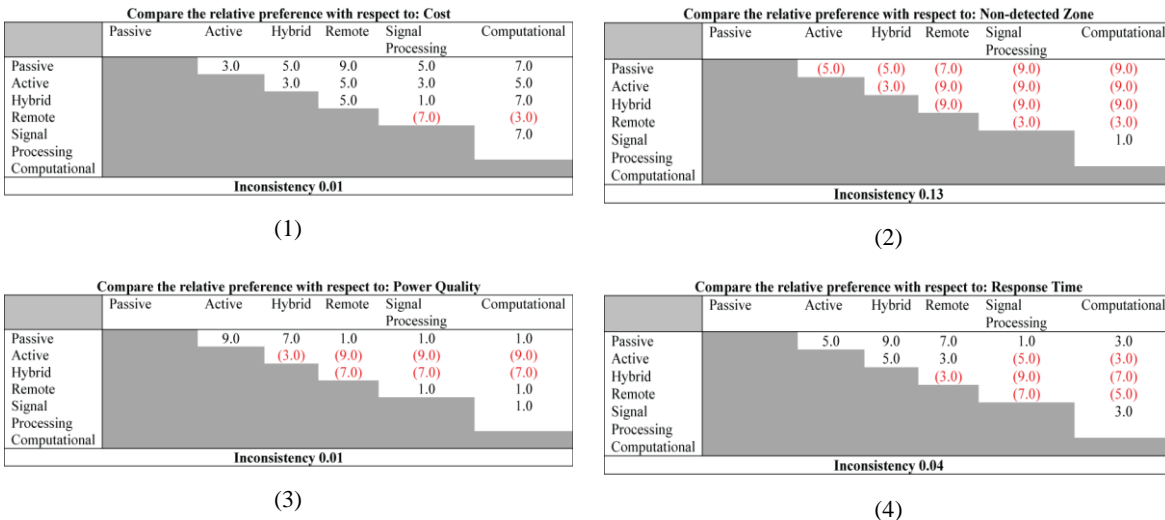


Fig. 3.5. Pair-wise assessment in relation to (1) execution expense, (2) undetectable area, (3) quality of power, and (4) time to respond

Priority values are determined after the process of comparing each pair is finished. This study assigns equivalent importance to execution expense, undetectable area, quality of power, and time to respond as they relate to the core purpose. The properties, as seen in Figure 3.6, are established by comparing the corresponding preferences for every criterion.

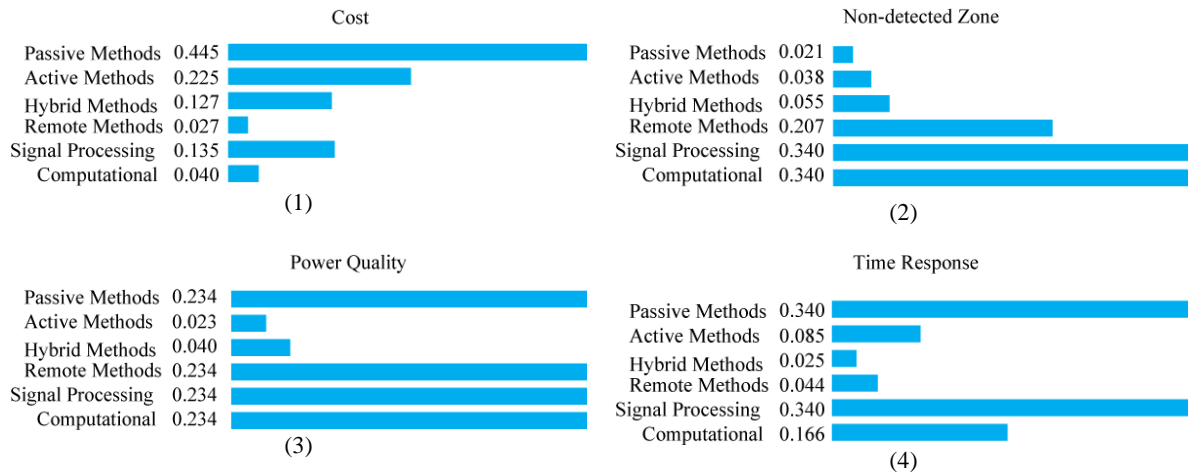


Fig. 3.6. The determination of priorities pair-wise assessment for (1) execution expense, (2) undetectable area, (3) quality of power, and (4) time to respond

The optimum mode is utilized to merge the local preferences across all criteria and ascertain the global priority. According to Figure 3.7, the total consistency is 0.04. The relative weights assigned to different schemes are as follows: (24.7%, 7.8%, 5.6%, 14.5%, 14.5%, 26.6%, 20.8%) for passive, active, hybrid, remote, signal processing, and computational intelligence schemes respectively. These weights are determined by comparing all criteria together. Based on the total weight, signal processing schemes are the most proper options to pick up, while hybrid schemes are the least proper. Sensitivity assessment may be employed in decision-making by making modest alterations to the input data in order to see the resulting influence on the outputs. When the ranking remains unchanged, the results are considered reliable. The sensitivity assessment, which is shown in Figure 3.8, ensures that whenever all criteria are given the same importance the greatest alternative and objectives priority go refer to schemes of signal processing with percentages of 55% and 27% respectively and the least goes to hybrid schemes with percentages of 10% and 5% respectively.

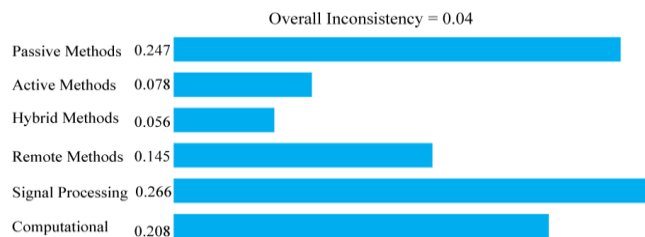


Fig. 3.7. Optimizing global priorities using the optimum mode

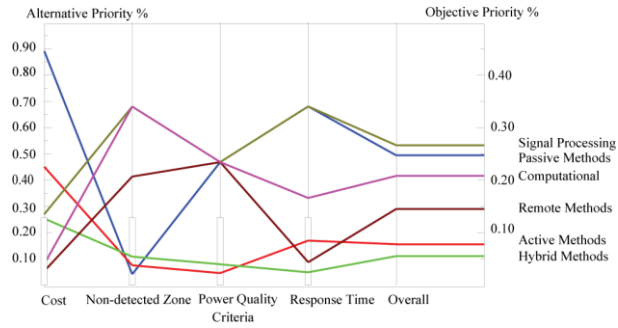


Fig. 3.8. Functioning sensitivity

3.13 Conclusion

In this chapter the four categories of islanding identification schemes are evaluated using AHP analysis model. The effectiveness of this model is validated by evaluation of those four categories using various parameters such as execution expense, undetectable area, quality of power, and time to respond. If the only aspect being examined is the execution expense, then passive schemes are the optimal choice. If the only aspect being examined is the undetectable area, then computational intelligence or signal processing schemes are the optimal choice. If the only aspect being examined is the quality of power, then computational intelligence, signal processing, remote, or passive schemes are the optimal choice. If the only aspect being examined is the time to respond, then signal processing, and passive schemes are the optimal choice. Nevertheless, if the whole aspects are being examined together, then signal processing, and passive schemes are the optimal choice to pick up.

4. Phasor Measurement Estimation

7.1 Background

An increasingly dynamic power grid is being created by the unbundling of vertically integrated electrical utilities, the involvement of multiple independent players in the energy markets, the integration of renewables to fulfill the ever-growing need for load, and the requirement to eliminate emission footprints. This makes real-time wide-area monitoring, protection, and control (WAMPAC) of the electrical grid crucial. Regarding the typical SCADA system and the corresponding asynchronous measurements, WAMPAC's low reporting rate renders it insufficiently prepared.

Phasor measurement unit (PMU) innovation is a result of advancements in phasor estimate methodologies and technology of synchronized measurement (SMT) with the aid of the Global Positioning System (GPS). PMU will strengthen WAMPAC's tendency even more.

Synchrophasor refers to a phasor that is synced in time. PMUs are the measurement instruments used to measure synchrophasors. In essence, a PMU is a digital recorder with synchronization capabilities. A PMU that is located at each node monitors the voltage phasor there as well as any branch current phasors that are incident to the node, depending on the frequency, rate of frequency change, and availability of channel capacity. Coordination of system-wide measurements can be achieved by placing several PMUs. Phasor measurements of power system events can also be time-stamped, recorded, and stored by PMUs. Table 4.1 lists the fundamental characteristics of the PMU in relation to the SCADA measurements. As a result, the power system's visibility will be improved by the PMUs' integration into the system and their aid in the power system state estimate process.

Table 4.1. A comparison between PMU and SCADA data.

SCADA Data	PMU Data
Rate of scan: 2s	Rate of scan: 25-30 samples/s
solely provides magnitude measurements.	provides phasor measurements
Not quick enough to react to changing circumstances	Quick enough to show the behavior of the system
Time stamping for particular values and cases	GPS-synchronized data that is fully time-tagged

4.2 Wide Area Measurement System

A wide-area measurement system is also known as a monitoring system that, as Figure 4.1 illustrates, gathers more coarse-grained data that is characterized by parameters collected via the coordinate system in real time and synchronization and uses that data for harmless functioning, optimized acquisition, and network dependability. This cutting-edge measurement technology offers excellent operational structure and informative tools to support the analysis and examination of the intricate performance displayed by high voltage grids. If the readings gained from different areas of the grid were not made at precisely the same moment, they would lack complete integration. The synchronization of the readings is the primary prerequisite for WAMS. The readings are perfectly chrono-synchronized with the GPS, which is based on satellites. After this, an integrated and highly-resolution picture of the operational conditions of the power system is obtained by combining these measurements. The PMU, that generates excellent bus angles and frequencies measurements together with more traditional characteristics, is the main and primary source of data for this specific network [146]. In its current configuration, WAMS can be utilized as an independent framework to enhance the network's conventional SCADA approach. WAMS is primarily designed as a complimentary technique to enhance conditional awareness and surveillance in actual time by operator involvement and the information shared amongst systems to confirm a protected and dependable electrical network functioning. In particular, this wide-area data visualizes the system's overall dynamic condition.

When the Western power grid failed on the 10th of August 1996, a major contribution incorporating WAMS technologies was demonstrated. The Western power system experienced a significant loss of load and was split into four asynchronous islanded areas during this specific blackout. Comparing to the dynamic data that WAMS offers, the results of this particular separation have prompted the power utilities to implement remedial action schemes (RAS), which are just one of many strategic methods. The data reaffirmed how heavily the present strategy models rely on the operation of the power grid in the WECC. Furthermore, it was shown that the models were insufficient for forecasting the responses of the network. With WAMS, data that comprise the early warning signs of an imminent power outage are by far its greatest benefit. The impact of the disturbance might have been reduced if the operators had been able to use this information to respond cautiously. One of the main forces behind further WAMS improvement and augmentation was the cascading failure of 1996.

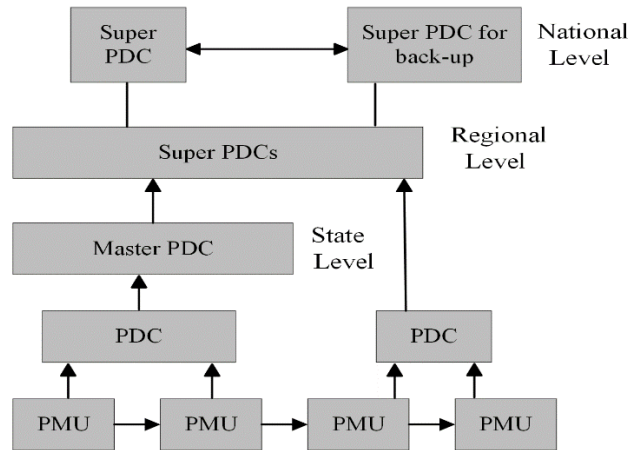


Fig. 4.1. WAM structure

5.3.1 Phasor Measurement Unit

The Phasor Measurement Unit (PMU) is used to measure various parameters of the grid system such as frequency, current, and voltage. It has the ability to measure the synchronized voltage and current phasors. This synchronization may be achieved by a time sampling of the current and voltage waveforms using a common synchronizing signal from the GPS. As a result, the PMU is the most effective and significant measuring tool for network safety, management, and supervising mentioned above. The PMU synchronizes the sample clocks with GPS transmission to calculate phasors using a shared reference. The Virginia Tech laboratory built the first PMU. PMUs offer real-time power system status information. The GPS delivers pulses with a precision of $1 \mu\text{s}$ which corresponds to 0.018° for a 50 Hz system. A PLL generates the sample pulses for the GPS signal with 1PPS [147]. The Phasor Measurement Unit's functional representation is presented in Figure 4.2.

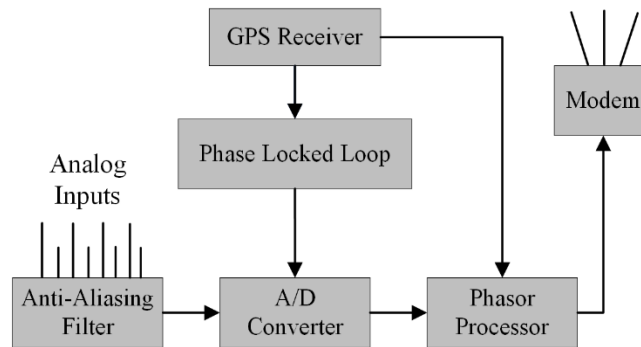


Fig. 4.2. The PMU's functional block diagram

A modem is a device that connects PMU to other components of a power network, like state estimation and wide-area management. Information generated by PMU is transmitted and received by the modem. The majority of anti-aliasing filters are analogue devices that process the signal prior to sampling. It is easier to limit a signal's bandwidth by using an anti-aliasing filter before the signal in order to satisfy the Nyquist-Shannon sampling principle. The signal's sampling frequency ought to be doubled to the highest frequency when the sampling operation is finished. If the sampling rate is lower than twice the highest frequency of a signal, the data from the original signal cannot be recovered. Anti-aliasing filters are therefore employed to restrict a signal's bandwidth in order to satisfy the sampling theorem's requirement. The output of anti-aliasing filters is obtained through the use of analog to digital converters in order to transform sampled signals. These signals are first received and subsequently converted via an analogue to a digital converter in order to get a suitable range of input signals. These analog signals are sent from anti-aliasing filters into analog to digital (A/D) converters for the digitalization process. Following conversion, a signal's sampling rate is established by phase lock loop (PLL). Subsequently these signals are sent to the microprocessor by the A to D converter (ADC). To precisely track a system reaction, one uses the Global Positioning System. It offers facts, data, and the location of an object on any given section. These satellites are delivering a signal of "one pulse per second" with an accuracy of $1\mu\text{s}$ in order to sample input signals. Additionally, GPS is essential for improving the performance of wide-area management and effectively offers a route for PMU measurement monitoring. The PLL fundamental idea is to recognize the behavior of signals and create a phase difference between them. By adjusting the loop frequency and creating a phase difference between two phasor signals, this process is accomplished. A phase lock oscillator splits the GPS data, which is one pulse per second, into an appropriate range of pulses per second for the purpose of sampling the data. To obtain precise and accurate measurements, a phase lock loop circuit (PLLC) in a PMU device immediately synchronizes the data. The PMU device then produces data at up to ten kHz high sampling rate. When the circuits of PLL of PMU tools are utilized, phasor differentiation between more than two phasor quantities becomes simple. Phasor microprocessors get the GPS information and the sampled data from PLL. The current and voltage magnitudes are next optimistically blended. A recursive approach of Discrete Fourier transform (DFT) is employed to handle the data. The phasor microprocessor, which regulates a signal's information flow throughout the system, is regarded as the PMU device's heart. Furthermore, the two algorithms-

recursive and non-recursive-that are used to determine a signal's amplitude, magnitude, and phase angle refer to DFT's component parts.

- **Recursive method**

The following is the equation for the recursive process used to calculate and compute the signal response:

$$x^{-N+r} = x^{-N+r-1} + \frac{\sqrt{2}}{N} (X_{N+r} - XR)e^{-jr\theta} \quad (4.1)$$

A recursive algorithm divides the problem into smaller inputs for ease of use, and then combines the solution after the problem has been solved. Recursive algorithms are also helpful in computing signal behavior because they are more dependable, efficient, and useful in signal computation. For a sinusoidal waveform to continue, the phasor rotates counterclockwise. A recursive algorithm eliminates error (irrelevant information) in order to make this waveform systematically stable. The discrete Fourier transform (DFT) computation is regenerated in all phasors, making the recursive technique computationally demanding.

- **Non-recursive method**

For the purpose of calculating the matrices, or input/output size, which indicates the signal behavior as described below, the non-recursive equation is employed.

$$x^{-N+r} = \frac{\sqrt{2}}{N} \sum_{K=0}^{N1} 1x_k e^{-jK\theta} \quad (4.2)$$

A non-recursive algorithm is a method for solving mathematical problems that has been implemented in a programming language. It addresses every issue without the need for more methods and does not need recursion. Despite having a larger code size, it is simple to implement and doesn't require much time. Recursive methods are the only ones that can execute complex operations, though occasionally both recursive and non-recursive methods can do a given task. It is found that MATLAB is used to carry out the majority of these methods.

4.2.2 Phasor Measurement Technique

A pure sinusoidal waveform can be represented as a phasor, a unique complex number.

Consider a sinusoidal signal like follows:

$$X(t) = X_m \cos(\omega t + \theta) \quad (4.3)$$

This signal's phasor representation is expressed as:

$$X(t) = \frac{X_m}{\sqrt{2}} e^{j\theta} = \frac{X_m}{\sqrt{2}} (\cos\theta + j\sin\theta) \quad (4.4)$$

In Figure 4.3, the sinusoidal signal and its phasor representation are presented. Typically, a signal's phasor representation can be determined by applying the input signal to the Discrete Fourier Transform (DFT).

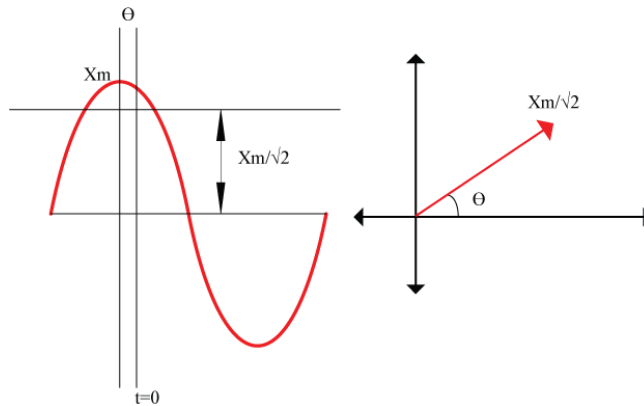


Fig. 4.3. A sinusoidal signal's phasor representation

4.2.3 Discrete Fourier Transform

The phasor computation needs sampled data; hence a filter that prevents aliasing should be added to the signal before capturing data samples. The pass band's bandwidth is limited by an anti-aliasing filter to be below or equal to (\leq) 50% of the frequency of data sampling.

The Nyquist criterion must be satisfied by this requirement. Subsequently, the phasor estimator computes the input signal's phasor representation.

If N samples of a time-varying signal evaluated for single period are represented by X_k ($k=1, 2, 3 \dots N-1$), hence the phasor notation is given by,

$$X = \frac{\sqrt{2}}{N} \sum_{k=0}^{N-1} X_k e^{-j2\pi k/N} \quad (4.5)$$

It is noted that the DFT produces complex conjugate components at ' $\pm\omega$ ' for real input signals. The input signal's harmonics are eliminated by the DFT. Because phasor calculation is a continuous operation, PMUs employ several updating formulas. Both recursive and non-recursive methods can be used to estimate phasors under nominal frequency conditions. The computing complexity of the non-recursive calculations prevents them from being recommended, even though they are numerically stable. A recursive formula that maintains the same multipliers for common samples in two windows can solve this issue.

4.2.4 Estimation of Frequency Amplitude and Frequency Rate of Change

Frequency and ROCOF are measured, computed, and reported by a PMU. Synchrophasors are always calculated with respect to the nominal frequency (f_o) of the system. The phasor ought to be calculated ten, twenty-five, or fifty times every single second with a rated frequency $f_o = 50$ Hz. The instantaneous (time-varying) frequency f_{in} of (4.3) is provided by:

$$f_{in}(t) = f_o + \frac{1}{2\pi} \frac{d\theta(t)}{dt} \quad (4.6)$$

Moreover, ROCOF is described as:

$$ROCOF(t) = \frac{1}{2\pi} \frac{d^2\theta(t)}{d^2t} = \frac{df_{in}(t)}{dt} \quad (4.7)$$

The accuracy, disturbance susceptibility, and response time of the various phasor computation techniques can differ. The fully compliant approach employed in this research is employed with flat-top Finite Input Response (FIR) filters [148, 149]. The flat-top FIR filters were utilized to

compute phasors [148] using time-based signals that were first recorded at 0.1 MHz sampling frequency and then resampled to 800 Hz sampling frequency.

Cosine windows were the flat-top windows presented as [148]:

$$W_M[n] = \begin{cases} \sum_{m=0}^M a_M[m] \cos\left(m \frac{\pi}{N} n\right), & n = -N, \dots, N \\ 0, & \text{otherwise} \end{cases} \quad (4.8)$$

where $a_M[m]$ representing the coefficients of the M order window and M is the window's order. The window $w_M[n]$ (4.6) length is $L = 2N + 1$ and it is symmetrical:

$$W_M[n] = W_M[-n] \quad (4.9)$$

The window coefficients $a_5 = [1.004854; 2.007611; 1.917918; 1.451047; 0.666862; 0.130977]$ were utilized for phasor estimation. Phasors were reported with a nominal frequency of 50 Hz and estimated over a period of time equivalent to ten periods of the rated frequency, or 200 ms.

4.3 Phasor Measurement Unit Techniques for Islanding Detection

The distribution of PMUs at numerous sites and the vibrant outcome of PMUs in grid network are utilized to calculate multiple-area estimation. Therefore, PMU detection can be achieved by analyzing the basic phasors of frequency, current, and voltage with synced harmonic phasors. Power systems need to be coordinated and controlled across a wider area in order to enhance detection when islanding occurs [150]. This is especially the case for long-distance electricity transmission on the island. Wide-range detection without network disturbance is possible with the PMU when the transmission of power is engaged within several control zones [151]. PMU has the capability to solve complex problems of a big size that traditional approaches are unable to manage. Additionally, it is capable of receiving data from extensive distances. Nevertheless, the comprehensive foundation for detecting islanding on a broad scale is not easily solved. Some of the most crucial elements of the PMU technique are as follows:

- The measured parameters are precise.
- Capable of providing more accurate data.

- Compared to conventional measures, the error is minimal.
- Ability to detect islanding when DG and the utility have matching frequency conditions.

For more accurate and precise islanding detection, a synchronized PMU is required. The required features can be computed and recorded by PMU. The PMU's margin of error is negligible in comparison to conventional measures.

When injecting network disturbances, several conventional techniques have the potential to affect the system; however, PMU is not affected by this problem. But that PMU method has the following shortcomings:

- Communication delays occur because of the shared or dedicated medium when transferring the time stamp in real time [152].
- Technical problems with the PMU's numerous components could result in missing data points [153,154].

A PMU that is part of the method group focused on communication needs to be competent to detect fluctuations within the threshold values of voltage and frequency in order to operate safely. However, aliasing can contaminate oscillations if they happen more than 0.5 Hz above or below the rated frequency. It also happens if the frequency is lower than 0.5 Hz compared to the rated frequency. The safe limit for voltage and frequency can be reached, which can then activate the islanding detecting mechanism. The sampling scheme report for the transmission network, presented in [154], stated that when the error is less than 1%, the PMU approaches can be considered precise. The PMU schemes for islanding identification are shown in Table 4.2.

Table 4.2. Techniques for detecting islanding using PMU parameters.

Ref.	Objectives	Contributions	Limitations
[155]	The PMU's frequency parameter is used for islanding detection. Utilize the PMU's data to observe islanding incident by calculating the phasor and angle of rotor [79]. Uses PMU to assist in islanding identification by employing the voltage at the coupling point, the rate of change of the inverse hyperbolic cosecant function, and the islanding detection monitoring factor [80].	Through establishment of a suitable threshold, the suggested algorithm can prevent false tripping. The timing of fault occurrence and clearing can be predicted by the proposed method. The algorithm's ability to distinguish between scenarios with and without islanding is fast, dependable, and secure.	The algorithm did not take the NDZ into consideration.

[156-160]	For controlled islanding, a hybrid transient stability evaluation model has been put out [80]. Developed a approach for regulated system separation Argentine power system based on PMUs [81]. proposed a voltage angle-based PMU-based islanding detection technique [82,83].	The proposed islanding technique is effective in averting transient instability. able to lessen the impact of serious fault incidents. From a practical and real-time implementation standpoint, this approach shows to be simple, quick, and economical.	The DG-utility match frequency conditions were not considered via the suggested approach.
[161]	The PMU is being used to detect the islanding of a huge photovoltaic power plant by collecting frequencies.	With fewer false triggers during islanding events, the proposed approach may observe islanding incidents.	There isn't a set method or procedure for figuring out threshold frequency and time.
[162]	An islanding detection approach based on linear programming formulation was implemented out.	The decision time of the proposed scheme is quicker.	When the inverter and main grid have a match frequency condition,
[163]	Frequency data obtained by the PMU to detect instances of abnormal conditions.	Reducing the number of necessary communications resulted in a reduction of processing time.	the algorithm fails to detect islanding events.
[164]	To employ the angle of voltage angle to enter to a shield DG against islanding occurrences.	The suggested approach is straightforward and simple to use.	When calculating the threshold values, there is no comprehensive explanation or formula.

As discussed earlier, there are a number of islanding detection techniques, but only a select handful are effective in the conditions of match frequency islanding. Nevertheless, the current algorithm's extended detection time was necessary to identify the match frequency. Furthermore, distinguishing between a transient fault and a real islanding event is a crucial aspect of the islanding detection algorithm. However, the majority of cases in the literature simply display the abnormal conditions within the system, leaving out the formation of islanding.

4.4 Phasor Measurement Unit Technique for Feature Extraction

Various features and system parameters have been selected from PMU with a focus on synchronous and inverter-based distributed generation. To incorporate as many factors as feasible that may be impacted by islanding within the network, three characteristics were measured locally. On the island side, measurements are obtained. Among the features that were extracted are the following:

Table 4.3. Features extracted from PMU.

Features	Description
Voltage	Potential energy of electricity per unit charge.
Frequency in Hz	The frequency with which an event repeats itself in a certain amount of time.
Rate of change of frequency	Time-to-frequency variation ratio $\frac{\Delta f}{\Delta t}$

The behavior of voltage and current has been observed during unintentionally islanding for three scenarios. Firstly, the system combined both the PV inverter and the main power supply side. Secondly, the utility grid was connected to the synchronous generator. Thirdly, both the PV inverter and synchronous generator were connected to the utility grid. The waveforms of voltage during the normal and abnormal conditions were simultaneously gained via PMUs regarding each envisioned scenario. The National Instruments NI6040E platform, shown in Figure 4.4, served as the foundation for developing the measurement.

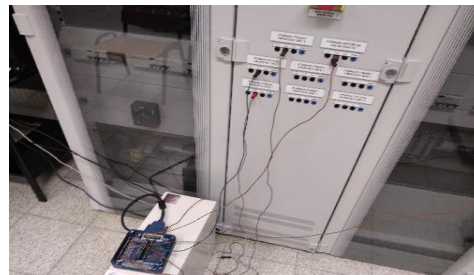


Fig. 4.4. Measurement platform

- **Case 1:** Grid linked- PV Inverter

Based on this case, the inverter output power of PV system was 1 KW, 1.5 KW, and 3 KW respectively. The connected load was linear, non-linear load and both, as illustrated by Table 4.4.

Table 4.4. Scenarios of islanding for grid-linked PV Inverter.

Scenario	PV Power [W]	Load Type
1	1000	Linear
2	1500	Non-linear
3	3000	Linear +non-linear

Figure 4.5 presents microgrids main bus voltage as well as a current of PV inverter for scenarios 1, 2, and 3 respectively. Figure 4.6 presents voltage amplitude, frequency and ROCOF of voltage for scenarios 1, 2, and 3 respectively.

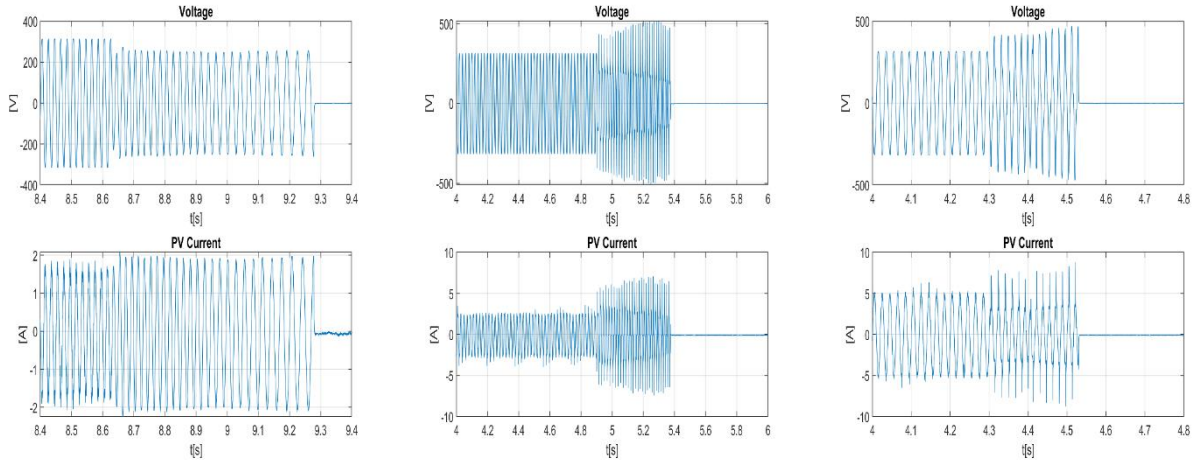


Fig. 4.5. Voltage and current for first, second , and third scenarios

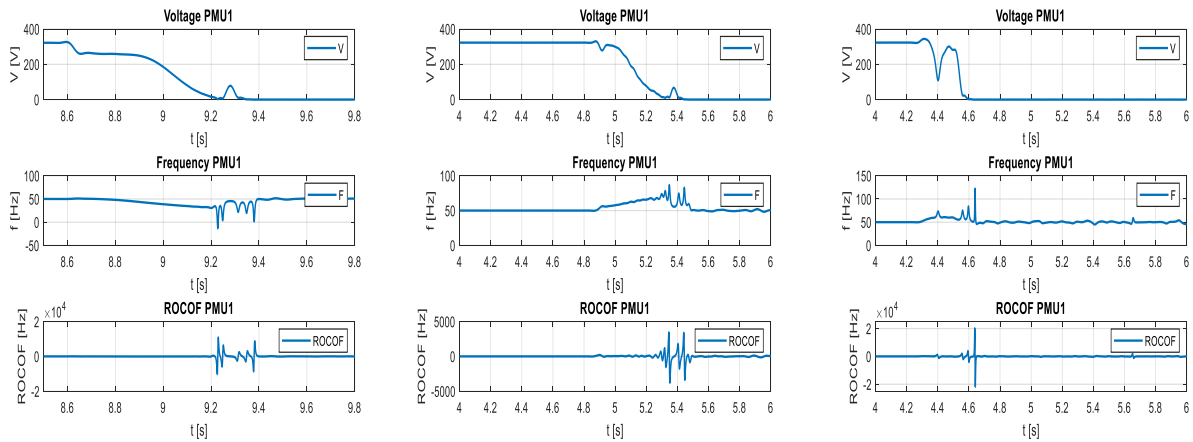


Fig. 4.6. Amplitude of voltage phasor, frequency and ROCOF for scenarios 1, 2, and 3

Table 4.5 displays the highest, lowest, and average values of phasors for the inverters that were evaluated. The voltage values recorded for scenario 3 ranged from the lowest (0.0040 V) to the highest (344 V).

Table 4.5. Phasors readings.

Scenario	Highest Phasor [V]	Lowest Phasor [V]	Average Phasor [V]
1	340.2	0.0333	175.7
2	341.4	0.1152	204.6
3	344	0.0040	175.1

Table 4.6 displays the highest, lowest, and average frequency values for the inverters that were evaluated. The frequency values recorded for scenario 1 ranged from -13.5 Hz to 149.36 Hz, with -13.5 Hz being the lowest and 149.36 Hz being the highest.

Table 4.6. Frequency readings.

Scenario	Highest Freq. [Hz]	Lowest Freq. [Hz]	Average Freq. [Hz]
1	149.36	-13.5	49.74
2	86.86	47.25	50.96
3	122.48	44.66	50.43

Table 4.7 displays the highest, lowest, and average rate of change of frequency (ROCOF) for the inverters that were evaluated. The frequency for scenario 1 was recorded with both the lowest value (-3.21×10^4 Hz/s) and the greatest value (3.2×10^4 Hz/s).

Table 4.7. ROCOF readings.

Scenario	Highest ROCOF [Hz/s]	Lowest ROCOF [Hz/s]	Average ROCOF [Hz/s]
1	3.2×10^4	-3.21×10^4	-0.0054
2	3.4×10^3	-3.8×10^3	-0.1153
3	2.02×10^4	-2.17×10^4	-0.2106

- **Case 2:** Grid Linked-Synchronous Generator

Based on this case, the inverter output power of synchronous generator was 10 KW, 10 KW, and 18KW respectively. The connected load was linear, non-linear load and both, as illustrated by Table 4.8.

Table 4.8. Scenarios of islanding for grid linked synchronous generator system.

Scenario	Synchronous Generator Power [W]	Load Type
4	10,000	Linear
5	10,000	Non-linear
6	15,000	Linear +non-linear

Figure 4.7 presents microgrids' main bus voltage as well as a current of synchronous generator inverter for scenarios 4, 5, and 6. Figure 4.8 presents voltage amplitude, frequency and ROCOF of voltage for scenarios 4, 5, and 6.

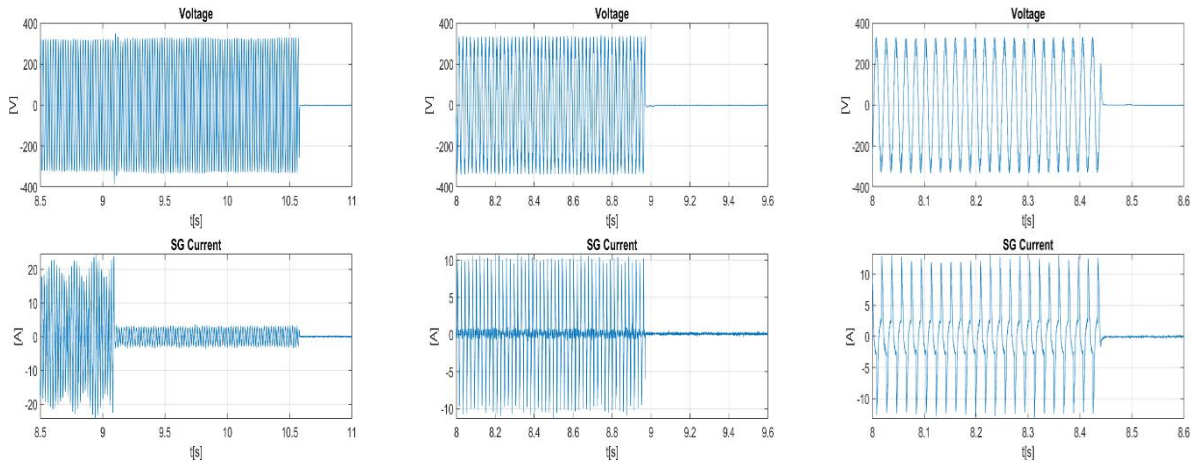


Fig. 4.7. Voltage and current for scenarios 4, 5, and 6

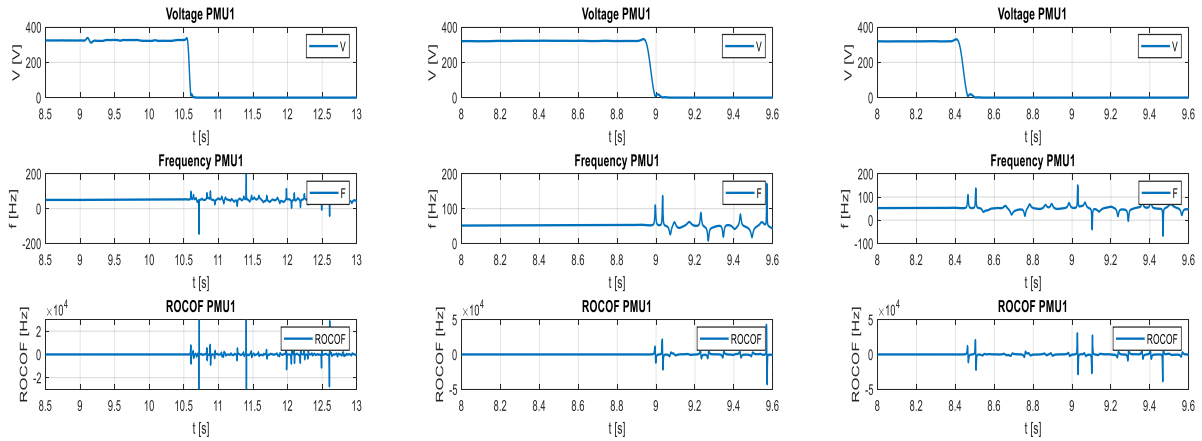


Fig. 4.8. Amplitude of voltage phasor, frequency and ROCOF for scenarios 4, 5, and 6

Table 4.9 displays the highest, lowest, and average values of the phasor for the synchronous generator that was evaluated. Scenario 6 recorded the lowest voltage value of 0.0001 V, while scenario 5 recorded the highest voltage value of 349 V.

Table 4.9. Phasors readings.

Scenario	Highest Phasor [V]	Lowest Phasor [V]	Average Phasor [V]
4	342.72	0.0005	77.05
5	349	0.0013	235.34
6	342.87	0.0001	267.25

Table 4.10 displays the highest, lowest, and average frequency values obtained from the tested synchronous generator. The lowest frequency value (-151.7 Hz) was recorded for scenario 4, while the highest frequency value (244.64 Hz) was recorded for scenario 6.

Table 4.10. Frequency readings.

Scenario	Highest Freq. [Hz]	Lowest Freq. [Hz]	Average Freq. [Hz]
4	236.64	-151.7	49.95
5	175.33	-104.8	50.56
6	244.64	-95.46	50.31

Table 4.11 displays the highest, lowest, and average rate of change of frequency (ROCOF) for the synchronous generator that was evaluated. The frequency values recorded for scenario 4 ranged from -8.05×10^4 Hz/s to 8.06×10^4 Hz/s, with -8.05×10^4 Hz/s being the smallest and 8.06×10^4 Hz/s being the highest.

Table 4.11. ROCOF readings.

Scenario	Highest ROCOF [Hz/s]	Lowest ROCOF [Hz/s]	Average ROCOF [Hz/s]
4	8.06×10^4	-8.05×10^4	0.0211
5	5.63×10^4	-5.97×10^4	-0.1080
6	7.84×10^4	-7.82×10^4	-0.2980

- **Case 3:** Grid linked- PV Inverter and Synchronous Generator

Based on this case, the output power of PV inverter and synchronous generator are presented in Table 4.12, and the connected load was linear.

Table 4.12. Scenarios of islanding for grid linked PV system and synchronous generator.

Scenario	PV Power [W]	Synchronous Generator Power [W]	Load Type
7	500	4,000	Linear
8	500	4,000	Linear +non-linear
9	400	6,000	Linear +non-linear

Figure 4.8 presents microgrids main bus voltage as well as a current of PV inverter for scenarios 8, 9, and 10. Figure 4.9 presents voltage amplitude, frequency and ROCOF of voltage for scenarios 8, 9, and 10.

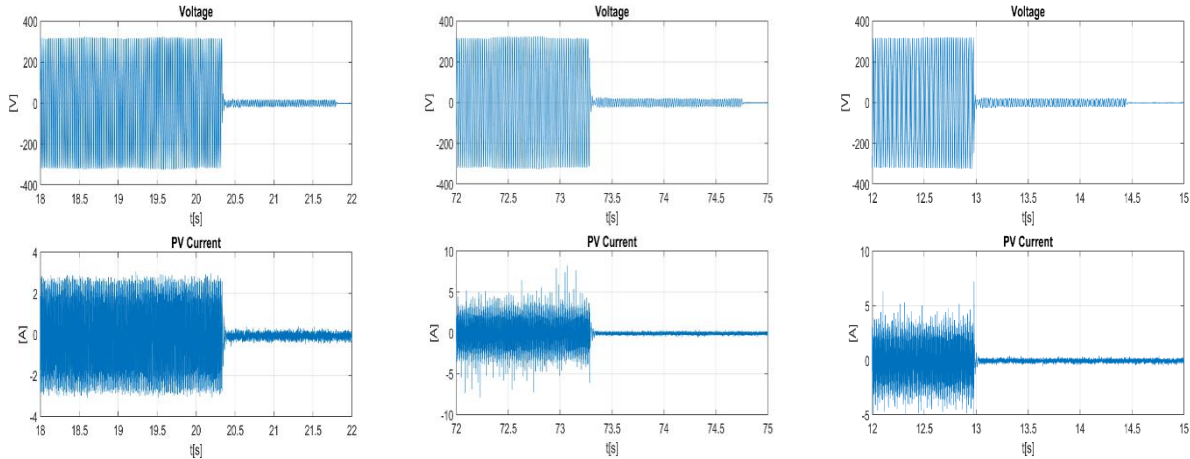


Fig. 4.9. Voltage and current for scenarios 8, 9, and 10

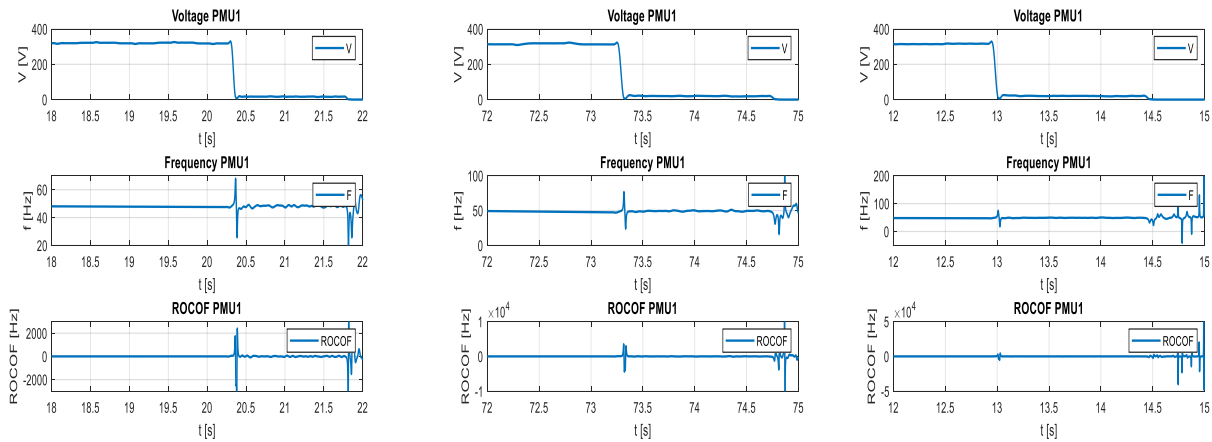


Fig. 4.10. Amplitude of voltage phasor, frequency and ROCOF for scenarios 8, 9, and 10

Table 4.13 displays the highest, lowest, and average values of the phasor for the tested system. The voltage values recorded for scenario 7 ranged from the smallest value of 0.0004 V to the highest value of 343.52 V.

Table 4.13. Phasors readings.

Scenario	Highest Phasor [V]	Lowest Phasor [V]	Average Phasor [V]
7	343.52	0.0004	225.32
8	342.77	0.0028	310.21
9	342.11	0.0015	263.19

Table 4.14 displays the highest, lowest, and average frequency values for the tested system. The lowest frequency value (-120.55 Hz) was recorded for scenario 7, while the highest frequency value (189.56 Hz) was recorded for scenario 8.

Table 4.14. Frequency readings.

Scenario	Highest Freq. [Hz]	Lowest Freq. [Hz]	Average Freq. [Hz]
7	170.94	-120.55	49.39
8	189.56	-13.89	49.94
9	213.68	-104.14	49.61

Table 4.15 displays the highest, lowest, and average rate of change of frequency (ROCOF) for the evaluated system. The frequency values recorded for scenario 7 ranged from -6.33×10^4 Hz/s to 6.49×10^4 Hz/s, with -6.33×10^4 Hz/s being the smallest and 6.49×10^4 Hz/s being the highest.

Table 4.15. Results for ROCOF.

Scenario	Highest ROCOF [Hz/s]	Lowest ROCOF [Hz/s]	Average ROCOF [Hz/s]
7	6.49×10^4	-6.33×10^4	0.0389
8	4.50×10^4	-5.0×10^4	0.0155
9	6.33×10^4	-6.14×10^4	-0.0798

4.5 Conclusion

PMUs are essential components of the islanding detection algorithms used in power systems. They offer the real-time data required to put several islanding detection methods into practice. Using PMUs to detect islanding, feature extraction is essential. The most important parameters are the absolute frequency value and its variation from the nominal frequency. The abrupt disconnecting of a section of the grid during islanding occurrences usually results in a large divergence in frequency. Setting thresholds to cause islanding detection alerts and keeping an eye on the frequency variation are two aspects of feature extraction. The rate of change in frequency over time is indicated by ROCOF. ROCOF values are raised when islanding events cause a sudden change in frequency. Finding the rate at which frequency changes over brief time intervals is necessary to extract ROCOF features. The abnormal frequency dynamics connected to islanding are subsequently identified by algorithms analyzing these ROCOF values. The features that are extracted and analyzed from PMU data allow islanding detection algorithms to detect abnormal grid circumstances that are linked to islanding events. This allows for timely measures to be taken in order to maintain grid stability and reliability.

5. Islanding Detection Classification

The developed scheme uses the waveform of voltage to precisely identify the incident of islanding by obtaining some significant features such as the voltage amplitude, the frequency, and ROCOF from the system. Following the utilization of every feature that was extracted as input for the classification procedure. The classification procedure is detailed below.

7.1 An overview of Theory of Artificial Neural Network

The idea of artificial neural networks (ANN), or just neural networks as a broad term, originated with neurobiological ideas that emphasized highly advanced computational capabilities. The digital computations that mimic the processing power of a human brain are not the same as the standard ANN approaches. Because the human brain performs the same computational tasks, the full ANN task may be replicated.

When using standard logic programs, a large amount of data memory is needed, and if the input sample is not in the lookup table, an error may be produced. The severity level can be more accurately determined with ANN, even inside shorting levels of 0.01%. In the event of unexpected inputs, it will classify it to the closest class and never provide an incorrect output.

The ANN uses multiple separate processing units to operate on the concepts of parallel distributed computing. For effective calculation, a large variety of knowledge can be stored in each processing unit. An electrical component or software may be used in its development.

An artificial neural network (ANN) resembles the human brain, which is analogous to how humans learn by assimilating data from their surroundings. The synaptic and interneuron connection is the primary unit in charge of gathering information. These neurons serve as the primary computational source. Information is exchanged across the many neurons using the available space, and the results are represented as weights. To achieve the intended goals, the data and weights are arranged using mathematical models such as sigmoid, linear, and others.

An artificial neural network (ANN) is a highly networked structure made up of many small processing units known as neurons. These processing units are interconnected through a cost known as links or weights. These properties enable ANN to learn from and gain knowledge of the

gathered environmental data. The many learning algorithms that are now in use can also teach the ANN new things.

The different forms of learning and training mechanisms can be used to characterize ANN learning designs. A few ANNs use the term "efficient learning process" to describe how well they can learn and solve problems depending on their training. Training ANNs are robust and have 0% fault tolerance when exposed to different unknown instances of the problem. Even if the pattern contains noisy information, the ANN can anticipate a new solution using the provided pattern based on its learning. With its computing development, this computation procedure can be completed quickly.

ANNs are widely used in a variety of applications, including as pattern recognition, label classification for given features, function approximation, weather forecasting, clustering similar objects without labels, optimization, control, and pattern completion. There are several ways to accomplish all of these conceptual applications. The classification mechanism, which classifies the pattern supplied into the network according to the activation set, is one of the often-used ANN mechanisms. Throughout the entire network, the activation functions-the primary mathematical calculation model-are distributed to produce the output units, which can be considered the classification's outcome.

5.2 Artificial Neural Network Model

An ANN's core processing unit is its neuronal architecture. These units are the ANN's designed models, as shown in Figure 5.1. Three key components are required for the neuron to function correctly in this basic model, and they are as follows:

- **Neurons:** A neural network's elementary processing unit.
- **Synapses:** An assemblage of multiple interconnected links, each of which is assigned a weight. In general, the particular signal X_j for each of the input lines of the synapse j is connected to the neuron k and multiplied by the weight that is supplied to each link at the synaptic W_{kj} . The final product, W_{kj} , denotes the weight and neurons, respectively, by the first and second subscripts.
- **An adder:** The function that determined the summation of the weight of each individual synapses and the input signals that were received.

- Activation function:** The primary computing component of the ANN, which primarily sets a limit on the neuron's output amplitude. Because of its limited amplitude within a range specified for the output signal, which is frequently a limited value, the function is referred to squashing function. For the amplitude, the single intervals $[0,1]$ or $[-1,1]$ will roughly match to its general and usual output range.

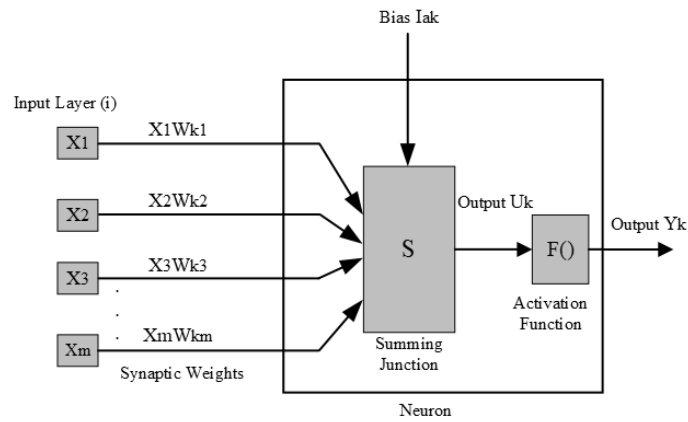


Fig. 5.1 ANN model

5.3 Artificial Neural Network Architecture

In general, ANN falls into two categories: Recurrent Architecture and Feed Forward (FF) Architecture. Three further categories exist for feed forward architecture: radial basis function (RBFN), multilayer ANN, and single-layered ANN. With its structure, Multilayer ANN is one of the most popular ANN kinds among them [165]. Here, each connected processing unit is set up separately inside the specified network structure. The ANN topologies that determine how the complete ANN processes information are shown in Figure 5.2.

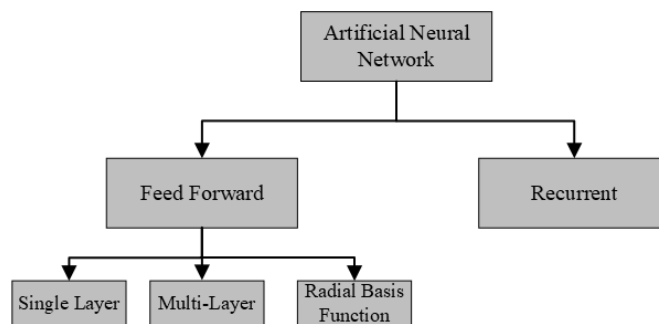


Fig. 5.2 ANN architecture classification

5.3.1 Single Layered Feed Forward ANN

The FF network illustrates how one input is provided to one unit as its output. A unit weight layer, which connects the inputs directly to the weight series, is included with the single FFN. The weights for each output are carried by each synaptic link in a distinct direction. A FFN typical is shown in Figure 5.3. In the final nodes, the input value is multiplied by utilizing the neuron node's activation function to get the weight.

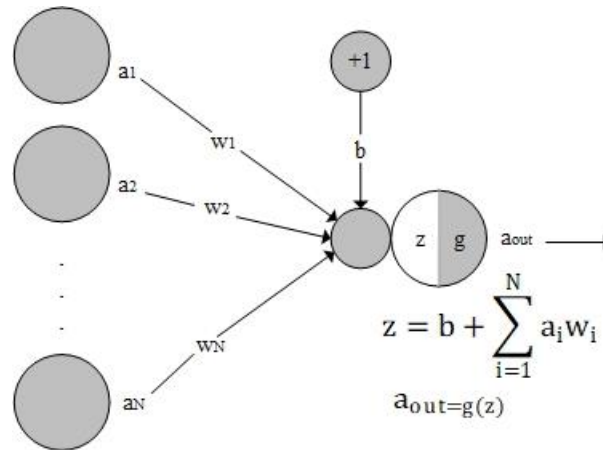


Fig. 5.3 FNN-single layer

5.3.2 Multilayered Feed Forward Network (MFFN)

The single-layered architecture FFN and the multilayered FFANN have comparable basic architectures and modes of operation. This type of network class is not only single-layered but also includes a second computational layer known as Hidden Layers and processing nodes known as Hidden Neurons.

In order to establish communication with inputs and outputs from the other layers and to extract knowledge based on the information, the neuron in the hidden layer is crucial. An artificial neural network (ANN) with more hidden layers and a larger unit will produce more accurate and efficient information.

The MFFN can be expressed simply as in Figure 5.4, where the layers at the input side, hidden network side, and output network are denoted by the letters i, j , and k , respectively. Layer " i " is an input layer (IL) made up of " l " neurons, which are represented as computation units by the letters $X_1, X_2, X_3, \dots, X_l$. The " m " neurons that make up the hidden layer (HL) j ' computing units are

denoted by the letters $H_1, H_2, H_3, \dots, H_m$. $Y_1, Y_2, Y_3, \dots, Y_n$ are the computing units that comprise the 'n' neurons that make up the output layer (OL) 'k'. The weights between the two distinct neurons of various layers will be assigned using this initial data to establish the feed forward network. As seen below, Figure 5.4 depicts the links:

W_{ij} : weighted links connecting the input layer to the hidden layer, or layer "i" to layer "j",.

W_{jk} : Weighted links between the nodes in the hidden layer and the output layer, or layers "j" and "k".

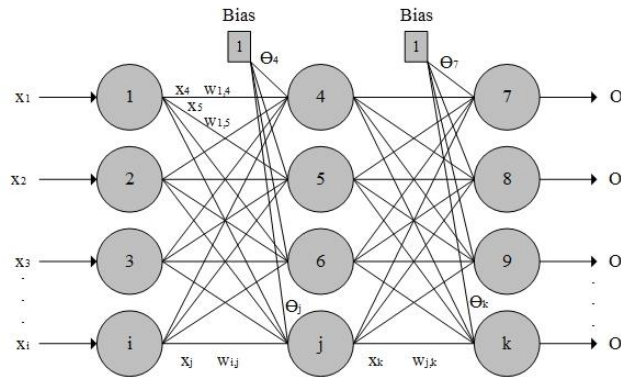


Fig. 5.4 Multilayered FNN

The MLP classification problem, in which the units are arranged into multiple layers, is an essential part of the neural network's architecture [166]. For all ANN learning algorithms, this will be a difficult task. Additionally, because the activation computation propagates unidirectionally, the neural network is referred to as feed forward [167]. Regarding each layer's neuron, the computing flow will be from the input layers to the hidden layers and the hidden layers to the output layers.

Electrical system difficulties and challenges can be effectively solved by integrating ANN mechanisms based on classification. Using the ANNs-based concept to identify the incidents of islanding in microgrids linked to different kinds of inverters is the main goal of this research project.

5.3.3 Back Propagation (BP) Algorithm

BP is among the most frequently applied algorithms for MLP training based on the ANN. Figure 5.5 depicts the two computational learning phases of this algorithm: the forward pass and the backward pass.

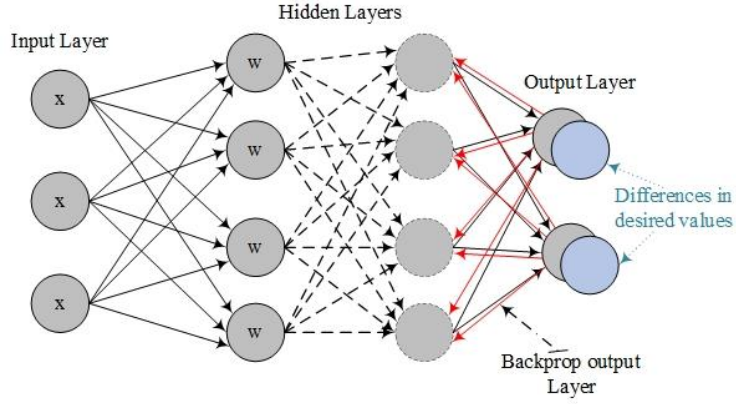


Fig. 5.5 ANN structure with backpropagation algorithm

Given is the forward pass output:

$$y_k^{(0)}(t) = \phi_k \left[\sum_{i=0}^Q m_{ki} \phi_i \left(\sum_{j=0}^p w_{ij} x_j(t) \right) \right] \quad (5.1)$$

P represents the input vector's size, Q the hidden layer's number of neurons, M the output layer's number of neurons, and w_{ij} the weight which links input j to hidden neuron i . The activation functions are represented by $\phi(\cdot)$, and the weight that links the hidden neuron i to the output neuron k ($k=1,2,\dots, M$) is denoted by m_{ki} .

In the backward pass,

The value of produced error $e_k^{(0)}(t)$ is

$$e_k^{(0)}(t) = d(t) - y_k^{(0)}(t), k=1, \dots, M \quad (5.2)$$

$$\varphi'_k u_k^{(0)}(t) = \partial \phi_k / \partial u_k^{(0)} \quad (5.3)$$

Local gradient of the neuron k output

$$\delta_k^{(0)}(t) = \phi'_k u_k^{(0)}(t) e_k^{(0)}(t) \quad (5.4)$$

The local gradient of hidden neuron I is expressed as

$$\delta_i^{(h)}(t) = \phi_i[u_i^{(h)}(t)] \sum m_{ki}(t) \delta_k^{(0)}(t) = \phi_i^{(h)}[u_i^{(h)}(t)] e_i^{(h)}(t), \text{ for } i = 0, \dots, Q \quad (5.5)$$

Updating the neurons' synaptic weights,

$$m_{ik}(t+1) = m_{ik}(t) + \eta \delta_k^{(0)}(t) y_i^{(k)}(t), \text{ for } i = 0, \dots, Q \quad (5.6)$$

$$w_{ij}(t+1) = w_{ij}(t) + \eta \delta_k^{(h)}(t) x_j(t), \text{ for } j = 0, \dots, P \quad (5.7)$$

In which η denotes the rate of learning.

5.4 Proposed Islanding Detection Method

In an influencing system, transient signals of voltage and current should have unique possibilities that point to the origin of the transient occurrence. The methodology presented here depends on the undeniable fact that a transitory state possesses particular features that can be tailored to offer a novel means of differentiating island events from other types of events. Furthermore, the options made available by fleeting signals are rarely considered carefully. There should be a mechanism to extract these options in order to expedite the classification process. Consequently, PMU is used to transient voltage and current data to extract the features needed for the classification process. The retrieved features-voltage amplitude, voltage frequency, and ROCOF-are used by an efficient classifier known as a neural network to differentiate between non-islanding and islanding conditions. Figure 5.6 presents the proposed approach.

Figure 5.7 illustrates the general procedures in the proposed approach for determining islanding. The input voltage is processed to extract a few features. The process is made simpler and faster by using the PMU algorithm to choose the most advantageous features among those retrieved. At that point, the prepared features are used by a neural network classifier that has been trained to categorize the sign as either islanding or non-islanding. The DG can be guarded and regulated by using neural network classifier learning.

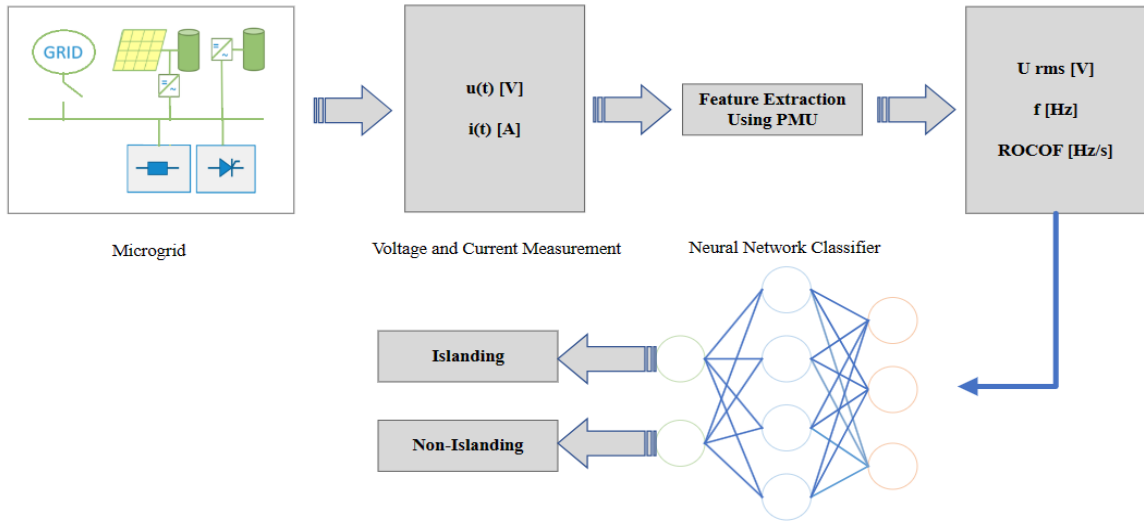


Fig. 5.6 Proposed islanding identification scheme

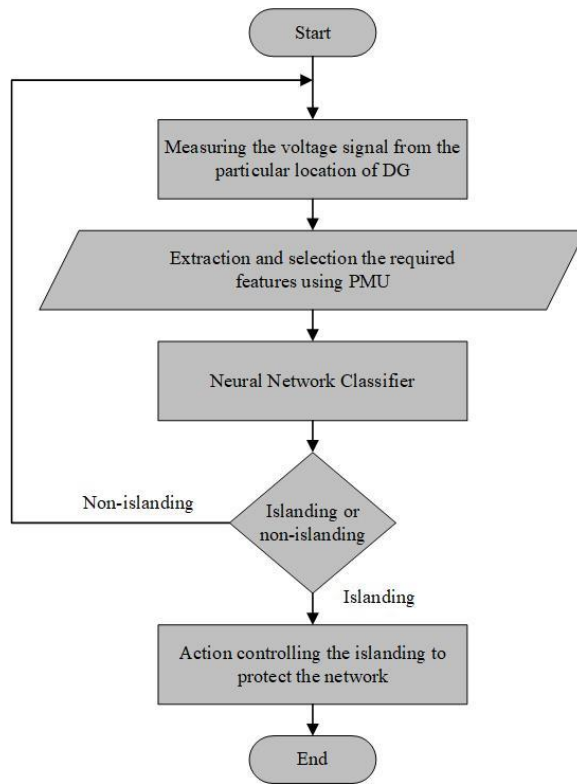


Fig. 5.7 Flowchart of the proposed scheme

5.5 Microgrid Systems under Test

Three different laboratories, each with their own particular procedures and objectives, were used to conduct experiments on islanding scenarios as presented below:

- **Relflex Laboratory:** Located in B1 at AGH University of Krakow

In this laboratory, a low-power AC microgrid was used for tests. The most important part of the microgrid is a 20-kW synchronous generator driven by an induction motor. The system also includes three inverters. The first inverter drives the induction motor, while the other two are used to transfer energy from the synchronous generator to the main microgrid bus, similar to the components of wind turbines installed in power grids in Poland and worldwide. The system can operate synchronously with the grid but also allows for islanded operation. It is powered from separate switchgear, ensuring that the system does not affect the overall energy balance of the microgrid. The other elements of the microgrid are:

- 10 kWh lithium-ion battery storage system,
- The photovoltaic installation consists of a 3.2 kW hybrid inverter and a 5-kWh lithium-ion battery storage system. This setup enables energy storage, allowing for the accumulation and utilization of solar energy,
- Programmable linear and non-linear load,
- Heat pump.

Figure 5.8 presents the schematic describing the used microgrid. An overall view of the system is illustrated in Figure 5.9.

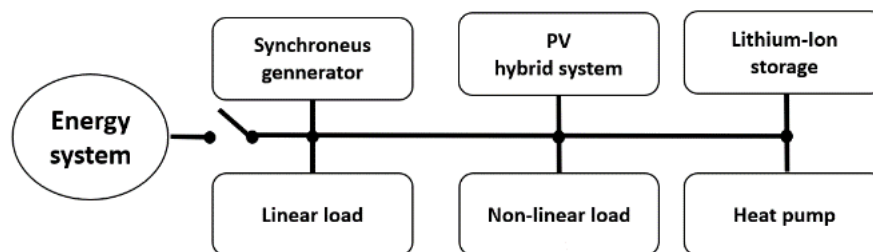


Fig. 5.8 Schematic diagram of reflex laboratory

In this work, the behavior of voltage and current has been observed during unintentionally islanding for three scenarios. Firstly, the system included the utility grid linked to a PV inverter.

Secondly, the main energy system was connected to the synchronous generator. Thirdly, both the PV inverter and synchronous generator were connected to the utility grid.

By shutting off the main switch, the constructed system was placed into islanding, and the voltage waveforms were simultaneously recorded using PMUs regarding each envisioned scenario. The National Instruments NI6040E platform served as the foundation for developing the measurement.

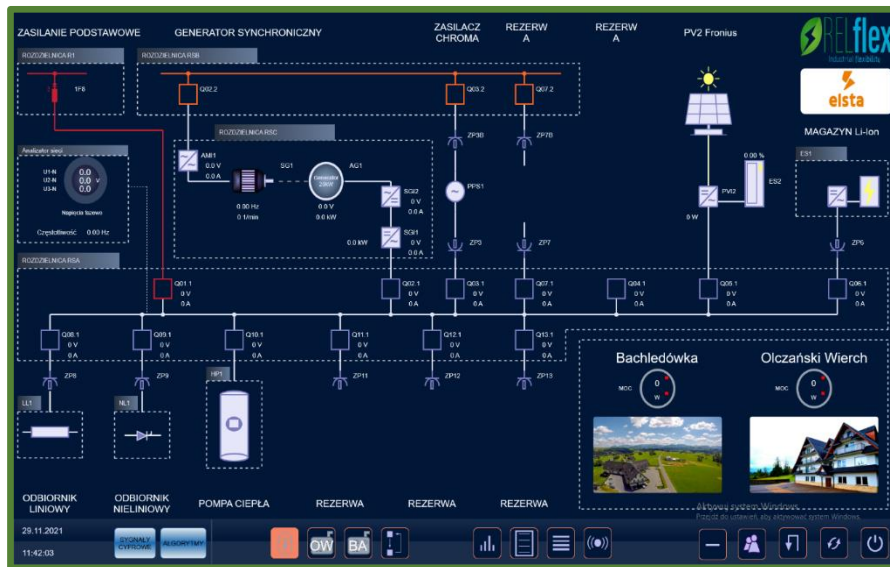


Fig. 5.9 Relflex laboratory system

- **Energy Center Laboratory:** Located in C5 at AGH University of Krakow

Twenty fourth different brands of PV inverters used in industry were investigated at the Laboratory of Energy Center at AGH University of Kraków during the unintentional islanding mode. The tests were carried out in compliance with the standards, considering the European standard PN-EN 62116, the IEEE 15471-2020 standard, and the requirements of the local electrical distributor. The guidelines also outline the testing procedures for inverters, indicating that numerous operational points should be examined due to the power generated and the degree of imbalance between the load side and generation of the energy island.

For testing, a Regenerative Grid Simulator Chroma 61815-powered system was employed. By using this testing technique, the devices may be examined free of the distortions and interruptions present in the real power grid. The network simulator was connected in parallel to an adjustable RLC load. Accurate processing power calibration was made possible by connecting the tested

inverter to the Photovoltaic Panels Simulator. The complete system diagram for laboratory testing is displayed in Figure 5.10.

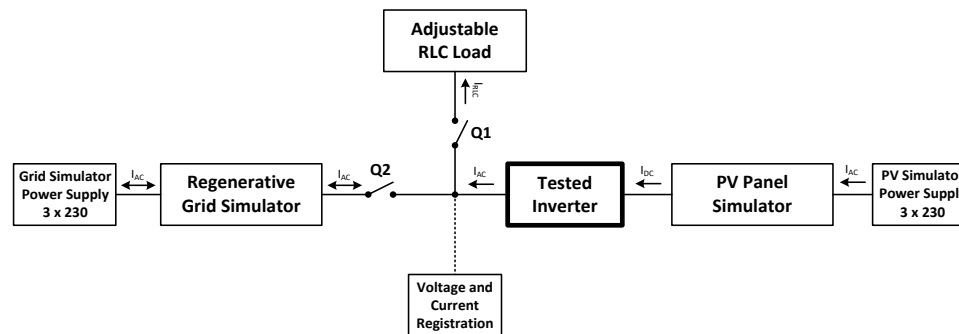


Fig. 5.10 Schematic diagram of energy center laboratory

A voltage recorder was connected to the inverter terminals. Using the National Instruments cRIO-9024 measuring apparatus, the measurements were carried out. 24-bits was the resolution and 25-kHz was the sample frequency of the AD converter. An overall view of the inverters test bench is pointed in Figure 5.11.



Fig. 5.11 Test bench for inverters

The evaluated inverter was attached, linked to a load, and run in island mode with the appropriate power output and consumption as part of the tests. Consequently, during the experiment, a precise switching sequence is needed, as seen in Figure 5.9. The six steps listed below had to be taken in order to switch the inverter into island mode:

- **The network simulator is launched:** first, the RMS value and voltage frequency were adjusted. The network simulator enables two-way energy flow, allowing the system to carrying out their duties regardless of whether the power balance is partial (generation of the tested inverter greater than load).

- **The circuit breaker Q2 is closed:** once the Q2 circuit breaker was connected and the test network was powered on, the tested inverter was able to operate.
- **The photovoltaic panel simulator is turned on:** the inverter was configured with its rated voltage, power, and MPPT voltage using the simulator program. Furthermore, the MPP power generated by the simulator was set up. The tested inverter increases power in accordance with the testing protocol until it reaches the maximum power point. At this operating point, the grid simulator feeds the power generated by the panel simulator into the electrical grid via the inverter.
- **Q1, the circuit breaker, is closed:** the RLC load is connected to the grid in parallel when the Q1 breaker is closed. Setting the load-adjusting receiver to ON allowed for the simulation of the tested inverter's shift to island mode.
- **Balance between produced and load power:** before putting the inverter in island working mode, it was necessary to equalize the amount of power that the regulated load consumes from the inverter, according to the assumptions listed in Table 5.1. This was accomplished by carefully adjusting the photovoltaic panel power produced by the simulator to a predetermined load value. The grid simulator was neither creating power nor consuming power from the system as a result, and its power was equal to zero. The inverters were tested using the procedure described in PN-EN 62116. The inverter initially operated at maximum capacity. The regulated load's input power value was kept constant. When the island operation began, the system was totally balanced, which corresponds with the conditions that make island operation identification particularly difficult. Points 2 and 3 were used for a similarly balanced system operating at 33% and 66% of power, respectively. After switching to island operation, the system lost equilibrium since the inverter's generated power was 5% higher in point 4 and 5% lower in point 5.

Table 5.1. Power assumption for inverters and loads.

Test	P_{EUT}	P_{LOAD}
1	100%	100%
2	66%	66%
3	33%	33%
4	105%	100%
5	95%	100%

* P_{EUT} : Power of equipment under test

- **The circuit break Q2 is opened:** prior to the Q2 switch being opened, the measurement system was activated, and the tested inverter was operating in the island mode. Following the activation of the protection against the inverter's island operation, the measurement system was turned off.
- **Dynamic Power Systems Lab:** Located at University of Strathclyde, Glasgow, UK

The operation of wind turbine generators during unintentionally islanding were investigated. When the inverter-load system switches to islanded operation, the voltage and current waveforms are captured. The complete diagram for the laboratory testing system is displayed in Figure 5.12. In Figure 5.13, the test setup schematic is displayed. The power of the controllable load and the converter utilized in the experiments should be determined based on the mentioned scenarios.

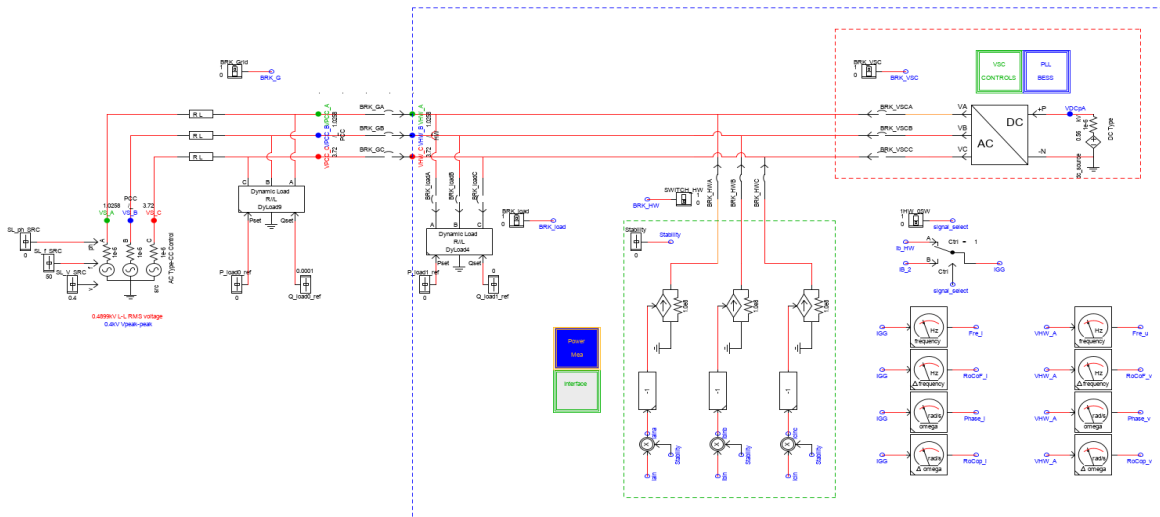


Fig. 5.12 Schematic diagram of dynamic power system laboratory

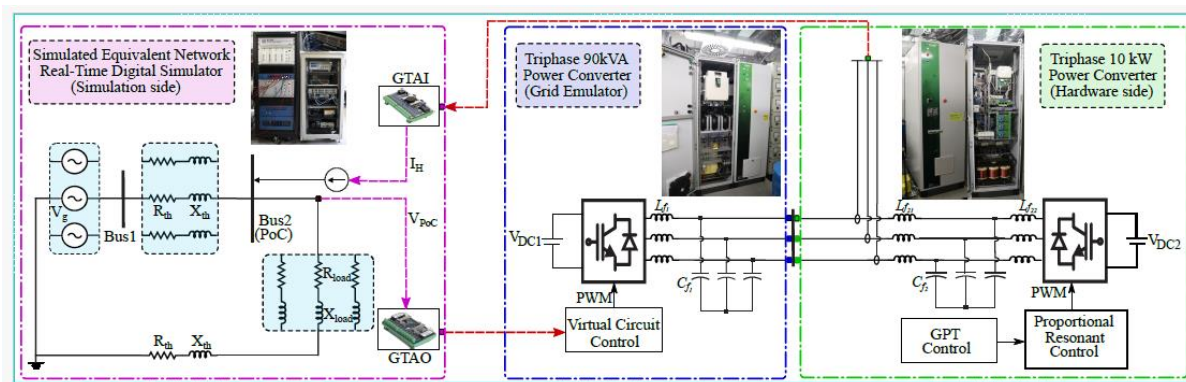


Fig. 5.13 Dynamic power systems laboratory setup

A network simulator, a controllable RL load, and the tested power converter (equipment under test EUT) supplying power to the grid were all part of a series of tests on a balanced and unbalanced system. Table 5.2 contains a list of the planned tests.

Table 5.2. Power assumption for inverters and loads.

Test	P_{EUT}	P_{LOAD}	Load type
1	100%	100%	R, cosj = 1
2	66%	66%	R, cosj = 1
3	33%	33%	R, cosj = 1
4	100%	100%	RL, cosj = 0.8
5	66%	66%	RL, cosj = 0.8
6	33%	33%	RL, cosj = 0.8
7	105%	100%	R, cosj = 1
8	95%	100%	R, cosj = 1
9	105%	100%	RL, cosj = 0.8
10	95%	100%	RL, cosj = 0.8

5.6 Conclusion

In order to ensure the stability and dependability of electrical grids, neural networks are useful classifiers for islanding identification in power systems. By examining numerous power system data and parameters, including voltage, frequency, and ROCOF measurements, neural networks are able to identify islanding events. Through training on historical information encompassing normal and islanding circumstances, the neural network obtains the ability to identify patterns indicative of islanding.

The neural network's design can change based on the particular needs of the islanding detection task. For processing fixed-length input signals, for instance, a feedforward neural network would be appropriate. For evaluating sequential or spatial data, on the other hand, recurrent or convolutional neural networks might be used.

The neural network uses supervised learning methods like backpropagation to minimize the difference between expected and actual islanding occurrences during training. After that, the trained neural network may be used in real-time to quickly detect any occurrences of islanding and continuously monitor the power supply.

Neural networks have the ability to handle complicated, nonlinear relationships in the data and adapt to changing operating conditions, which makes them an excellent choice for islanding identification. Neural networks can also be trained to achieve high accuracy with low false alarms, which lowers the possibility of unneeded power outages.

Comprehensive islanding mode testing in three distinct laboratories has produced encouraging findings, supporting the viability of using a control method that is highly compatible with real-world situations. The varied evaluations of inverters in different settings highlight the adaptability and effectiveness of the suggested technique. In the end, neural networks prove to be a dependable and effective method for detecting islanding in power systems, which is critical for maintaining grid stability and reducing hazards to infrastructure and public safety.

6. Results and Discussion

This chapter presents the results of the proposed method. The proposed method's accuracy is compared to other approaches to showcase its efficacy. In addition, the suggested model's response time is calculated and compared to the response times of the tested inverters to determine whether or not it meets the standard.

7.1 Islanding Detection Scenarios

This section presents the results of the proposed islanding detection. For the construction of the distribution system under study, the experiments were carried out in three different laboratories as mentioned in the previous chapter. In the Reflex lab, the main grid is connected to PV inverter Synchronous generator inverter, linear load, non-linear load, and the measurement was developed using the National Instruments NI6040E platform. In the Energy center lab, the main grid is a Regenerative Grid Simulator Chroma 61815-powered system which is connected to Photovoltaic Panels Simulator that is connected to the tested inverter and adjustable RLC load. The measurements were performed using the National Instrument Crio-9024 measuring equipment. In the Dynamic Power System lab, the main grid is a Simulated Equivalent Network Real-Time Digital Simulator which is connected to a Tri-phase 10 kW power inverter. The measurements were recorded using current and voltage sensors using RCAD software. The required PMU and ANN were programmed using MATLAB software. Some examples of the studied cases are presented in Figure 6.1, Figure 6.2, 6.3, and 6.4 respectively in which the inverter voltage is recorded during the unintentional islanding event for different scenarios of power match between the inverter and load, then the PMU is applied to extract the required features (phasor voltage, frequency, and ROCOF) as Figure 6.5 (a),(b),(c), and (d) that needed for the ANN classifier to determine the islanding and non-islanding conditions.

The rated power of one of the tested inverters is 3.5 kW, the power match between the inverter and load is presented below:

- The inverter output power is equivalent to the power consumed by load

The power of inverter is 100% (3.5 kW), and the load power is 100% (3.5 kW).

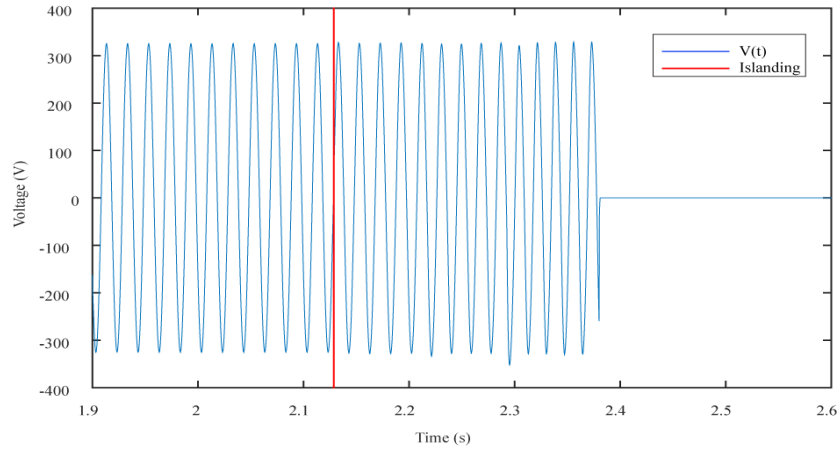


Figure 6.1 Inverter voltage during unintentional islanding for scenario 1

As seen from Figure 6.1, the islanding happens after round 2.1 s and due to the match between the inverter and load powers; the voltage fluctuation is not big which leads to have bigger non-detected zone accordingly. The islanding mode was detected during 0.25253 s.

- The inverter output power is equivalent to the power consumed by load

The power of inverter is 66% (2.31 kW), and the load power is 66% (2.31 kW).

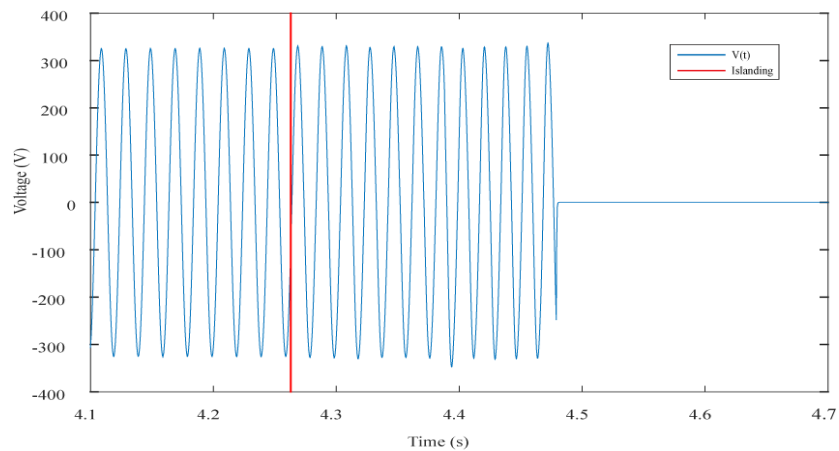


Figure 6.2 Inverter voltage during unintentional islanding for scenario 2

As seen from Figure 6.2, the islanding happens after round 4.25 s and due to the match between the inverter and load powers; the voltage fluctuation is not big which leads to have bigger non-detected zone accordingly. The islanding mode was detected during 0.21708 s.

- The inverter power is greater than the load power (over voltage)

The inverter power is 105% (3.675 kW), and the load power is 100% (3.5 kW).

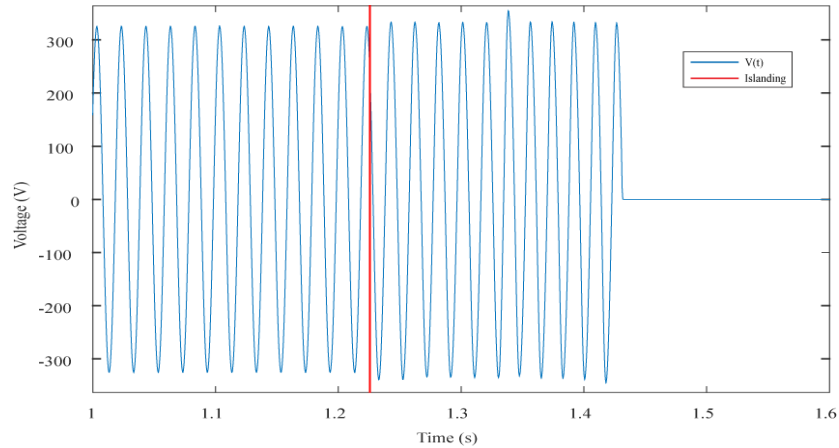


Figure 6.3 Inverter voltage during unintentional islanding for scenario 3

As seen from Figure 6.3, the islanding happens after around 1.2 s and due to the mismatch between the inverter and load powers; the voltage level increased above the boundary limits which leads to have smaller non-detected zone and faster detection time accordingly. The islanding mode was detected during 0.2067 s.

- The power of inverter power is smaller than the power consumed by load (under voltage)

The inverter power is 95% (3.325 kW), and the load power is 100% (3.5 kW).

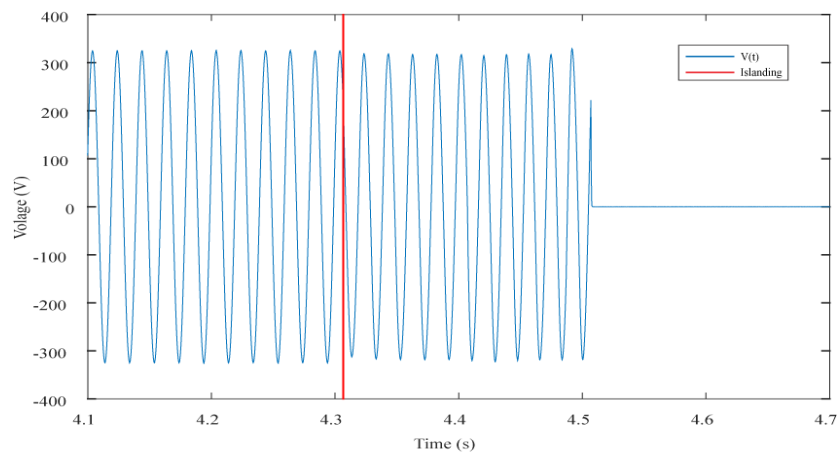


Figure 6.4 Inverter voltage during unintentional islanding for scenario 4

As seen from Figure 6.4, the islanding happens after round 4.3 s and due to the mismatch between the inverter and load powers; the voltage level decreased above the boundary limits which leads to have smaller non-detected zone and faster detection time accordingly. The islanding mode was detected during 0.20082 s.

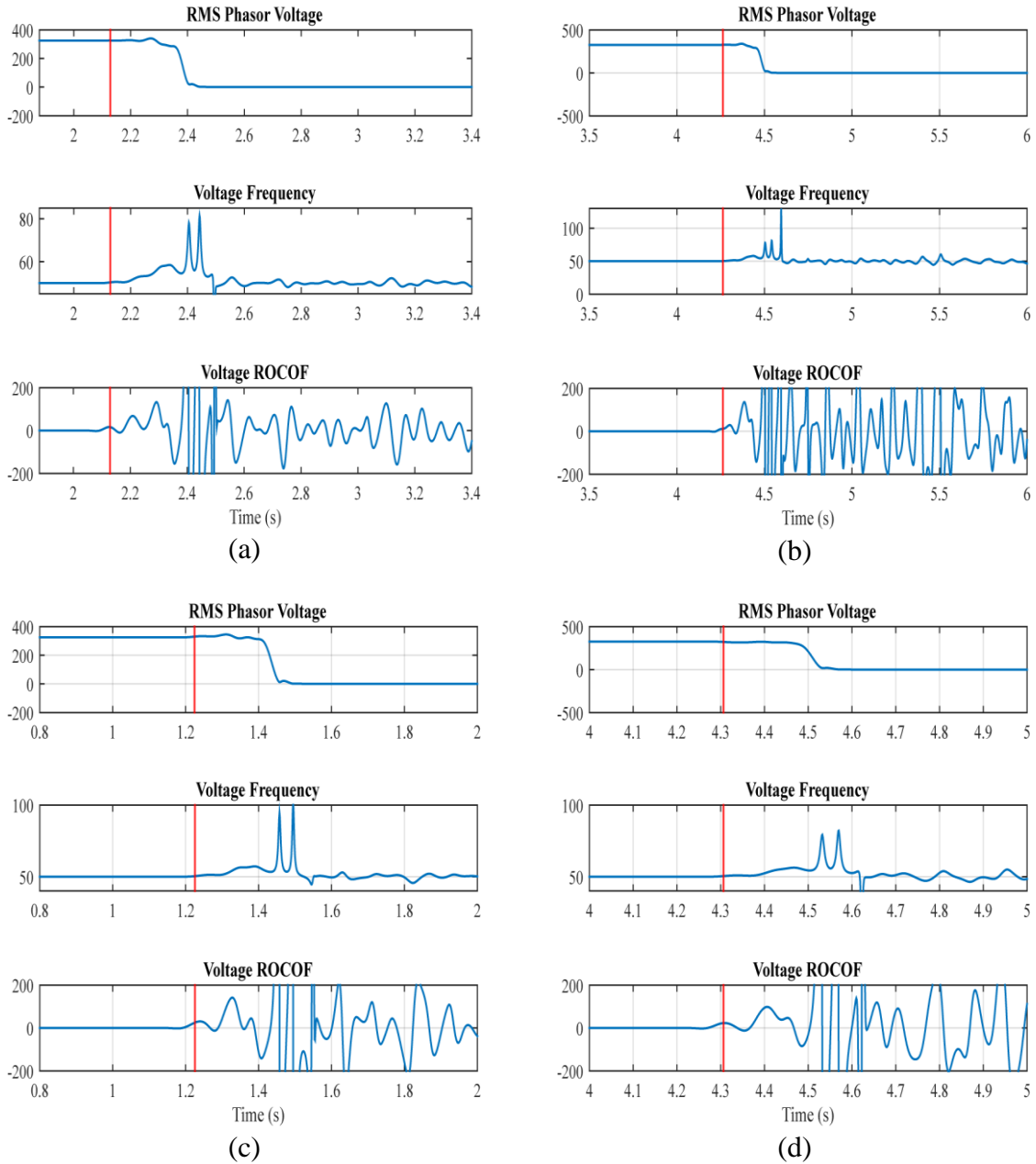


Figure 6.5 Inverter phasor voltage, frequency, and ROCOF during unintentional islanding for (a) scenario 1, (b) scenario 2, (c) scenario 3, and (d) scenario 4

The investigation of the unintentional islanding detection was carried out on different types of industrial inverters that are used in real-world. As mentioned previously, the evaluation of each inverter was done using a separate set of tests for power assumptions between the tested inverter and load. During the assessment of inverters during the unintentional islanding mode, the exact time of islanding occurrence and the time period which the inverter needed to disconnect were known which used to prepare the training and testing data set required for the ANN classifier.

6.2 ANN Classifier Model Parameters and Training

The data set which was used for the purpose of ANN training process includes hundreds of thousand observations for islanding and non-islanding events. The training data set is a matrix with hundreds of thousand rows and 4 columns. The whole rows present the number of various situations and cases of non-islanding and unintentional islanding events, the first 3 columns present the predictors (input parameters) values specifically the phasor voltage, frequency, and ROCOF, and the last column presents the response or the outcome. The outcome is either 0 which designates that the system is under non-islanding condition or 1 which implies that the system is under unintentional islanding condition as illustrated in Table 6.1.

Table 6.1. Some samples of the data set used for training the classifier.

Case no.	Phasor Voltage [V]	Frequency [Hz]	ROCOF [Hz/s]	Outcome
1	325.6311	50.00336	-0.00113	0
1061	334.2130	53.76710	137.4227	1
1253	325.4371	50.00054	0.003009	0
2830	332.5613	55.03513	116.613	1
2997	325.591	50.00065	0.0169	0
6159	310.393	57.02548	46.9333	1
6422	325.721	50.00056	0.00616	0
7730	297.354	49.47087	-12.8572	1
8310	325.724	50.00045	0.01449	0
9932	320.047	45.61211	-1.3501	1
10356	325.64	50.00066	0.01228	0
12577	207.391	53.43756	26.9291	1
13769	325.547	49.99661	0.06308	0
13924	329.051	50.29849	5.65685	1
57414	325.607	50.00061	0.00341	0
60097	307.08	55.82833	179.016	1
60374	325.753	50.00058	-0.00029	0
63968	333.0892	52.175534	72.42099	1
70395	325.6145	50.000623	-0.0019	0
78070	319.2818	49.976431	15.60329	1
79650	325.6507	50.00045	0.001316	0
80107	298.9276	50.535499	-18.7912	1
83909	325.642	49.999962	0.033554	0

84713	324.5224	52.736807	82.71616	1
86945	325.684	50.00066	-0.00269	0
89237	340.4295	53.860815	160.1389	1
91553	325.6295	50.000389	-0.00883	0
92546	322.4447	48.97164	7.26551	1
95930	325.5419	49.99986	0.02075	0
97584	325.8385	47.188339	-22.4117	1
100239	325.6212	50.000649	0.028159	0
102484	317.3278	47.318808	-134.54	1
104737	325.5797	50.001108	0.005606	0
107144	343.9238	53.149936	197.3891	1
107533	325.6944	50.000658	-0.0235	0
108851	347.2253	52.278491	176.2884	1
110531	325.5919	49.999875	0.00946	0
114107	329.2767	54.303263	29.55277	1
114349	325.5534	50.000508	0.021124	0
115783	326.3335	54.060305	100.0834	1
164998	325.5046	50.000121	-0.03925	0
175783	318.697	50.174623	2.742095	1
187882	325.7082	50.000873	0.02608	0
198650	203.5668	49.495963	-23.5036	1

The trained ANN is multilayered feed forward neural network (FNN) comprises three layers and the size of each layer is ten. The specification parameters of the trained ANN are presented in Table 6.2.

Table 6.2. ANN parameters specification.

Parameter	Value
No. of fully linked layers	3
First layer size	10
Second layer size	10
Third layer size	10
Activation Function	Rectified liner Unit
Standardize data	Yes

7.1 ANN Model Parameters Evaluation

The performance of the classification model is described by the confusion matrix as shown in Figure. 6.6. The actual classification of islanding cases known as true positive (TP) matches the prediction of the proposed model by 14782 islanding cases. As well. 34574 cases were classified correctly by the proposed model as non-islanding case which known as true negative (TN). 253 cases were classified as islanding case by the classifier model, but in real these cases were non-islanding occurrences; this term is known as false positives (FP). In addition, 74 cases were identified as islanding cases, but these cases in real are non-islanding events which related to the term false negative (FN). Table 6.3 presents the contingency table for the classification of neural network model.

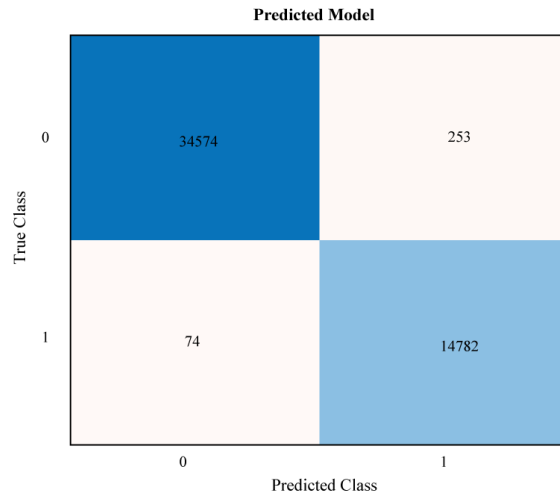


Figure 6.6 Confusion matrix for training

Table 6.3. ANN contingency table.

Actual classes	Predicted Model	
	Islanding	Non-islanding
Islanding	TP (14782)	FN (74)
Non-islanding	FP (253)	TN (34574)

In which TP refers to the number of true positive points.

FP is the number of false positive points.

TN is the number of true negative points.

FN is the number of false negative points.

Definition 1: A true positive test result occurs when the model detects the islanding when the islanding is present.

Definition 2: A false positive test result occurs when the model detects the islanding when the islanding is absent.

Definition 3: A true negative test result occurs when the model detects the non-islanding when the non-islanding is present.

Definition 4: A false negative test result occurs when the model detects the non-islanding when the non-islanding is absent.

Let TP refer to the count of true positives, TN the count of true negatives, FP the count of false positives, and FN the count of false negatives.

The effectiveness of the classification model is assessed using the performance parameters known as sensitivity, specificity, positive predictive value (PPV), negative predictive value (NPV), and classification accuracy. According to the contingency table given previously, the constraint values of the developed ANN model are presented in Table. 6.4.

Table 6.4. Constraint values of the ANN model.

Parameter	Percentage
Sensitivity	99.5%
Specificity	99.27%
Positive predictive value	98.31%
Negative predictive value	99.78%
Accuracy	99.34%

- **Sensitivity:** it is described as the system ability to identify the condition when the condition is present. It might be computed using the following formula:

$$Sensitivity = \frac{TP}{TP + FN} \times 100\% \quad (6.1)$$

$$Sensitivity = \frac{14782}{14782 + 74} \times 100\%$$

$$Sensitivity = \frac{14782}{14856} \times 100\% = 99.5\%$$

- **Specificity:** it is described as the system ability to accurately exclude the condition when the condition is absent. It can be calculated using the following formula:

$$Specificity = \frac{TN}{TN + FP} \times 100\% \quad (6.2)$$

$$Specificity = \frac{34574}{34574 + 253} \times 100\%$$

$$Specificity = \frac{34574}{34827} \times 100\% = 99.27\%$$

- **Positive predictive value (PPV):** it is defined as the ratio of positives which correspond to the presence of the condition. It can be calculated using the following formula:

$$PPV = \frac{TP}{TP + FP} \times 100\% \quad (6.3)$$

$$PPV = \frac{14782}{14782 + 253} \times 100\%$$

$$PPV = \frac{14782}{15035} \times 100\% = 98.31\%$$

- **Negative predictive value (NPV):** it is defined as the ratio of negatives that correspond to the absence of the condition. It can be calculated using the following formula:

$$NPV = \frac{TN}{TN + FN} \times 100\% \quad (6.4)$$

$$NPV = \frac{34574}{34574 + 74} \times 100\%$$

$$NPV = \frac{34574}{34648} \times 100\% = 99.78\%$$

- **Accuracy:** it is defined as the percentage of correctly classified cases. The accuracy can be calculated in the context of the confusion matrix as the following formula:

$$Accuracy = \frac{TP + TN}{TP + TN + FP + FN} \times 100\% \quad (6.1)$$

$$Accuracy = \frac{14782 + 34574}{14782 + 34574 + 253 + 74} \times 100\%$$

$$Accuracy = \frac{49356}{49683} \times 100\% = 99.3\%$$

The relationship and distribution of voltage, frequency, and ROCOF are visualized via a scatter plot as shown in Figure 6.7. The correct prediction is indicated by dots, and the wrong prediction is indicated by cross signs.

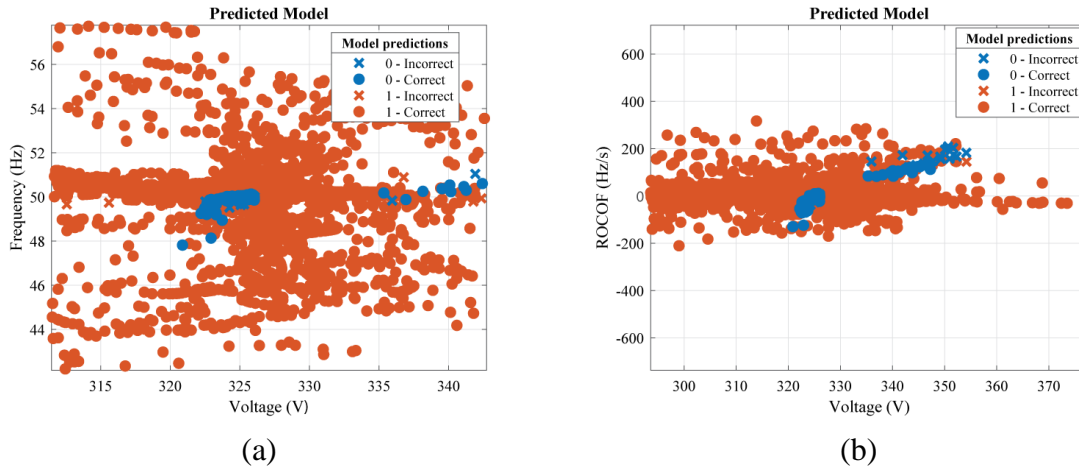


Figure 6.7 Confusion matrix for training (a) voltage vs frequency (b) voltage vs ROCOF

The model was validated using holdout validation with 25% held out. The model accuracy during training and testing was 99.3% and 99% respectively as presented in Table 6.5.

Table 6.5. ANN model results.

Accuracy (Validation)	Accuracy (Test)	Prediction Speed (obs/sec)	Time of Training (sec)
99.3%	99%	901516	130.6

6.4 Comparisons

This section presents a contrast between the suggested strategy and several present techniques such as Naïve Bayes, Generalized Linear Model Logistic Regression, and Linear Discriminant are provided.

a. Naïve Bayes

The Naïve Bayes technique is commonly employed for islanding recognition in distribution systems because this approach is considered simple and efficient for complex data analysis. During the assessment of islanding identification schemes, the accuracy of Naïve Bayes was 85.4% which is lower than the accuracy of the proposed method. Comparing with various methods ensures the importance of choosing the most suitable method according to certain requirements and dataset characteristics. The contingency table for Naïve Bayes classification is provided in Table 6.6. The constraint values of the Naïve Bayes model are presented in Table 6.7.

Table 6.6. Naïve Bayes contingency table.

Actual classes	Predicted Model	
	Islanding	Non-islanding

Islanding	TP (7720)	FN (7136)
Non-islanding	FP (131)	TN (34696)

Table 6.7. Constraint values of the ANN model.

Parameter	Percentage
Sensitivity	51.96%
Specificity	99.6%
Positive predictive value	98.33%
Negative predictive value	82.94%
Accuracy	85.37%

b. Generalized Liner Model (GLM) Logistic Regression

The Logistic Regression method is contingent upon the characteristics of the data and the distribution classes which can affect the method performance. This method presupposes a linear correlation between the predictor's variables and the response, hence if the relationship is non-linear or more complex this method may have difficulty to capture the patterns efficiently, leading to decrease the model accuracy which was 77.4%. The contingency table for GLM Logistic Regression classification is provided in Table 6.8. The constraint values of the GLM Logistic Regression model are presented in Table 6.9.

Table 6.8. GLM Logistic Regression contingency table.

Actual classes	Predicted Model	
	Islanding	Non-islanding
Islanding	TP (3628)	FN (11228)
Non-islanding	FP (6)	TN (34821)

Table 6.9. Constraint values of the GLM Logistic Regression model.

Parameter	Percentage
Sensitivity	24.42%
Specificity	99.9%
Positive predictive value	99.8%
Negative predictive value	75.6%
Accuracy	77.38%

c. Liner Discriminant (LD)

The liner discriminant is a statistical approach which is used for classification purposes to get linear combinations of features that effectively divide numerous classes. During the assessment of islanding detection, the accuracy of liner discriminant method was 76% which the lowest among

other tested methods. The contingency table for LD classification is provided in Table 6.10. The constraint values of the Linear Discriminant model are presented in Table 6.11.

Table 6.10. Linear Discriminant contingency table.

Actual classes	Predicted Model	
	Islanding	Non-islanding
Islanding	TP (2937)	FN (11919)
Non-islanding	FP (3)	TN (34824)

Table 6.11. Constraint values of the GLM Logistic Regression model.

Parameter	Value
Sensitivity	19.76%
Specificity	99.9%
Positive predictive value	99.8%
Negative predictive value	74.5%
Accuracy	76%

The graphical comparison between the accuracies of the proposed model and other classifiers is shown in Figure 6.8.

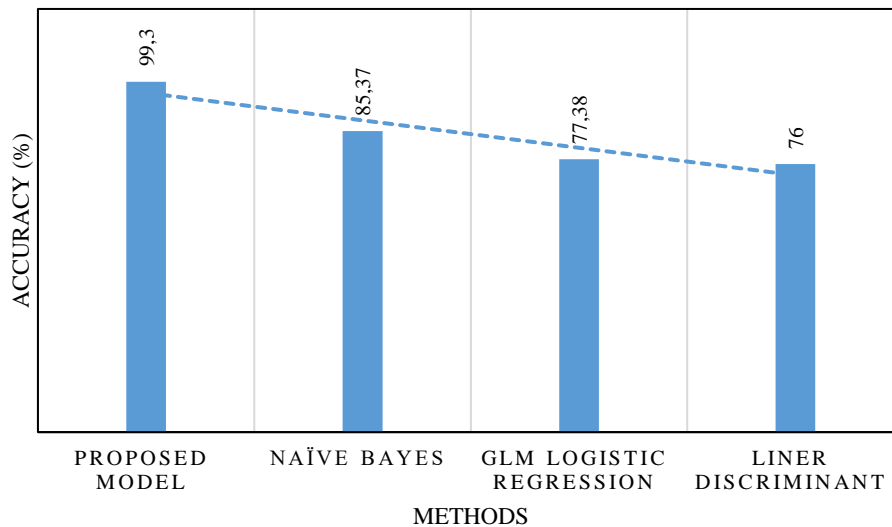


Figure 6.8 Comparison of accuracies between the proposed model and other methods

6.5 Detection Time

The DG inverter must identify and disconnect the power supply during unintended islanding within 2 seconds according to IEEE standards. The scenario which was considered while recoding the detection time of the examined inverters and proposed model is when there was a power

equilibrium existed between the inverter and load sides, since this scenario results in a bigger non-detection zone compared to previous instances, necessitating additional time for the inverters to identify the islanding event. Table 6.12 presents a comparison of detection times between the designed model and the evaluated inverters.

Table 6.12. Comparison of response time between the proposed model and tested inverters.

Detection Time (Seconds)		
	Tested Inverters	Proposed Model
Inv.1	0.66	0.20
Inv.2	0.43	0.25
Inv.3	0.26	0.18
Inv.4	1.03	0.15
Inv.5	6.47	0.18
Inv.6	0.74	0.20
Inv.7	6.24	0.39
Inv.8	0.22	0.12
Inv.9	0.45	0.10
Inv.10	1.51	0.10
Inv.11	1.09	0.12
Inv.12	0.14	0.20
Inv.13	0.17	0.16
Inv.14	0.02	0.16
Inv.15	0.19	0.11
Inv.16	0.83	0.31
Inv.17	0.12	0.13
Inv.18	0.10	0.18
Inv.19	0.61	0.42
Inv.20	0.32	0.15
Inv. 21	0.22	0.18
Inv.22	0.20	0.17
Inv.23	0.55	0.12
Inv.24	0.27	0.17
Inv.25	0.35	0.17
Inv.26	0.63	0.18
Inv.27	0.87	0.18

As seen from Table 6.13, Inverter 5, and inverter 6 fail to detect the islanding incident within 2 seconds while the other tested inverters were able to distinguish the islanding incident within the acceptable time ranges. In addition, when it comes to the proposed model, it was able to detect the islanding incident within the acceptable time frames. The proposed model was faster to detect the islanding incident than the algorithms that were implemented in the tested inverters in most cases. Only inverter 12, inverter 14, inverter 17, and inverter 18 were slightly faster than the proposed method.

6.6 Conclusion

To identify the occurrence of islanding circumstances effectively and efficiently, a hybrid method that includes both phasor measuring unit and artificial neural network is developed in this study. The islanding detection technique that uses PMU-ANN is a workable way to distinguish between islanding and non-islanding events in power systems. This approach achieved outstanding results during thorough laboratory tests by utilizing the capabilities of Phasor Measurement Units (PMUs) to extract essential features such as phasor voltage, voltage frequency, and voltage rate of change of frequency (ROCOF), as well as the effectiveness of artificial neural networks (ANNs) as a classification algorithm. The rigorous evaluation, involving testing on several types of inverters in accordance with the PN-EN 62116 procedure guidelines, yielded remarkable findings, with a testing accuracy of 99.05% and a training accuracy of 99.34%. Furthermore, the presented method's resilience and durability are demonstrated by the utilization of a large dataset containing more than 100 thousand samples covering both islanding and non-islanding occurrences for both training and evaluating the proposed algorithm. This research makes an important contribution to the area of islanding detection by providing an affordable and viable technique that could be simply incorporated into a variety of power grid applications. This strategy offers an opportunity to significantly enhance the security and effectiveness of global energy supply and distribution networks by boosting the ability to identify islanding incidents more accurately and efficiently. It has the ability to increase the general efficiency, security, and dependability of today's electrical systems.

7. Conclusion and Future Scope

7.1 Conclusion

This work presents the associate islanding detection methods used in distribution networks that are connected with multi-DG inverters. The islanding phenomenon is considered a serious problem in the distributed networks due to the side effects that can be caused by this phenomenon. Therefore, when this phenomenon occurs within the distributed system, it is essential to detect it and shut down the system within the permissible ranges determined by the international standards. Various islanding detection methods which depend on the system parameters such as voltage and frequency were proposed by different researchers. Those methods can be classified into different categories namely as conventional and modern methods. The selection of these islanding detection methods to be used in the distributed system depends on different criteria to be considered, especially the non-detected zone criterion (NDZ). Therefore, an assessment of these methods was carried out using a decision-making approach known as analytical hierarchy process (AHP) accordingly. To avoid any failure of islanding detecting and to get higher response time, a hybrid islanding detection method which combined both phasor measurement estimation and artificial neural network is proposed. The principal operation of this proposed method depends on two stages. In the first stage, the phasor measurement estimation is employed to extract some features from the system voltage waveform during the non-islanding and islanding incidents. In the second stage, the extracted features are used to form the dataset that is required to train the neural network model for the classification process.

The main term which was calculated to examine the effectiveness of the proposed model was accuracy. The accuracy of the proposed model was compared with other machine learning approaches which ensure that the model is proper to detect the islanding effectively and accurately. Also, the other important criterion which was evaluated is the response time of the proposed model. The response time of the proposed model was recorded and compared with the response time of the tested inverter which ensures that the proposed model is capable of detecting the islanding faster than most of the tested inverters.

7.2 Major Contribution

Below is a summary of the major contribution of this dissertation.

Problem formulation

- A comprehensive analysis of the islanding detection problem is considered in this work. The detection and classification of islanding phenomenon is studied to propose a better approach of comparing with the existing islanding detection techniques.
- According to the main purpose of fault analysis of microgrid integrated with DGs, three different practical microgrid systems were examined to carry out the experiments. Also, to achieve the feasibility of real-time operation of the tests, IEEE standards are taken into consideration.
- In this work, different types of DGs such as PV system, wind turbine, and synchronous generator are considered.

Methodologies

- A decision-making approach is used to assess the existing islanding detection methods according to different criteria such as the response time and non-detected zone to compare between those methods based on the selected criterion.
- In the second part of the work, an advanced signal processing approach based on phasor measurement estimation is designed. This approach is helpful to be applied for the feature extraction that is needed in the third part.
- In the third part, the phasor measurement estimation approach is combined with ANN classifier to build the whole proposed model. This proposed model is compared with other approaches such as Naïve bayes, GLM logistic regression, and LD. The proposed model gives better results comparing with other techniques and other tested inverters in terms of accuracy and response time respectively.

Performance and Implementation

- The performance is evaluated on different real-time experimental systems according to IEEE standards.
- The performance of the PMU-ANN approach is better than the others compared methods for islanding detection with large non-detected zones.
- This work has culminated in plenty of articles published and under review in Journals and conferences, as shown in the table of publications.

Results

- The performance of the proposed model is evaluated in terms of accuracy, which was 99.3% and 99% during training and testing respectively.
- The performance of the proposed model was better than other approaches such as Naïve bayes, GLM logistic regression, and LD.
- The response time of the proposed model was compared with different inverters. It was recorded as an average time equals 0.18s.
- The response time of the proposed model was faster than all tested inverters except inverters 12, 14, 17 and 18.

7.3 Future Scope

The outcome of is study is very beneficial for researchers, scholars, and engineers in both academia and industry. Below there are some recommendations of this research for further extension and enhancement.

- In this work, the used approach of phasor measurement estimation is measurement class (M class). In the future, the implementation of protective class (P class) to M class phasor measurement unit will be considered.
- In this work, the islanding detection is examined on AC microgrids only. The influence of islanding phenomena on the AC and DC networks are not similar, hence the proposed model for islanding detection in AC network may not provide the same results when it applies to DC systems.

References

- 1.Fang, X., Misra, S., Xue, G. and Yang, D., 2011. Smart grid—The new and improved power grid: A survey. *IEEE communications surveys & tutorials*, 14(4), pp.944-980.
- 2.Ipakchi, A. and Albuyeh, F., 2009. Grid of the future. *IEEE power and energy magazine*, 7(2), pp.52-62.
- 3.Le Ray, G. and Pinson, P., 2020. The ethical smart grid: Enabling a fruitful and long-lasting relationship between utilities and customers. *Energy Policy*, 140, p.111258.
- 4.Rathor, S.K. and Saxena, D., 2020. Energy management system for smart grid: An overview and key issues. *International Journal of Energy Research*, 44(6), pp.4067-4109.
- 5.Lasseter, R.H., 2011. Smart distribution: Coupled microgrids. *Proceedings of the IEEE*, 99(6), pp.1074-1082.
- 6.Bode, H., Heid, S., Weber, D., Hüllermeier, E. and Wallscheid, O., 2020. Towards a Scalable and Flexible Simulation and Testing Environment Toolbox for Intelligent Microgrid Control. *arXiv preprint arXiv:2005.04869*.
- 7.Hatziargyriou, N., Asano, H., Iravani, R. and Marnay, C., 2007. Microgrids. *Power and energy magazine. IEEE*, 5(4), pp.78-94.
- 8.Parag, Y. and Ainspan, M., 2019. Sustainable microgrids: Economic, environmental and social costs and benefits of microgrid deployment. *Energy for Sustainable Development*, 52, pp.72-81.
- 9.Peyghami, S., Palensky, P. and Blaabjerg, F., 2020. An overview on the Reliability of Modern Power Electronic Based Power Systems. *IEEE Open Journal of Power Electronics*, 1, pp.34-50.
- 10.Hirsch, A., Parag, Y. and Guerrero, J., 2018. Microgrids: A review of technologies, key drivers, and outstanding issues. *Renewable and sustainable Energy reviews*, 90, pp.402-411.
- 11.Soshinskaya, M., Crijns-Graus, W.H., Guerrero, J.M. and Vasquez, J.C., 2014. Microgrids: Experiences, barriers and success factors. *Renewable and Sustainable Energy Reviews*, 40, pp.659-672.
- 12.Cagnano, A., De Tuglie, E. and Mancarella, P., 2020. Microgrids: Overview and guidelines for practical implementations and operation. *Applied Energy*, 258, p.114039.
- 13.Tan, X., Li, Q. and Wang, H., 2013. Advances and trends of energy storage technology in microgrid. *International Journal of Electrical Power & Energy Systems*, 44(1), pp.179-191.
- 14.Guerrero, J.M., Loh, P.C., Lee, T.L. and Chandorkar, M., 2012. Advanced control architectures for intelligent microgrids—Part II: Power quality, energy storage, and AC/DC microgrids. *IEEE Transactions on industrial electronics*, 60(4), pp.1263-1270.
- 15.Microgrids-Benefits, M., 2014. Barriers and suggested policy initiatives for the commonwealth of massachusetts. KEMA Inc.: Burlington, MA, USA.
- 16.IEC, I., 2003. 61970-301: Energy management system application program interface (EMS-API)-Part 301: Common Information Model (CIM) Base. Technical report, IEC-International Electrotechnical Commission.
- 17.Zia, M.F., Elbouchikhi, E. and Benbouzid, M., 2018. Microgrids energy management systems: A critical review on methods, solutions, and prospects. *Applied energy*, 222, pp.1033-1055.
- 18.Salam, A.A., Mohamed, A. and Hannan, M.A., 2008. Technical challenges on microgrids. *ARNP Journal of engineering and applied sciences*, 3(6), pp.64-69.
- 19.Hatziargyriou, N.D., Jenkins, N., Strbac, G., Lopes, J.A.P., Ruela, J., Engler, A., Oyarzabal, J., Kariniotakis, G. and Amorim, A., 2006, August. Microgrids-large scale integration of microgeneration to low voltage grids.

20. Zamora, R. and Srivastava, A.K., 2010. Controls for microgrids with storage: Review, challenges, and research needs. *Renewable and Sustainable Energy Reviews*, 14(7), pp.2009-2018.
21. Hooshyar, A. and Iravani, R., 2017. Microgrid protection. *Proceedings of the IEEE*, 105(7), pp.1332-1353.
22. Shiles, J., Wong, E., Rao, S., Sanden, C., Zamani, M.A., Davari, M. and Katiraei, F., 2017, July. Microgrid protection: An overview of protection strategies in North American microgrid projects. In 2017 IEEE Power & Energy Society General Meeting (pp. 1-5). IEEE.
23. Che, L., Khodayar, M.E. and Shahidehpour, M., 2014. Adaptive Protection System for Microgrids: Protection practices of a functional microgrid system. *IEEE Electrification magazine*, 2(1), pp.66-80.
24. Beheshtaein, S., Cuzner, R., Savaghebi, M. and Guerrero, J.M., 2019. Review on microgrids protection. *IET Generation, Transmission & Distribution*, 13(6), pp.743-759.
25. Monadi, M., Zamani, M.A., Candela, J.I., Luna, A. and Rodriguez, P., 2015. Protection of AC and DC distribution systems Embedding distributed energy resources: A comparative review and analysis. *Renewable and sustainable energy reviews*, 51, pp.1578-1593.
26. Hosseini, S.A., Abyaneh, H.A., Sadeghi, S.H.H., Razavi, F. and Nasiri, A., 2016. An overview of microgrid protection methods and the factors involved. *Renewable and Sustainable Energy Reviews*, 64, pp.174-186.
27. Min, B.W., Jung, K.H., Choi, M.S., Lee, S.J., Hyun, S.H. and Kang, S.H., 2003, May. Agent-based adaptive protection coordination in power distribution systems. In *Proceedings of the 17th International Conference on Electricity Distribution (CIRED)*.
28. Hussain, B., Sharkh, S.M., Hussain, S. and Abusara, M.A., 2010. Integration of distributed generation into the grid: Protection challenges and solutions. In 10th IET International Conference on Developments in Power System Protection (DPSP 2010). *Managing the Change*.
29. Memon, A.A. and Kauhaniemi, K., 2015. A critical review of AC Microgrid protection issues and available solutions. *Electric Power Systems Research*, 129, pp.23-31.
30. Kauhaniemi, K. and Kumpulainen, L., 2004. Impact of distributed generation on the protection of distribution networks.1.pp.315–318.
31. Priolkar, J.G. and Shet, V.N., 2013. A Review on Protection Issues in microgrid. *ion sources*, 2, pp.6-11.
32. Conti, S., 2009. Analysis of distribution network protection issues in presence of dispersed generation. *Electric Power Systems Research*, 79(1), pp.49-56.
33. Kashem, M.A. and Ledwich, G., 2002. Impact of distributed generation on protection of single wire earth return lines. *Electric Power Systems Research*, 62(1), pp.67-80.
34. Merino, J., Mendoza-Araya, P., Venkataramanan, G. and Baysal, M., 2014. Islanding detection in microgrids using harmonic signatures. *IEEE Transactions on Power Delivery*, 30(5), pp.2102-2109.
35. IEEE Standards Board, 2003. IEEE Standard for Interconnecting Distributed Resources with Electric Power Systems: 1547-2003. IEEE.
36. Dutta, S., Sadhu, P.K., Reddy, M.J.B. and Mohanta, D.K., 2018. Shifting of research trends in islanding detection method-a comprehensive survey. *Protection and Control of Modern Power Systems*, 3(1), p.1.
37. Mishra, M., Sahani, M. and Rout, P.K., 2017. An islanding detection algorithm for distributed generation based on Hilbert–Huang transform and extreme learning machine. *Sustainable Energy, Grids and Networks*, 9, pp.13-26.

38. Biaz, B.M., Ferreira, V.H., Fortes, M.Z., Lopes, T.T. and Lima, G.B.A., 2018. Islanding detection in distributed generation using unsupervised learning techniques. *IEEE Latin America Transactions*, 16(1), pp.118-125.
39. Zeineldin, H.H., Abdel-Galil, T., El-Saadany, E.F. and Salama, M.M.A., 2007. Islanding detection of grid connected distributed generators using TLS-ESPRIT. *Electric Power Systems Research*, 77(2), pp.155-162.
40. Basso, T.S. and DeBlasio, R., 2004. IEEE 1547 series of standards: interconnection issues. *IEEE Transactions on Power Electronics*, 19(5), pp.1159-1162.
41. I. V. Banu et al., "Passive anti-Islanding protection for Three-Phase Grid-Connected photovoltaic power systems," *International Journal of Electrical Power and Energy Systems*, vol. 148, no. January, p. 108946, 2023. <https://doi.org/10.1016/j.ijepes.2023.108946>.
42. X. Xie, C. Huang, and D. Li, "A new passive islanding detection approach considering the dynamic behavior of load in microgrid," *International Journal of Electrical Power and Energy Systems*, vol. 117, no. October 2019, p. 105619, 2020. <https://doi.org/10.1016/j.ijepes.2019.105619>.
43. A. Abyaz et al., "An effective passive islanding detection algorithm for distributed generations," *Energies*, vol. 12, no. 16, pp. 1–19, 2019. <https://doi.org/10.3390/en12163160>.
44. M. S. Kim, R. Haider, G. J. Cho, C. H. Kim, C. Y. Won, and J. S. Chai, "Comprehensive review of islanding detection methods for distributed generation systems," *Energies*, vol. 12, no. 5, pp. 1–21, 2019. <https://doi.org/10.3390/en12050837>.
45. C. R. Reddy, B. S. Goud, B. N. Reddy, M. Pratyusha, C. V. Vijay Kumar, and R. Rekha, "Review of Islanding Detection Parameters in Smart Grids," *8th International Conference on Smart Grid, icSmartGrid 2020*, pp. 78–89, 2020. <https://doi.org/10.1109/icSmartGrid49881.2020.9144923>.
46. N. Gupta, R. Dogra, R. Garg, and P. Kumar, "Review of islanding detection schemes for utility interactive solar photovoltaic systems," *International Journal of Green Energy*, vol. 19, no. 3, pp. 242–253, 2022. <https://doi.org/10.1080/15435075.2021.1941048>.
47. J. A. Cebollero, D. Cañete, S. Martín-Arroyo, M. García-Gracia, and H. Leite, "A Survey of Islanding Detection Methods for Microgrids and Assessment of Non-Detection Zones in Comparison with Grid Codes," *Energies*, vol. 15, no. 2, 2022. <https://doi.org/10.3390/en15020460>.
48. C. Rami Reddy et al., "Hybrid ROCOF Relay for Islanding Detection," *Journal of Electrical Engineering and Technology*, vol. 17, no. 1, pp. 51–60, 2022. <http://dx.doi.org/10.1007/s42835-021-00856-9>.
49. B. Hariprasad., P. Bharat Kumar, P. Sujatha, and G. Sreenivasan, "Island Detection in Inverter Based Distributed Generation Using a Hybrid Method," *Proceedings of the 2nd International Conference on Artificial Intelligence and Smart Energy, ICAIS 2022*, pp. 1702–1707, 2022. <https://doi.org/10.1109/ICAIS53314.2022.9742815>.
50. M. A. Ajith and R. M. Shereef, "Islanding Detection of Inverter based Distributed Generations using Wavelet Transform and KNN," *PESGRE 2022 - IEEE International Conference on "Power Electronics, Smart Grid, and Renewable Energy"*, pp. 1–6, 2022. <https://doi.org/10.1109/PESGRE52268.2022.9715940>.
51. M. Tajdinian, H. Khosravi, H. Samet, and Z. M. Ali, "Islanding Detection Scheme Using Potential Energy Function Based Criterion," *Electric Power Systems Research*, vol. 209, no. September 2021, p. 108047, 2022. <https://doi.org/10.1016/j.epsr.2022.108047>.
52. S. K. G. Manikonda and D. N. Gaonkar, "Comprehensive review of IDMs in DG systems," *IET Smart Grid*, vol. 2, no. 1, pp. 11–24, 2019. <https://doi.org/10.1049/iet-stg.2018.0096>.
53. S. C. Paiva, R. L. de A. Ribeiro, D. K. Alves, F. B. Costa, and T. de O. A. Rocha, "A wavelet-based hybrid islanding detection system applied for distributed generators interconnected to AC

- microgrids,” *International Journal of Electrical Power and Energy Systems*, vol. 121, no. March, p. 106032, 2020. <https://doi.org/10.1016/j.ijepes.2020.106032>.
- 54.A. Taheri Kolli and N. Ghaffarzadeh, “A novel phaselet-based approach for islanding detection in inverter-based distributed generation systems,” *Electric Power Systems Research*, vol. 182, no. February 2019, 2020. <https://doi.org/10.1016/j.epr.2020.106226>.
 - 55.N. A. Larik, M. F. Tahir, Z. M. S. Elbarbary, M. Z. Yousaf, and M. A. Khan, “A comprehensive literature review of conventional and modern islanding detection methods,” *Energy Strategy Reviews*, vol. 44, no. November, p. 101007, 2022. <https://doi.org/10.1016/j.esr.2022.101007>.
 - 56.I. Bhushan, S. Chandra, and A. Yadav, “A Comprehensive Portrayal of Research Drifts in Islanding Detection Methods towards Soft Computing,” *2022 2nd International Conference on Power Electronics and IoT Applications in Renewable Energy and its Control, PARC 2022*, pp. 1–5, 2022. <https://doi.org/10.1109/PARC52418.2022.9726246>.
 - 57.S. S. Mohapatra, M. K. Maharana, A. Pradhan, P. K. Panigrahi, and R. C. Prusty, “Detection and diagnosis of islanding using artificial intelligence in distributed generation systems,” *Sustainable Energy, Grids and Networks*, vol. 29, p. 100576, 2022. <https://doi.org/10.1016/j.segan.2021.100576>.
 - 58.Teoh, W.Y.; Tan, C.W. An overview of islanding detection methods in photovoltaic systems. *Int. J. Electr. Comput. Eng.* 2011, 5, 1341–1349.
 - 59.Bower, W.I.; Ropp, M. *Evaluation of Islanding Detection Methods for Photovoltaic Utility-Interactive Power System*; Sandia National Lab: Albuquerque, NM, USA, 2002.
 - 60.Antony, A.; Menon, D. *Islanding Detection Technique of Distribution Generation System*. In *Proceedings of the 2016 International Conference on Circuit, Power and Computing Technologies, Nagercoil, India, 18–19 March 2016*.
 - 61.Jones, R.A.; Sims, T.R.; Imece, A.F. Investigation of potential islanding of a self-commutated static power converter in photovoltaic systems. *IEEE Trans. Energy Convers.* 1990, 5, 624–631.
 - 62.Kim, M.S.; Haider, R.; Cho, G.J.; Kim, C.H.; Won, C.Y.; Chai, J.S. Comprehensive review of islanding detection methods for distributed generation systems. *Energies* 2019, 12, 837.
 - 63.Li, C.; Cao, C.; Cao, Y.; Kuang, Y.; Zeng, L.; Fang, B. A review of islanding detection methods for microgrid. *Renew. Sustain. Energy Rev.* 2014, 35, 211–220.
 - 64.Ahmad, K.N.E.K.; Selvaraj, J.; Rahim, N.A. A review of the islanding detection methods in grid-connected PV inverters. *Renew. Sustain. Energy Rev.* 2013, 21, 756–766.
 - 65.Jang, S.I.; Kim, K.H. An islanding detection method for distributed generations using voltage unbalance and total harmonic distortion of current. *IEEE Trans. Power Deliv.* 2004, 19, 745–752.
 - 66.Cebollero, J.A.; Cañete, D.; Martín-Arroyo, S.; García-Gracia, M.; Leite, H. A Survey of Islanding Detection Methods for Microgrids and Assessment of Non-Detection Zones in Comparison with Grid Codes. *Energies* 2022, 15, 460.
 - 67.Hatata, F.A.Y.; Abd-Raboh, E.H.; Sedhom, B.E. A review of anti-islanding protection methods for renewable distributed generation systems. *J. Electr. Eng.* 2016, 16, 235–246.
 - 68.Singam, B.; Hui, L.Y. Assessing SMS and PJD schemes of anti-islanding with varying quality factor. In *Proceedings of the 2006 IEEE International Power and Energy Conference, Putra Jaya, Malaysia, 28–29 November 2006*.
 - 69.Zhou, X.; Wu, J.; Ma, Y. A review of islanding detection method of grid-connected PV power system. *Adv. Mater. Res.* 2013, 614–615, 815–818.
 - 70.Mishra, M.; Chandak, S.; Rout, P.K. Taxonomy of Islanding detection techniques for distributed generation in microgrid. *Renew. Energy Focus* 2019, 31, 9–30.

71. Kunte, R.S.; Gao, W. Comparison and review of islanding detection techniques for distributed energy resources. In Proceedings of the 40th North American Power Symposium, Calgary, AB, Canada, 29–30 September 2008.
72. Mukarram, M.J.; Murkute, S.V. Sandia Frequency Shift Method for Anti-Islanding Protection of a Grid-tied Photovoltaic System. In Proceedings of the 2020 IEEE International Students' Conference on Electrical, Electronics and Computer Science, Bhopal, India, 22–23 February 2020.
73. Reis, M.V.; Barros, T.A.; Moreira, A.B.; Ruppert, E.; Villalva, M.G. Analysis of the Sandia Frequency Shift (SFS) islanding detection method with a single-phase photovoltaic distributed generation system. In Proceedings of the 2015 IEEE PES Innovative Smart Grid Technologies Latin America, Montevideo, Uruguay, 5–7 October 2015.
74. Worku, M.Y.; Hassan, M.A.; Maraaba, L.S.; Abido, M.A. Islanding detection methods for microgrids: A comprehensive review. *Mathematics* 2021, 9, 3174.
75. Chaitanya, B.K.; Yadav, A.; Pazoki, M.; Abdelaziz, A.Y. A comprehensive review of islanding detection methods. *Uncertainties Mod. Power Syst.* 2021, 211–256.
76. Liu, F.; Kang, Y.; Zhang, Y.; Duan, S.; Lin, X. Improved SMS islanding detection method for grid-connected converters. *IET Renew. Power Gener.* 2010, 4, 36–42.
77. Trujillo, C.L.; Velasco, D.; Figueres, E.; Garcerá, G. Analysis of active islanding detection methods for grid-connected micro inverters for renewable energy processing. *Appl. Energy* 2010, 87, 3591–3605.
78. Panigrahi, B.K.; Bhuyan, A.; Shukla, J.; Ray, P.K.; Pat, S. A comprehensive review on intelligent islanding detection techniques for renewable energy integrated power system. *Int. J. Energy Res.* 2021, 45, 14085–14116.
79. Manikonda, S.K.; Gaonkar, D.N. Comprehensive review of IDMs in DG systems. *IET Smart Grid* 2019, 2, 11–24.
80. Velasco, D.; Trujillo, C.; Garcera, G.; Figueres, E. An active anti-islanding method based on phase-PLL perturbation. *IEEE Trans. Power Electron.* 2010, 26, 1056–1066.
81. Dong, D.; Wen, B.; Mattavelli, P.; Boroyevich, D.; Xue, Y. Modeling and design of islanding detection using phase-locked loops in three-phase grid-interface power converters. *IEEE J. Emerg. Sel. Top. Power Electron.* 2014, 2, 1032–1040.
82. Chiang, W.J.; Jou, H.L.; Wu, J.C. Active islanding detection method for inverter-based distribution generation power system. *Int. J. Electr. Power Energy Syst.* 2012, 42, 158–166.
83. Jou, H.L.; Chiang, W.J.; Wu, J.C. Virtual inductor-based islanding detection method for grid-connected power inverter of distributed power generation system. *IET Renew. Power Gener.* 2007, 1, 175–181.
84. Menon, V.; Nehrir, M.H. A hybrid islanding detection technique using voltage unbalance and frequency set point. *IEEE Trans. Power Syst.* 2007, 22, 442–448.
85. Mahat, P.; Chen, Z.; Bak-Jensen, B. A hybrid islanding detection technique using average rate of voltage change and real power shift. *IEEE Trans. Power Deliv.* 2009, 24, 764–771.
86. Vahedi, H.; Noroozian, R.; Jalilvand, A.; Gharehpetian, G.B. Hybrid SFS and Q-f Islanding Detection Method for Inverter-Based DG. In Proceedings of the 2010 IEEE International Conference on Power and Energy, Kuala Lumpur, Malaysia, 29 November– 1 December 2010.
87. Sundar, D.J.; Kumaran, M.S. A comparative review of islanding detection schemes in distributed generation systems. *Int. J. Renew. Energy Res.* 2015, 5, 1016–1023.
88. Funabashi, T.; Member, S.; Koyanagi, K.; Yokoyama, R. A Review of Islanding Detection Methods for Distributed Resources. In Proceedings of the 2003 IEEE Power Tech Conference Proceedings, Bologna, Italy, 23–26 June 2003.

- 89.Chandrakar, C.S.; Dewani, B.; Chandrakar, D. An assessment of distributed generation islanding detection methods. *Int. J. Adv. Eng. Technol.* 2012, 5, 218.
- 90.Barcentewicz, S.; Lerch, T.; Bie ´n, A.; Duda, K. Laboratory evaluation of a phasor-based islanding detection method. *Energies* 2021, 14, 1953.
- 91.Schweitzer, E.O.; Whitehead, D.; Zweigle, G.; Ravikumar, K.G. Synchrophasor-based power system protection and control applications. In Proceedings of the 2010 63rd Annual Conference for Protective Relay Engineers, College Station, TX, USA, 29 March–1 April 2010.
- 92.Yılmaz, A.; Bayrak, G. A new signal processing-based islanding detection method using pyramidal algorithm with undecimated wavelet transform for distributed generators of hydrogen energy. *Int. J. Hydrog. Energy* 2022, 47, 19821–19836.
- 93.Mohanty, S.R.; Kishor, N.; Ray, P.K.; Catalo, J.P. Comparative study of advanced signal processing techniques for islanding detection in a hybrid distributed generation system. *IEEE Trans. Sustain. Energy* 2014, 6, 122–131.
- 94.Paiva, S.C.; de Araujo Ribeiro, R.L.; Alves, D.K.; Costa, F.B.; Rocha, T.D. A wavelet-based hybrid islanding detection system applied for distributed generators interconnected to AC microgrids. *Int. J. Electr. Power Energy Syst.* 2020, 121, 106032.
- 95.Barros, J.; Diego, R.I. Application of the wavelet-packet transform to the estimation of harmonic groups in current and voltage waveforms. *IEEE Trans. Power Deliv.* 2005, 21, 533–535.
- 96.Samantaray, S.R.; Samui, A.; Babu, B.C. Time–frequency transform-based islanding detection in distributed generation. *IET Renew. Power Gener.* 2011, 5, 431–438.
- 97.Merlin, V.L.; Santos, R.C.; Grilo, A.P.; Vieira, J.C.; Coury, D.V.; Oleskovicz, M. A new artificial neural network based method for islanding detection of distributed generators. *Int. J. Electr. Power Energy Syst.* 2016, 75, 139–151.
- 98.Khamis, A.; Shareef, H.; Mohamed, A.; Bizkevelci, E. Islanding detection in a distributed generation integrated power system using phase space technique and probabilistic neural network. *Neurocomputing* 2015, 148, 587–599.
- 99.Heidari, M.; Seifossadat, G.; Razaz, M. Application of decision tree and discrete wavelet transform for an optimized intelligent-based islanding detection method in distributed systems with distributed generations. *Renew. Sustain. Energy Rev.* 2013, 27, 525–532.
- 100.Dash, P.K.; Padhee, M.; Panigrahi, T.K. A hybrid time–frequency approach based fuzzy logic system for power island detection in grid connected distributed generation. *Int. J. Electr. Power Energy Syst.* 2012, 42, 453–464.
- 101.Lin, F.J.; Tan, K.H.; Chiu, J.H. Active islanding detection method using wavelet fuzzy neural network. In Proceedings of the 2012 IEEE International Conference on Fuzzy Systems, Brisbane, QLD, Australia, 10–15 June 2012.
- 102.Matic-Cuka, B.; Kezunovic, M. Islanding detection for inverter-based distributed generation using support vector machine method. *IEEE Trans. Smart Grid* 2014, 5, 2676–2686.
- 103.Baghaee, H.R.; Mlaki ´c, D.; Nikolovski, S.; Dragic ´cvi ´c, T. Anti-islanding protection of PV-based microgrids consisting of PHEVs using SVMs. *IEEE Trans. Smart Grid* 2019, 11, 483–500.
- 104.Faqhruldin, O.N.; El-Saadany, E.F.; Zeineldin, H.H. Naive Bayesian islanding detection technique for distributed generation in modern distribution system. In Proceedings of the 2012 IEEE Electrical Power and Energy Conference, London, ON, Canada, 10–12 October 2012.
- 105.Faqhruldin, O.N.; El-Saadany, E.F.; Zeineldin, H.H. A universal islanding detection technique for distributed generation using pattern recognition. *IEEE Trans. Smart Grid* 2014, 5, 1985–1992.
- 106.Manikonda, S.K.; Gaonkar, D.N. IDM based on image classification with CNN. *J. Eng.* 2019, 2019, 7256–7262.

- 107.Kong, X.; Xu, X.; Yan, Z.; Chen, S.; Yang, H.; Han, D. Deep learning hybrid method for islanding detection in distributed generation. *Appl. Energy* 2018, 210, 776–785.
- 108.Dietmannsberger, M.; Schulz, D. Different load types and their effect on islanding detection and control in low voltage grids. In *Proceedings of the 2016 10th International Conference on Compatibility, Power Electronics and Power Engineering*, Bydgoszcz, Poland, 29 June–1 July 2016.
- 109.Larik, N.A.; Tahir, M.F.; Elbarbary, Z.S.; Yousaf, M.Z.; Khan, M.A. A comprehensive literature review of conventional and modern islanding detection methods. *Energy Strategy Rev.* 2022, 44, 101007.
- 110.Shukla, A.; Dutta, S.; Sahu, S.K.; Sadhu, P.K. A narrative perspective of island detection methods under the lens of cyber-attack in data-driven smart grid. *J. Electr. Syst. Inf. Technol.* 2023, 10, 14.
- 111.Aruldoss, M.; Lakshmi, M.T.; Venkatesan, V.P. A survey on multi criteria decision making methods and its applications. *Am. J. Inf. Syst.* 2013, 1, 31–43.
- 112.Velasquez, M.; Hester, P.T. An analysis of multi-criteria decision making methods. *Int. J. Oper.* 2013, 10, 56–66.
- 113.Shahsavarani, A.M.; Azad Marz Abadi, E. The Bases, Principles, and Methods of Decision-Making: A review of literature. *IJMR* 2015, 2, 214–225.
- 114.Baczkiwicz, A.; Watróbski, J.; Kizielewicz, B.; Sałabun, W. Towards Objectification of Multi-Criteria Assessments: A Comparative Study on MCDA Methods. In *Proceedings of the 2021 16th Conference on Computer Science and Intelligence Systems (FedCSIS)*, online, 2–5 September 2021.
- 115.Hajduk, S. Multi-Criteria Analysis in the Decision-Making Approach for the Linear Ordering of Urban Transport Based on TOPSIS Technique. *Energies* 2021, 15, 274.
- 116.A. Datta, A. Ray, D. Mukherjee, and H. Saha, “Selection of islanding detection methods based on multi-criteria decision analysis for grid-connected photovoltaic system applications,” *Sustainable Energy Technologies and Assessments*, vol. 7, pp. 111–122, 2014. <https://doi.org/10.1016/j.seta.2014.04.003>.
- 117.Habenicht, W.; Scheubrein, B.; Scheubrein, R. Multiple-criteria Decision Making. *Optim. Oper. Res.* 2002, 4, 257–279.
- 118.Trendowicz, A.; Kopczynska, S. Adapting Multi-Criteria Decision Analysis for Assessing the Quality of Software Products. *Current Approaches and Future Perspectives*. In *Advances in Computers*; Elsevier: Amsterdam, The Netherlands, 2014; pp. 153–226.
- 119.Zopounidis, C.; Doumpos, M. Multicriteria classification and sorting methods: A literature review. *Eur. J. Oper. Res.* 2002, 138, 229–246.
- 120.Sabaei, D.; Erkoyuncu, J.; Roy, R. A review of multi-criteria decision making methods for enhanced maintenance delivery. *Procedia CIRP* 2015, 37, 30–35.
- 121.Hwang, C.-L.; Yoon, K. *Multiple Attribute Decision Making: Methods and Applications—A State-of-the-Art Survey*; Springer: New York, NY, USA, 1981; Volume 186.
- 122.Saaty TL, Sagir M. Extending the measurement of tangibles to intangibles. *International Journal of Information Technology & Decision Making*. 2009 Mar;8(01):7-27.
- 123.Saaty TL, Shang JS. An innovative orders-of-magnitude approach to AHP-based mutli-criteria decision making: Prioritizing divergent intangible humane acts. *European Journal of Operational Research*. 2011 Nov 1;214(3):703-15.
- 124.Aydin O, Arslan G. Optimal hospital location with fuzzy AHP. *The Business Review*, Cambridge. 2010;15:262-8.
- 125.Podvezko V, Mitkus S, Trinkūniene E. Complex evaluation of contracts for construction. *Journal of civil Engineering and management*. 2010 Jan 1;16(2):287-97.

126. Dong Y, Zhang G, Hong WC, Xu Y. Consensus models for AHP group decision making under row geometric mean prioritization method. *Decision Support Systems*. 2010 Jun 1;49(3):281-9.
127. Machiwal D, Jha MK, Mal BC. Assessment of groundwater potential in a semi-arid region of India using remote sensing, GIS and MCDM techniques. *Water resources management*. 2011 Mar;25:1359-86.
128. Stoklasa J, Jandová V, Talasová J. Weak consistency in Saaty's AHP-evaluating creative work outcomes of Czech art colleges. *Neural network world*. 2013;23(1):61.
129. Zhang H, Dong Y, Chiclana F, Yu S. Consensus efficiency in group decision making: A comprehensive comparative study and its optimal design. *European Journal of Operational Research*. 2019 Jun 1;275(2):580-98.
130. Stoklasa J, Jandová V, Talasová J. Weak consistency in Saaty's AHP-evaluating creative work outcomes of Czech art colleges. *Neural network world*. 2013;23(1):61.
131. Kravchenko T, Seredenko N. Decision-making with modeling of problem situations using the analytic network hierarchy process. *International Journal of the Analytic Hierarchy Process*. 2011 Jun 14;3(1).
132. Amponsah CT. Application of multi-criteria decision making process to determine critical success factors for procurement of capital projects under public-private partnerships. *International Journal of the Analytic Hierarchy Process*. 2011 Dec 27;3(2).
133. Wu W, Kou G, Peng Y, Ergu D. Improved AHP-group decision making for investment strategy selection. *Technological and Economic Development of Economy*. 2012 Jun 1;18(2):299-316.
134. Saaty TL. *Fundamentals of decision making and priority theory with the analytic hierarchy process*. RWS publications; 2001.
135. Forman EH, Gass SI. The analytic hierarchy process—an exposition. *Operations research*. 2001 Aug;49(4):469-86.
136. Lipovetsky S. An interpretation of the AHP eigenvector solution for the lay person. *International Journal of the Analytic Hierarchy Process*. 2010 Dec 31;2(2).
137. Zakaria NF, Dahlan HM, Hussin AR. Prioritization method in the analytic hierarchy process using evolutionary computing. *International Journal of Innovative Computing*. 2012;1:555-60.
138. Wang YM, Chin KS. A linear programming approximation to the eigenvector method in the analytic hierarchy process. *Information Sciences*. 2011 Dec 1;181(23):5240-8.
139. Lipovetsky S. Priority eigenvectors in Analytic Hierarchy/Network Processes with outer dependence between alternatives and criteria. *International Journal of the Analytic Hierarchy Process*. 2011 Dec 27;3(2).
140. Barfod MB, Leleur S. Scaling transformation in the Rembrandt technique: Examination of the progression factors. *International Journal of Information Technology & Decision Making*. 2013 Sep;12(05):887-903.
141. Ricciardo G. AN EVALUATION OF METHODS TO MAKE TRANSITIVE THE MULTIPLE COMPARISONS MATRICES. *International Journal of the Analytic Hierarchy Process*. 2011 Jun 14;3(1).
142. Wang X, Chan HK, Yee RW, Diaz-Rainey I. A two-stage fuzzy-AHP model for risk assessment of implementing green initiatives in the fashion supply chain. *International journal of production economics*. 2012 Feb 1;135(2):595-606.
143. Sipahi S, Timor M. The analytic hierarchy process and analytic network process: an overview of applications. *Management decision*. 2010 Jun 1;48(5):775-808.
144. Zakaria NF, Dahlan HM, Hussin AR. Deriving priority in AHP using evolutionary computing approach. *WSEAS transactions on information science and applications*. 2010 May 1;7(5):714-24.

145. Tsyganok VV. About one approach to AHP/ANP stability measurement. *International Journal of the Analytic Hierarchy Process*. 2011 Jun 14;3(1).
146. Bobba RB, Dagle J, Heine E, Khurana H, Sanders WH, Sauer P, Yardley T. Enhancing grid measurements: Wide area measurement systems, NASPInet, and security. *IEEE Power and Energy Magazine*. 2011 Dec 15;10(1):67-73.
147. Phadke AG, Thorp JS. History and applications of phasor measurements. In 2006 IEEE PES Power Systems Conference and Exposition 2006 Oct 29 (pp. 331-335). IEEE.
148. Duda K, Zieliński TP, Barczentewicz SH. Perfectly flat-top and equiripple flat-top cosine windows. *IEEE Transactions on Instrumentation and Measurement*. 2016 Mar 11;65(7):1558-67.
149. Duda K, Zieliński TP. FIR filters compliant with the IEEE standard for M class PMU. *Metrology and Measurement Systems*. 2016;23(4).
150. Lee SH, Park JW. New islanding detection method for inverter-based distributed generation considering its switching frequency. *IEEE Transactions on Industry Applications*. 2010 May 10;46(5):2089-98.
151. Vieira JC, Freitas W, Xu W, Morelato A. An investigation on the non-detection zones of synchronous distributed generation anti-islanding protection. *IEEE transactions on power delivery*. 2008 Mar 31;23(2):593-600.
152. Eghbali O, Kazemzadeh R, Amiri K. Multi-area state estimation based on PMU measurements in distribution networks. *Journal of Operation and Automation in Power Engineering*. 2020 Feb 1;8(1):65-74.
153. Zargar B, Angioni A, Ponci F, Monti A. Multiarea parallel data-driven three-phase distribution system state estimation using synchrophasor measurements. *IEEE Transactions on Instrumentation and Measurement*. 2020 Jan 17;69(9):6186-202.
154. Appasani B, Jha AV, Mishra SK, Ghazali AN. Communication infrastructure for situational awareness enhancement in WAMS with optimal PMU placement. *Protection and Control of Modern Power Systems*. 2021 Dec;6:1-2.
155. Osipov D, Chow JH. PMU missing data recovery using tensor decomposition. *IEEE Transactions on Power Systems*. 2020 May 1;35(6):4554-63.
156. Saber A. PMU-Based fault location method for Three-terminal transmission lines with outage of one line branch. *Electric Power Systems Research*. 2020 May 1;182:106224.
157. Tang Y, Sun R, Thomas K, Burgos R. Synchrophasor based transmission system anti-islanding scheme. In 2017 IEEE Power & Energy Society General Meeting 2017 Jul 16 (pp. 1-5). IEEE.
158. Kamali S, Amraee T. Prediction of unplanned islanding in power systems using pmu data. In 2018 IEEE International Conference on Environment and Electrical Engineering and 2018 IEEE Industrial and Commercial Power Systems Europe (EEEIC/I&CPS Europe) 2018 Jun 12 (pp. 1-5). IEEE.
159. Radhakrishnan RM, Sankar A, Rajan S. A combined islanding detection algorithm for grid connected multiple microgrids for enhanced microgrid utilisation. *International Transactions on Electrical Energy Systems*. 2020 Feb;30(2):e12232.
160. Tang Y, Li F, Zheng C, Wang Q, Wu Y. PMU measurement-based intelligent strategy for power system controlled islanding. *Energies*. 2018 Jan 7;11(1):143.
161. Candelino M, Scheinkman M, Anello M, Del Rosso A. PMU-based Controlled System Separation Case Study for the Argentinean High Voltage Interconnection System. In 2019 IEEE PES Innovative Smart Grid Technologies Conference-Latin America (ISGT Latin America) 2019 Sep 15 (pp. 1-6). IEEE.

162. Dutta S, Sadhu PK, Reddy MJ, Mohanta DK. Smart inadvertent islanding detection employing p-type μ PMU for an active distribution network. *IET Generation, Transmission & Distribution*. 2018 Nov;12(20):4615-25.
163. Cao Q, Liu F, Zhu G, Chen W. PMU based islanding detection method for large photovoltaic power station. In 2015 IEEE 11th International Conference on Power Electronics and Drive Systems 2015 Jun 9 (pp. 126-131). IEEE.
164. Arefin AA, Baba M, Singh NS, Nor NB, Sheikh MA, Kannan R, Abro GE, Mathur N. Review of the Techniques of the Data Analytics and Islanding Detection of Distribution Systems Using Phasor Measurement Unit Data. *Electronics*. 2022 Sep 19;11(18):2967.
165. Gori M, Scarselli F, Tsoi AC. On the closure of the set of functions that can be realized by a given multilayer perceptron. *IEEE transactions on neural networks*. 1998 Nov;9(6):1086-98.
166. Kwon OJ, Bang SY. Design of a fault tolerant multilayer perceptron with a desired level of robustness. In *International Conference on Artificial Neural Networks 1997 Oct 8* (pp. 493-498). Berlin, Heidelberg: Springer Berlin Heidelberg.
167. Ghate VN, Dudul SV. Cascade neural-network-based fault classifier for three-phase induction motor. *IEEE Transactions on Industrial Electronics*. 2010 Jun 21;58(5):1555-63.